Physics – Uspekhi **60** (2) 121 – 148 (2017)

REVIEWS OF TOPICAL PROBLEMS PACS numbers: 74.20.Mn, 74.20.Rp, 74.25.Dw, 74.70.Tx, 75.40.Gb

Superconductivity in uranium ferromagnets

V P Mineev

DOI: https://doi.org/10.3367/UFNe.2016.04.037771

Contents

Abstract. The theoretical description and survey of the physical properties of superconducting states in uranium ferromagnetic materials are presented. On the basis of microscopic theory, we show that the coupling between electrons in these ferromagnetic metals by means of magnetization fluctuations gives rise to a triplet-pairing superconducting state, and establish the general form of the order parameter dictated by symmetry. The theory allows explaining some specific observations, including the peculiar phenomenon of reentrant superconductivity in URhGe in a magnetic field perpendicular to the spontaneous magnetization direction. In addition, we describe several particular topics related to uranium superconducting ferromagnets: (i) critical magnetic relaxation in dual localized–itinerant ferromagnets, (ii) phase transition to the ferromagnetic state in a Fermi liquid and UGe_2, (iii) superconducting ordering in ferromagnetic metals without an inversion center.

Keywords: ferromagnetism, superconductivity

V P Mineev Commissariat à l'Énergie Atomique, Université Grenoble Alpes, Institut Nanosciences et Cryogénie – FELIQS, 38000 Grenoble, France;
Landau Institute for Theoretical Physics, Russian Academy of Sciences, ul. Kosygina 2, 119334 Moscow, Russian Federation
E-mail: vladimir.mineev@cea.fr

Received 16 March 2016, revised 5 April 2016
Uspekhi Fizicheskikh Nauk **187** (2) 129 – 158 (2017)
DOI: https://doi.org/10.3367/UFNr.2016.04.037771
Translated by V P Mineev; edited by A M Semikhatov

1. Introduction

Superconductivity and ferromagnetic ordering are usually antagonists of each other. The reason is that the exchange field exceeds the paramagnetic limit field and destroys superconductivity by aligning the electron spins directed oppositely in Cooper pairs. Nevertheless, singlet superconductivity can coexist with ferromagnetism when the critical temperature of the transition to the superconducting state is greater than the Curie temperature, as is the case with so-called ternary compounds, which were actively investigated in

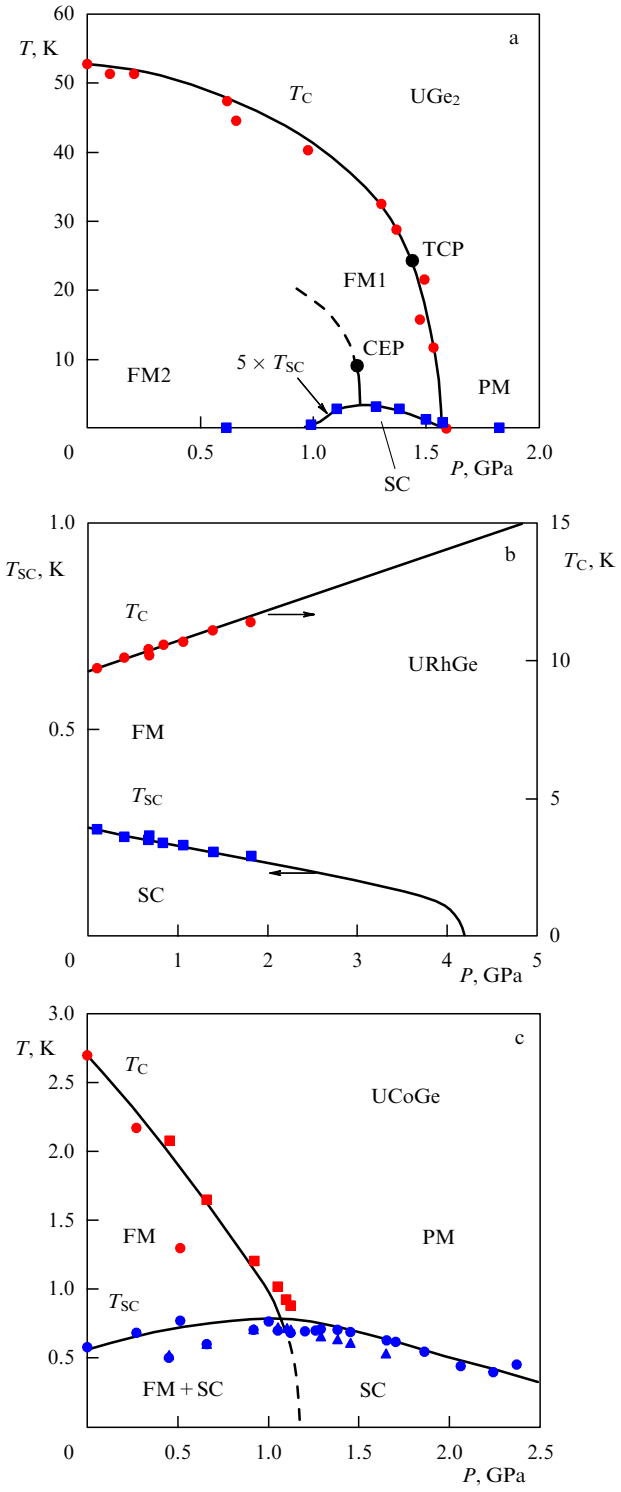

Figure 1. (Color online.) Temperature–pressure phase diagram of (a) UGe_2, (b) URhGe, and (c) UCoGe. FM, SC, and PM stand for ferromagnetic, superconducting, and paramagnetic phases; TCP is the tricritical point, and CEP is the critical end point [9].

the 1980s. The coexistence reveals itself in a form known as the Anderson–Suhl or crypto-ferromagnetic superconducting state [1, 2], characterized by the formation of a periodic domain-like magnetic structure. The structure period or the domain size λ is larger than the interatomic distance, but smaller than the superconducting coherence length ξ_0, which weakens the depairing effect of the exchange field, leading to an effective averaging of it to zero.

The coexistence of superconductivity and ferromagnetism recently discovered [3–6] in several uranium compounds — UGe_2, URhGe, UCoGe, and UIr — exhibits quite different properties. In the first two compounds, the Curie temperature T_C is higher than their critical temperatures for superconductivity T_{SC} by more than an order of magnitude (Fig. 1a, b). In UCoGe, the ratio T_C/T_{SC} at ambient pressure is about four (Fig. 1c). This, together with the fact that the upper critical field at low temperatures greatly exceeds the paramagnetic limit field in the first three compounds (see reviews [7–9]), indicates that we are dealing here with Cooper pairing in a triplet state. In UIr, the upper critical field is smaller than the paramagnetic limit field [6]. The reason is most likely in the low specimen quality: it is known that impurities and inhomogeneities strongly suppress the upper critical field in unconventional superconductors.

Ferromagnetism does not suppress the superconductivity with triplet pairing; hence, there is no reason for the formation of a cryptomagnetic state. Indeed, no traces of spatial modulation of magnetic moment directions on a scale smaller than the coherence length have been revealed [4, 10–12]. On the other hand, neutron depolarization measurements of UGe_2 down to 4.2 K (that is, in the ferromagnetic but not superconducting region) establish that the magnetic moment is strictly aligned along the a axis, with a typical domain size in the bc plane of the order of 4.4×10^{-4} cm [13], about two orders of magnitude larger than the largest superconducting coherence length in the b direction, $\xi_b \approx 7 \times 10^{-6}$ cm. A similar domain size was recently measured in UCoGe [14].

It is therefore natural to assume that these ferromagnetic superconductors are triplet superconductors similar to superfluid phases of He^3. It must be kept in mind, however, that unlike liquid helium, which is a completely isotropic neutral Fermi liquid, here we are dealing with superconductivity developing in strongly anisotropic ferromagnetic metals. Namely, UGe_2, URhGe, and UCoGe have an orthorhombic structure with the magnetic moment oriented along the a axis in the first of these compounds and along the c axis in the last two (Fig. 2). UIr has a monoclinic PbBi-type structure (space group P21) without inversion symmetry, with the magnetic moment oriented along the $[10\bar{1}]$ direction [15].

The magnetic moments in UGe_2 [16], URhGe [17], and UCoGe [18] are mostly concentrated around uranium ions. At $T = 0$, they are respectively equal to $1.4\mu_B$, $0.4\mu_B$, and $0.07\mu_B$. Although these values are much smaller than the

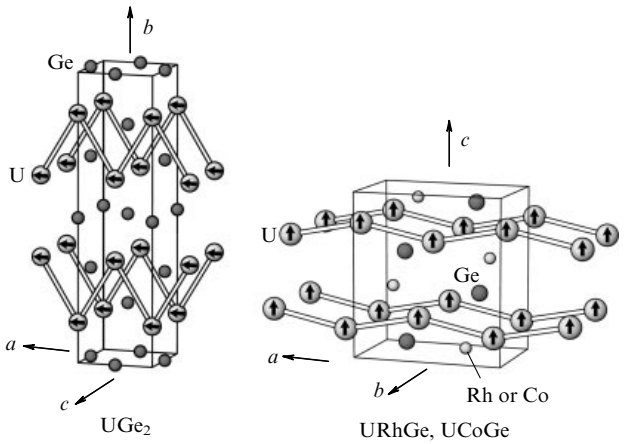

Figure 2. (Color online.) Crystal structures of UGe_2, URhGe, and UCoGe [9].

moment per uranium atom deduced from the susceptibility above T_C ($2.8\mu_B$, $1.8\mu_B$, and $1.5\mu_B$, respectively), this is still not sufficient to treat uranium compounds as completely itinerant ferromagnets. Instead, they are dual localized–itinerant ferromagnets. The most weakly delocalized material is UGe_2 [16, 19] and the most itinerant one is UCoGe [20, 21].

The interaction between conduction electrons by means of spin waves in a system of localized moments has been proposed as the most plausible pairing mechanism. Models of this type have been applied to the superconducting antiferromagnet UPd_2Al_3 [22] and to reentrant superconductivity in the ferromagnetic URhGe [23].

The general form of the order parameters of superconducting states in orthorhombic ferromagnets dictated by symmetry was found in [24–26]. Subsequently, a microscopic description of triplet superconductivity was developed based on the pairing interaction due to exchange of magnetization fluctuations in orthorhombic ferromagnets with strong magnetic anisotropy [27, 28]. This approach allowed explaining the interplay of the pressure dependence of the Curie temperature and the critical temperature of the superconducting transition and the magnetic field dependence of the pairing interaction for field orientations parallel or perpendicular to the spontaneous magnetization direction. The latter, in turn, allows explaining the peculiar phenomenon of reentrant superconductivity in URhGe in a magnetic field along the *b* direction [29].

Here, we present a survey of the theory and the physical properties of superconducting uranium compounds. Starting from the symmetry of superconducting states valid for a multiband orthorhombic ferromagnet, we limit ourselves to a description of the simplest two-band spin-up, spin-down superconducting ferromagnet. The structure of the superconducting order parameters and the quasiparticle spectrum are derived. We then explore the corresponding weak-coupling microscopic theory of pairing due to exchange by magnetic fluctuations in strongly anisotropic media with orthorhombic symmetry. The theory reproduces the superconducting order parameter dictated by the symmetry. The assumptions made in the previous treatments are demonstrated explicitly. We next discuss the low-temperature specific heat, the upper critical field, and other concrete properties of uranium ferromagnet superconductors.

Special attention is paid to the peculiar phenomenon of reentrant superconductivity in URhGe [30]. In the framework of the Landau theory of phase transitions, it is demonstrated that a magnetic field perpendicular to the easy magnetization direction decreases the Curie temperature, and the transition between the anisotropic ferromagnetic and paramagnetic states becomes a first-order phase transition in a strong enough field. The pairing interaction increases significantly in the vicinity of the transition, stimulating the reentrance to the superconducting state suppressed by the orbital mechanism.

We show that the magnetic field along the spontaneous magnetization direction suppresses the longitudinal fluctuations of magnetization. This allows us to explain the peculiar phenomena of the field-direction dependence of nuclear magnetic resonance relaxation [31] and the sharp anisotropy of the upper critical field [9, 32] in UCoGe.

In addition, we describe several particular topics related to superconductivity in uranium superconductors: (1) the origin of non-Landau damping of critical magnetic fluctuations in ferromagnets with a dual localized–itinerant nature of f-electrons [33, 34]; (2) the phase transition to the ferromagnetic state in UGe_2 [35] and in a Fermi liquid; (3) the general structure of superconducting ordering in ferromagnetic metals without inversion symmetry, as in UIr.

2. Order parameters, symmetry of states, and quasiparticle energy spectrum

2.1 Symmetry of superconducting states in orthorhombic ferromagnets

We consider a two-band ferromagnetic metal with the respective electron spectra

$$\varepsilon_\uparrow(\mathbf{k}) = \xi_\uparrow(\mathbf{k}) + \mu\,, \qquad \varepsilon_\downarrow(\mathbf{k}) = \xi_\downarrow(\mathbf{k}) + \mu \tag{1}$$

for the spin-up and spin-down bands (Fig. 3), where $\xi_\uparrow$ and $\xi_\downarrow$ are the energies measured from the chemical potential μ.

The spin-triplet superconducting state arising in a ferromagnetic metal consists of spin-up, spin-down, and zero-spin Cooper pairs described by the matrix order parameter [36]

$$\begin{aligned}\Delta_{\alpha\beta}(\mathbf{k},\mathbf{r}) &= \begin{pmatrix} \Delta^\uparrow(\mathbf{k},\mathbf{r}) & \Delta^0(\mathbf{k},\mathbf{r}) \\ \Delta^0(\mathbf{k},\mathbf{r}) & \Delta^\downarrow(\mathbf{k},\mathbf{r}) \end{pmatrix} \\ &= \Delta^\uparrow(\mathbf{k},\mathbf{r})|\uparrow\uparrow\rangle + \Delta^0(\mathbf{k},\mathbf{r})\big(|\uparrow\downarrow\rangle + |\downarrow\uparrow\rangle\big) + \Delta^\downarrow(\mathbf{k},\mathbf{r})|\downarrow\downarrow\rangle \\ &= \big(\mathbf{d}(\mathbf{k},\mathbf{r})\boldsymbol{\sigma}\big)\mathrm{i}\sigma_y = \begin{pmatrix} -d_x(\mathbf{k},\mathbf{r}) + \mathrm{i}d_y(\mathbf{k},\mathbf{r}) & d_z(\mathbf{k},\mathbf{r}) \\ d_z(\mathbf{k},\mathbf{r}) & d_x(\mathbf{k},\mathbf{r}) + \mathrm{i}d_y(\mathbf{k},\mathbf{r}) \end{pmatrix},\end{aligned} \tag{2}$$

where $\Delta^\uparrow(\mathbf{k},\mathbf{r})$, $\Delta^\downarrow(\mathbf{r},\mathbf{k},\mathbf{r})$, and $\Delta^0(\mathbf{k},\mathbf{r})$ are the spin-up, spin-down, and zero-spin amplitudes of the superconducting order parameter, depending on the Cooper pair center of gravity coordinate $\mathbf{r}$ and the momentum $\mathbf{k}$ of pairing electrons; $\boldsymbol{\sigma} = (\sigma_x, \sigma_y, \sigma_z)$ are the Pauli matrices. Equivalently, the order parameter can be written as the complex vector

$$\mathbf{d}(\mathbf{k},\mathbf{r}) = \frac{1}{2}\left[-\Delta^\uparrow(\mathbf{k},\mathbf{r})(\hat{\mathbf{x}} + \mathrm{i}\hat{\mathbf{y}}) + \Delta^\downarrow(\mathbf{k},\mathbf{r})(\hat{\mathbf{x}} - \mathrm{i}\hat{\mathbf{y}})\right] + \Delta^0(\mathbf{k},\mathbf{r})\hat{\mathbf{z}}\,. \tag{3}$$

Here and in what follows, $\hat{\mathbf{x}}$, $\hat{\mathbf{y}}$, $\hat{\mathbf{z}}$ are the unit vectors along the corresponding coordinate axes.

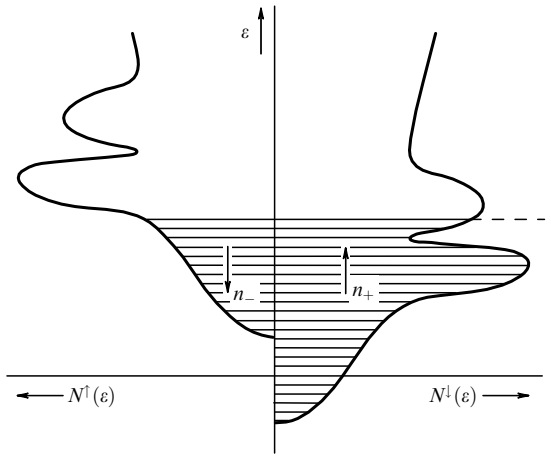

Figure 3. Density of states for spin-up $N^\uparrow(\varepsilon)$ and spin-down $N^\downarrow(\varepsilon)$ electron bands in a ferromagnetic metal.

We consider a ferromagnetic orthorhombic crystal with a strong spin–orbit coupling fixing the spontaneous magnetization along one of the second-order symmetry axes chosen as the z direction. Its point symmetry group, or black-white group, consists of rotation through the angle π around the z axis and rotations through π around the x and y directions combined with the operation of time reversal R, which changes the spontaneous magnetization direction to the opposite:

$$\mathrm{D}_2(\mathrm{C}_2^z) = (\mathrm{E}, \mathrm{C}_2^z, \mathrm{RC}_2^x, \mathrm{RC}_2^y)\,. \tag{4}$$

Because we are not interested in possible translation invariance breaking at the transition to the superconducting state, we do not consider the full space group of the normal state. Besides the point operations, the symmetry group of the normal state includes the U(1) group of gauge transformations

$$\mathrm{G_{FM}} = \mathrm{U}(1) \times \mathrm{D}_2(\mathrm{C}_2^z) = \mathrm{U}(1) \times (\mathrm{E}, \mathrm{C}_2^z, \mathrm{RC}_2^x, \mathrm{RC}_2^y)\,. \tag{5}$$

Superconducting states with *different critical temperatures* are described by the basis functions of *different irreducible corepresentations* of the symmetry group of the normal state. There are only two different corepresentations A and B of the group $\mathrm{G_{FM}}$ [24, 26]. The vector order parameters

$$\mathbf{d}_\mathrm{A}(\mathbf{k}, \mathbf{r}), \quad \mathbf{d}_\mathrm{B}(\mathbf{k}, \mathbf{r})$$

of the corresponding states are determined by the amplitudes

$$\begin{aligned} &\Delta_\mathrm{A}^\uparrow(\mathbf{k}, \mathbf{r}) = \hat{k}_x \eta_x^\uparrow(\mathbf{r}) + \mathrm{i}\hat{k}_y \eta_y^\uparrow(\mathbf{r})\,,\\ &\Delta_\mathrm{A}^\downarrow(\mathbf{k}, \mathbf{r}) = \hat{k}_x \eta_x^\downarrow(\mathbf{r}) + \mathrm{i}\hat{k}_y \eta_y^\downarrow(\mathbf{r})\,,\\ &\Delta_\mathrm{A}^0(\mathbf{k}, \mathbf{r}) = \hat{k}_z \eta_z^0(\mathbf{r})\,, \end{aligned} \tag{6}$$

$$\begin{aligned} &\Delta_\mathrm{B}^\uparrow(\mathbf{k}, \mathbf{r}) = \hat{k}_z \zeta_z^\uparrow(\mathbf{r})\,,\\ &\Delta_\mathrm{B}^\downarrow(\mathbf{k}, \mathbf{r}) = \hat{k}_z \zeta_z^\downarrow(\mathbf{r})\,,\\ &\Delta_\mathrm{B}^0(\mathbf{k}, \mathbf{r}) = \hat{k}_x \zeta_x^0(\mathbf{r}) + \mathrm{i}\hat{k}_y \zeta_y^0(\mathbf{r})\,. \end{aligned} \tag{7}$$

Here and in what follows, $\hat{k}_x, \hat{k}_y, \hat{k}_z$ are the components of the unit momentum vector $\hat{\mathbf{k}} = \mathbf{k}/|\mathbf{k}|$. For state A, the pair of scalar complex order parameter amplitudes for spin-up pairing have the common phase $(\eta_x^\uparrow, \eta_y^\uparrow) = (|\eta_x^\uparrow|, |\eta_y^\uparrow|) \times \exp(\mathrm{i}\varphi^\uparrow)$. The spin-down pair also have the common phase $(\eta_x^\downarrow, \eta_y^\downarrow) = (|\eta_x^\downarrow|, |\eta_y^\downarrow|) \exp(\mathrm{i}\varphi^\downarrow)$. The zero-spin amplitude has its own phase $\eta_z^0 = |\eta_z^0| \exp(\mathrm{i}\varphi^0)$. We assume that the three phases $\varphi^\uparrow$, $\varphi^\downarrow$, and φ^0 either coincide, $\varphi^\uparrow = \varphi^\downarrow = \varphi^0 = \varphi$, or differ by $\pm\pi$. The same holds for the spin-up, spin-down, and zero-spin order parameter components of the B state.

We can verify that the order parameter $\mathbf{d}_\mathrm{A}(\mathbf{k}, \mathbf{r})$ is invariant under all transformations of the group $\mathrm{G_A}$ that is isomorphic to the black-white group of the normal state $\mathrm{D}_2(\mathrm{C}_2^z)$, but contains the combined elements of time reversal and gauge transformations:

$$\mathrm{G_A} = \left(\mathrm{E}, \mathrm{C}_2^z, \exp(2\mathrm{i}\varphi)\mathrm{RC}_2^x, \exp(2\mathrm{i}\varphi)\,\mathrm{RC}_2^y\right). \tag{8}$$

For instance, the element RC_2^x, combining the transformations $\hat{\mathbf{y}} \to -\hat{\mathbf{y}}$, $\hat{\mathbf{z}} \to -\hat{\mathbf{z}}$, $\hat{k}_y \to -\hat{k}_y, \hat{k}_z \to -\hat{k}_z$ and complex conjugation of the order parameter, transforms into itself up to a phase factor $\exp(-\mathrm{i}\varphi)$, such that

$$\exp(2\mathrm{i}\varphi)\mathrm{RC}_2^x \mathbf{d}_\mathrm{A}(\mathbf{k}, \mathbf{r}) = \mathbf{d}_\mathrm{A}(\mathbf{k}, \mathbf{r})\,.$$

The order parameter $\mathbf{d}_\mathrm{B}(\mathbf{k}, \mathbf{r})$ is invariant under all transformations of the group

$$\begin{aligned} \mathrm{G_B} &= \mathrm{D}_2(\mathrm{E})\\ &= \left(\mathrm{E}, \mathrm{C}_2^z \exp(\mathrm{i}\pi), \exp(2\mathrm{i}\varphi)\mathrm{RC}_2^x \exp(\mathrm{i}\pi), \exp(2\mathrm{i}\varphi)\mathrm{RC}_2^y\right) \end{aligned} \tag{9}$$

that contains the combined elements of time reversal (complex conjugation) and multiplication by phase factors (gauge transformations).

It is important to note that the five-component order parameter of the A state, $\eta_x^\uparrow$, $\eta_y^\uparrow$, $\eta_x^\downarrow$, $\eta_y^\downarrow$, η_z^0, and the four-component order parameter of the B state, $\zeta_z^\uparrow, \zeta_z^\downarrow, \zeta_x^0, \zeta_y^0$, found from pure symmetry considerations include the zero-spin components. In other words, they are not *equal-spin-pairing states* consisting of Cooper pairs with opposite spins. This fact is explained below in the framework of the microscopic approach.

In writing Eqns (6) and (7), we were limited by the simplest form of the superconducting state order parameters. In general, the following complications must be taken into account.

(i) Each term in Eqns (6) and (7) can contain k_x^2, k_y^2, k_z^2-dependent factors invariant under all rotations of the orthorhombic group [24].

(ii) Equations (6) and (7) are written as they should be for a two-band spin-up and spin-down ferromagnet. For a multiband ferromagnet, the spin-up, spin-down, and zero-spin parts of the order parameter should consist of several terms related to different bands.

(iii) Also, if necessary, the higher-order harmonics (higher powers of $\hat{k}_x^l \hat{k}_y^m \hat{k}_z^n$) of the same symmetry as the one linear in the components of $\hat{\mathbf{k}}$ in Eqns (6) and (7) can be taken into account [24].

2.2 Superconducting states in UCoGe

Unlike URhGe and $\mathrm{UGe_2}$, where the superconducting state arises only in the ferromagnetic state, the phase diagram of UCoGe in Fig. 1c includes ferromagnetic (FM + SC) and paramagnetic (SC) superconducting states [37].[1] The symmetries of all the states shown in Fig. 1c obey the subordination rules usual for a second-order phase transition [37]. Namely, the symmetry group of the ferromagnetic superconducting state A,

$$\mathrm{G_{FM+SC}} = \left(\mathrm{E}, \mathrm{C}_2^z, \exp(2\mathrm{i}\varphi)\mathrm{RC}_2^x, \exp(2\mathrm{i}\varphi)\mathrm{RC}_2^y\right), \tag{10}$$

is a subgroup of the symmetry group of the ferromagnetic state

$$\mathrm{G_{FM}} = \mathrm{U}(1) \times \mathrm{D}_2(\mathrm{C}_2^z) = \mathrm{U}(1) \times \left(\mathrm{E}, \mathrm{C}_2^z, \mathrm{RC}_2^x, \mathrm{RC}_2^y\right) \tag{11}$$

and the symmetry group of the paramagnetic superconducting state

$$\mathrm{G_{SC}} = (\mathrm{E}, \mathrm{C}_2^z, \mathrm{C}_2^x, \mathrm{C}_2^y) + \exp(2\mathrm{i}\varphi)\mathrm{R} \times (\mathrm{E}, \mathrm{C}_2^z, \mathrm{C}_2^x, \mathrm{C}_2^y)\,. \tag{12}$$

Both of these groups are, in turn, subgroups of the group of the paramagnetic normal state

$$\mathrm{G_N} = \mathrm{U}(1) \times \left\{(\mathrm{E}, \mathrm{C}_2^z, \mathrm{C}_2^x, \mathrm{C}_2^y) + \mathrm{R} \times (\mathrm{E}, \mathrm{C}_2^z, \mathrm{C}_2^x, \mathrm{C}_2^y)\right\}. \tag{13}$$

[1] Any superconductor is a diamagnet; however, here and in what follows, we call a state that does not have a spontaneous magnetic moment a 'paramagnetic' superconducting state.

The order parameter of the paramagnetic superconducting state looks like the order parameter of the superfluid ^{3}He−B phase [36]:

$$\mathbf{d}(\mathbf{k},\mathbf{r}) = \hat{k}_x\eta_1(\mathbf{r})\hat{\mathbf{x}} + \hat{k}_y\eta_2(\mathbf{r})\hat{\mathbf{y}} + \hat{k}_z\eta_0(\mathbf{r})\hat{\mathbf{z}}\,. \tag{14}$$

Under the phase transition into a superconducting ferromagnet state, the exchange field lifts the Kramers degeneracy between the spin-up and spin-down electron states. Hence, unitary order parameter (14) transforms into a type-A nonunitary order parameter of superconducting ferromagnetic state (6):

$$\begin{aligned}
&\hat{k}_x\eta_x\hat{\mathbf{x}} + \hat{k}_y\eta_y\hat{\mathbf{y}} + \hat{k}_z\eta_z\hat{\mathbf{z}}\\
&= \frac{1}{2}\left[(\hat{k}_x\eta_x - \mathrm{i}\hat{k}_y\eta_y)(\hat{\mathbf{x}} + \mathrm{i}\hat{\mathbf{y}}) + (\hat{k}_x\eta_x + \mathrm{i}\hat{k}_y\eta_y)(\hat{\mathbf{x}} - \mathrm{i}\hat{\mathbf{y}})\right] + \hat{k}_z\eta_z\hat{\mathbf{z}}\\
&= \frac{1}{2}\left[-\Delta^{\uparrow}(\mathbf{k})(\hat{\mathbf{x}} + \mathrm{i}\hat{\mathbf{y}}) + \Delta^{\downarrow}(\mathbf{k})(\hat{\mathbf{x}} - \mathrm{i}\hat{\mathbf{y}})\right] + \Delta^0(\mathbf{k})\hat{\mathbf{z}}\\
&\Longrightarrow \frac{1}{2}\left(\hat{k}_x\eta_x^{\uparrow}(\mathbf{r}) - \mathrm{i}\hat{k}_y\eta_y^{\uparrow}(\mathbf{r})\right)(\hat{\mathbf{x}} + \mathrm{i}\hat{\mathbf{y}})\\
&+ \frac{1}{2}\left(\hat{k}_x\eta_x^{\downarrow}(\mathbf{r}) + \mathrm{i}\hat{k}_y\eta_y^{\downarrow}(\mathbf{r})\right)(\hat{\mathbf{x}} - \mathrm{i}\hat{\mathbf{y}}) + \hat{k}_z\eta_z^0(\mathbf{r})\hat{\mathbf{z}}.
\end{aligned} \tag{15}$$

A similar analysis of the phase symmetry and the order parameter transformation can also be performed for the transition from a paramagnetic superconducting state to the ferromagnetic superconducting state B.

A phase transition from the paramagnetic superconducting state to the ferromagnetic superconducting state in UCoGe has never been revealed experimentally.

2.3 Quasiparticle spectrum in ferromagnet superconductors with triplet pairing

We consider a two-band ferromagnetic metal with the electron spectra $\xi_{\uparrow}(\mathbf{k})$ and $\xi_{\downarrow}(\mathbf{k})$ for the spin-up and spin-down bands.

Even in the absence of an external field in a ferromagnet, there is an internal field H_{int} acting on the electron charges. The internal magnetic field in all uranium superconducting ferromagnets is larger than the lower critical field H_{c1} (see, e.g., [14]). Hence, the Meissner state is absent and the superconducting state is always the Abrikosov mixed state with a spatially inhomogeneous distribution of the order parameter and the internal magnetic field. In this case, to find the elementary excitation energies, we have to solve the coupled systems of Gor'kov and Maxwell differential equations. Some simplifications occur at low temperatures. Here, because $H_{\mathrm{int}} \ll H_{\mathrm{c2}}$, we can work in the London approximation, such that the internal magnetic field $\mathbf{H}_{\mathrm{int}}(\mathbf{r}) = \mathrm{rot}\,\mathbf{A}(\mathbf{r})$ is a slow function of coordinates. In the inter-vortex space, the order parameter is constant, and the electron (hole) momenta acquire a Doppler shift $\mathbf{k} \pm m\mathbf{v}_{\mathrm{s}}(\mathbf{r})$ due to the nonzero velocity of the superfluid component,

$$\mathbf{v}_{\mathrm{s}}(\mathbf{r}) = \frac{\hbar}{2m}\left(\nabla\varphi + \frac{2e}{\hbar c}\,\mathbf{A}(\mathbf{r})\right).$$

Then the Gor'kov equations become

$$\begin{aligned}
&\begin{pmatrix}
\mathrm{i}\omega_n - \frac{1}{2}(\xi_{\uparrow+} + \xi_{\downarrow+})\sigma_0 - \frac{1}{2}(\xi_{\uparrow+} - \xi_{\downarrow+})\sigma_z & -\mathrm{i}(\mathbf{d}\boldsymbol{\sigma})\sigma_y\\
\mathrm{i}\sigma_y(\mathbf{d}^*\boldsymbol{\sigma}) & \mathrm{i}\omega_n + \frac{1}{2}(\xi_{\uparrow-} + \xi_{\downarrow-})\sigma_0 + \frac{1}{2}(\xi_{\uparrow-} - \xi_{\downarrow-})\sigma_z
\end{pmatrix}\\
&\times\begin{pmatrix}
\hat{\mathrm{G}} & -\hat{\mathrm{F}}\\
-\hat{\mathrm{F}}^{\dagger} & -\tilde{\mathrm{G}}_{-k,-\omega}
\end{pmatrix} = \begin{pmatrix}\sigma_0 & 0\\ 0 & \sigma_0\end{pmatrix},
\end{aligned} \tag{16}$$

where

$$\xi_{\uparrow,\downarrow\pm}(\mathbf{k}) = \xi_{\uparrow,\downarrow}(\mathbf{k} \pm m\mathbf{v}_{\mathrm{s}}) \approx \xi_{\uparrow,\downarrow}(\mathbf{k}) \pm \mathbf{k}\mathbf{v}_{\mathrm{s}}\,. \tag{17}$$

As $\mathrm{i}\omega_n \to E$, the equality of the determinant of this system to zero gives the energy of elementary excitations

$$\begin{aligned}
E = \mathbf{k}\mathbf{v}_{\mathrm{s}} + \Bigg[&\frac{1}{2}(\xi_{\uparrow}^2 + \xi_{\downarrow}^2) + (\mathbf{d}\mathbf{d}^*) \pm \Big\{\frac{1}{4}\left[\xi_{\uparrow}^2 - \xi_{\downarrow}^2 + 2\mathrm{i}(\mathbf{d}\times\mathbf{d}^*)_z\right]^2\\
&- \left(\mathrm{i}(\mathbf{d}\times\mathbf{d}^*)_z\right)^2 + \mathrm{i}(\mathbf{d}\times\mathbf{d}^*)^2\Big\}^{1/2}\Bigg]^{1/2}.
\end{aligned} \tag{18}$$

The excitation energies acquire the simplest form in the so-called equal-spin-pairing state with $d_0 = 0$:

$$E_{\uparrow} = \mathbf{k}\mathbf{v}_{\mathrm{s}} + \sqrt{\xi_{\uparrow}^2 + \mathbf{d}\mathbf{d}^* + \mathrm{i}(\mathbf{d}\times\mathbf{d}^*)_z} = \mathbf{k}\mathbf{v}_{\mathrm{s}} + \sqrt{\xi_{\uparrow}^2 + \Delta_{\uparrow}^2}\,, \tag{19}$$

$$E_{\downarrow} = \mathbf{k}\mathbf{v}_{\mathrm{s}} + \sqrt{\xi_{\downarrow}^2 + \mathbf{d}\mathbf{d}^* - \mathrm{i}(\mathbf{d}\times\mathbf{d}^*)_z} = \mathbf{k}\mathbf{v}_{\mathrm{s}} + \sqrt{\xi_{\downarrow}^2 + \Delta_{\downarrow}^2}\,. \tag{20}$$

It is also instructive to write the energy of excitations in the nonunitary superconducting state [36],

$$E = \mathbf{k}\mathbf{v}_{\mathrm{s}} + \sqrt{\xi^2 + \mathbf{d}\mathbf{d}^* \pm \left|\mathrm{i}(\mathbf{d}\times\mathbf{d}^*)\right|}\,, \tag{21}$$

arising from a paramagnetic normal state with $\xi_{\uparrow} = \xi_{\downarrow} = \xi$. In all the cases, the Kramers degeneracy is lifted.

We next discuss what kind of pairing interaction gives rise to the A and B superconducting states in ferromagnets with orthorhombic symmetry.

3. Superconducting states in microscopic weak-coupling theory

3.1 Triplet pairing by spin-fluctuation exchange

The interaction between two electrons is assumed to be due to the attraction of one electron by the magnetic polarization cloud of the other. Unlike superfluid He^3, where the pairing of atoms originates from the magnetic polarization in an isotropic Fermi liquid, pairing of electrons in a ferromagnetic metal occurs in an anisotropic medium due to polarization of the electron liquid and the localized moments.

We therefore consider the pairing originating from the attraction

$$H_{\mathrm{elm}} = -\frac{1}{2}\mu_{\mathrm{B}}^2 I^2 \int \mathrm{d}^3\mathbf{r}\,\mathrm{d}^3\mathbf{r}'\; S_i(\mathbf{r})\,\chi_{ij}(\mathbf{r}-\mathbf{r}')\,S_j(\mathbf{r}') \tag{22}$$

between the electrons with magnetic moments μ_{B} by means of the electron–magnon interaction in a ferromagnetic medium with orthorhombic symmetry. Here,

$$\mathbf{S}(\mathbf{r}) = \psi_{\alpha}^{\dagger}(\mathbf{r})\boldsymbol{\sigma}_{\alpha\beta}\,\psi_{\beta}(\mathbf{r})$$

is the electron spin density operator, $\chi_{ij}(\mathbf{r})$ is the medium susceptibility, and I is an exchange constant.

Transforming the interaction Hamiltonian into the momentum representation and retaining only the odd-parity terms (with respect to $\mathbf{k}$ and $\mathbf{k}'$), after some straightforward algebra [38] we obtain the Bardeen–Cooper–Schrieffer (BCS) Hamiltonian for triplet pairing from Eqn (22):

$$H_{\mathrm{pairing}} = \frac{1}{2}\sum_{\mathbf{k}\mathbf{k}'} V_{\alpha\beta\gamma\delta}(\mathbf{k},\mathbf{k}')a_{\alpha}^{\dagger}(\mathbf{k})a_{\beta}^{\dagger}(-\mathbf{k})a_{\gamma}(-\mathbf{k}')a_{\delta}(\mathbf{k}')\,, \tag{23}$$

where

$$V_{\alpha\beta\gamma\delta}(\mathbf{k},\mathbf{k}') = V_{ij}(\mathbf{k},\mathbf{k}')(\mathrm{i}\sigma_i\sigma_y)_{\alpha\beta}(\mathrm{i}\sigma_j\sigma_y)^{\dagger}_{\gamma\delta}\,, \tag{24}$$

$$V_{ij}(\mathbf{k},\mathbf{k}') = -\mu_{\mathrm{B}}^2 I^2\left(\frac{1}{2}\,\mathrm{Tr}\,\hat{\chi}^{\mathrm{u}}(\mathbf{k},\mathbf{k}')\delta_{ij} - \chi^{\mathrm{u}}_{ij}(\mathbf{k},\mathbf{k}')\right) \tag{25}$$

is expressed through the odd part of the medium static susceptibility

$$\hat{\chi}^{\mathrm{u}}(\mathbf{k},\mathbf{k}') = \chi^{\mathrm{u}}_{ij}(\mathbf{k},\mathbf{k}') = \frac{1}{2}\left[\chi_{ij}(\mathbf{k}-\mathbf{k}') - \chi_{ij}(\mathbf{k}+\mathbf{k}')\right].$$

The critical temperature or the upper critical field is determined as an eigenvalue of the linear equation for the order parameter

$$\Delta_{\alpha\beta}(\mathbf{k},\mathbf{q}) = -T\sum_n\sum_{\mathbf{k}'} V_{\beta\alpha\lambda\mu}(\mathbf{k},\mathbf{k}')G_{\lambda\gamma}(\mathbf{k}',\omega_n) \times G_{\mu\delta}(-\mathbf{k}'+\mathbf{q},-\omega_n)\Delta_{\gamma\delta}(\mathbf{k}',\mathbf{q})\,. \tag{26}$$

Here, the matrix of the order parameter in the momentum representation is

$$\Delta(\mathbf{k},\mathbf{q}) = \int \Delta(\mathbf{k},\mathbf{r})\exp(\mathrm{i}\mathbf{q}\mathbf{r})\,\mathrm{d}^3 r = \begin{pmatrix} \Delta^{\uparrow}(\mathbf{k},\mathbf{q}) & \Delta^{0}(\mathbf{k},\mathbf{q}) \\ \Delta^{0}(\mathbf{k},\mathbf{q}) & \Delta^{\downarrow}(\mathbf{k},\mathbf{q}) \end{pmatrix}, \tag{27}$$

and $G_{\lambda\gamma}(\mathbf{k}',\omega_n)$ is the matrix of the normal-metal Green's function. *In the absence of an external field or when the external magnetic field is strictly parallel to the spontaneous magnetization*, this Green's function is diagonal,

$$G_{\mathrm{n}} = \begin{pmatrix} G^{\uparrow} & 0 \\ 0 & G^{\downarrow} \end{pmatrix}, \tag{28}$$

where

$$G^{\uparrow,\downarrow} = \frac{1}{\mathrm{i}\omega_{\mathrm{n}} - \xi^{\uparrow,\downarrow}_{\mathbf{k}}}\,. \tag{29}$$

Matrix equation (26) is a system of coupled linear equations for the order parameter components

$$\Delta^{\uparrow}(\mathbf{k},\mathbf{q}) = -T\sum_n\sum_{\mathbf{k}'}\left[V^{\uparrow\uparrow}(\mathbf{k},\mathbf{k}')G^{\uparrow}G^{\uparrow}\Delta^{\uparrow}(\mathbf{k}',\mathbf{q}) + V^{\uparrow\downarrow}(\mathbf{k},\mathbf{k}')G^{\downarrow}G^{\downarrow}\Delta^{\downarrow}(\mathbf{k}',\mathbf{q}) + V^{\uparrow 0}(\mathbf{k},\mathbf{k}')(G^{\downarrow}G^{\uparrow}+G^{\uparrow}G^{\downarrow})\Delta^{0}(\mathbf{k}',\mathbf{q})\right], \tag{30}$$

$$\Delta^{\downarrow}(\mathbf{k},\mathbf{q}) = -T\sum_n\sum_{\mathbf{k}'}\left[V^{\downarrow\uparrow}(\mathbf{k},\mathbf{k}')G^{\uparrow}G^{\uparrow}\Delta^{\uparrow}(\mathbf{k}',\mathbf{q}) + V^{\downarrow\downarrow}(\mathbf{k},\mathbf{k}')G^{\downarrow}G^{\downarrow}\Delta^{\downarrow}(\mathbf{k}',\mathbf{q}) + V^{\downarrow 0}(\mathbf{k},\mathbf{k}')(G^{\downarrow}G^{\uparrow}+G^{\uparrow}G^{\downarrow})\Delta^{0}(\mathbf{k}',\mathbf{q})\right], \tag{31}$$

$$\Delta^{0}(\mathbf{k},\mathbf{q}) = -T\sum_n\sum_{\mathbf{k}'}\left[V^{0\uparrow}(\mathbf{k},\mathbf{k}')G^{\uparrow}G^{\uparrow}\Delta^{\uparrow}(\mathbf{k}',\mathbf{q}) + V^{0\downarrow}(\mathbf{k},\mathbf{k}')G^{\downarrow}G^{\downarrow}\Delta^{\downarrow}(\mathbf{k}',\mathbf{q}) + V^{00}(\mathbf{k},\mathbf{k}')(G^{\downarrow}G^{\uparrow}+G^{\uparrow}G^{\downarrow})\Delta^{0}(\mathbf{k}',\mathbf{q})\right], \tag{32}$$

where the arguments in the Green's function products are the same as in matrix equation (26). For instance,

$$G^{\uparrow}G^{\uparrow} = G^{\uparrow}(\mathbf{k}',\omega_n)\,G^{\uparrow}(-\mathbf{k}'+\mathbf{q},-\omega_n)\,.$$

The pairing amplitudes found from Eqn (25) are

$$V^{\uparrow\uparrow}(\mathbf{k},\mathbf{k}') = V_{xx}+V_{yy}+\mathrm{i}V_{xy}-\mathrm{i}V_{yx} = -\mu_{\mathrm{B}}^2 I^2\chi^{\mathrm{u}}_{zz}\,, \tag{33}$$

$$V^{\downarrow\downarrow}(\mathbf{k},\mathbf{k}') = V_{xx}+V_{yy}-\mathrm{i}V_{xy}+\mathrm{i}V_{yx} = -\mu_{\mathrm{B}}^2 I^2\chi^{\mathrm{u}}_{zz}\,, \tag{34}$$

$$V^{\uparrow\downarrow}(\mathbf{k},\mathbf{k}') = -V_{xx}+V_{yy}+\mathrm{i}V_{xy}+\mathrm{i}V_{yx} = -\mu_{\mathrm{B}}^2 I^2(\chi^{\mathrm{u}}_{xx}-\chi^{\mathrm{u}}_{yy}-2\mathrm{i}\chi^{\mathrm{u}}_{xy})\,, \tag{35}$$

$$V^{\downarrow\uparrow}(\mathbf{k},\mathbf{k}') = -V_{xx}+V_{yy}-\mathrm{i}V_{xy}-\mathrm{i}V_{yx} = -\mu_{\mathrm{B}}^2 I^2(\chi^{\mathrm{u}}_{xx}-\chi^{\mathrm{u}}_{yy}+2\mathrm{i}\chi^{\mathrm{u}}_{xy})\,, \tag{36}$$

$$V^{00}(\mathbf{k},\mathbf{k}') = V_{zz} = -\frac{\mu_{\mathrm{B}}^2 I^2(\chi^{\mathrm{u}}_{xx}+\chi^{\mathrm{u}}_{yy}-\chi^{\mathrm{u}}_{zz})}{2}\,, \tag{37}$$

$$V^{\uparrow 0}(\mathbf{k},\mathbf{k}') = \left(V^{0\uparrow}(\mathbf{k},\mathbf{k}')\right)^{*} = -V_{xz}+\mathrm{i}V_{yz} = -\mu_{\mathrm{B}}^2 I^2(\chi^{\mathrm{u}}_{xz}-\mathrm{i}\chi^{\mathrm{u}}_{yz})\,, \tag{38}$$

$$V^{\downarrow 0}(\mathbf{k},\mathbf{k}') = \left(V^{0\downarrow}(\mathbf{k},\mathbf{k}')\right)^{*} = V_{xz}+\mathrm{i}V_{yz} = -\mu_{\mathrm{B}}^2 I^2(-\chi^{\mathrm{u}}_{xz}-\mathrm{i}\chi^{\mathrm{u}}_{yz})\,. \tag{39}$$

We see that the equations for $\Delta^{\uparrow}$, $\Delta^{\downarrow}$, and Δ^{0} are entangled. Moreover, the entanglement still exists in the case of a strong spin-up and spin-down band splitting, which allows us to omit all the terms that involve the combinations $G^{\downarrow}G^{\uparrow}+G^{\uparrow}G^{\downarrow}$ corresponding to interband pairing.[2] Ignoring the inter-band pairing, we find

$$\Delta^{\uparrow}(\mathbf{k},\mathbf{q}) = -T\sum_n\sum_{\mathbf{k}'}\left[V^{\uparrow\uparrow}(\mathbf{k},\mathbf{k}')G^{\uparrow}G^{\uparrow}\Delta^{\uparrow}(\mathbf{k}',\mathbf{q}) + V^{\uparrow\downarrow}(\mathbf{k},\mathbf{k}')G^{\downarrow}G^{\downarrow}\Delta^{\downarrow}(\mathbf{k}',\mathbf{q})\right], \tag{40}$$

$$\Delta^{\downarrow}(\mathbf{k},\mathbf{q}) = -T\sum_n\sum_{\mathbf{k}'}\left[V^{\downarrow\uparrow}(\mathbf{k},\mathbf{k}')G^{\uparrow}G^{\uparrow}\Delta^{\uparrow}(\mathbf{k}',\mathbf{q}) + V^{\downarrow\downarrow}(\mathbf{k},\mathbf{k}')G^{\downarrow}G^{\downarrow}\Delta^{\downarrow}(\mathbf{k}',\mathbf{q})\right], \tag{41}$$

$$\Delta^{0}(\mathbf{k},\mathbf{q}) = -T\sum_n\sum_{\mathbf{k}'}\left[V^{0\uparrow}(\mathbf{k},\mathbf{k}')G^{\uparrow}G^{\uparrow}\Delta^{\uparrow}(\mathbf{k}',\mathbf{q}) + V^{0\downarrow}(\mathbf{k},\mathbf{k}')G^{\downarrow}G^{\downarrow}\Delta^{\downarrow}(\mathbf{k}',\mathbf{q})\right]. \tag{42}$$

We see that Eqn (42) for the order parameter component Δ^{0} corresponding to the pairing of particles with opposite spins is still present. According to Eqn (42), the pairing with opposite spins is induced by the pairing terms with parallel spins. *Hence, in general, a superconducting state in a ferromagnetic metal is not an equal-spin-pairing state*. This property originates from the spin–orbit coupling. Indeed, we see in what follows that the pairing amplitudes $V^{0\uparrow}$ and $V^{0\downarrow}$ arise due to the spin–orbit terms in the ferromagnet gradient energy, which are presumably small. Therefore, with good accuracy, we can work with Eqns (40) and (41) corresponding to equal-spin-pairing superconductivity, ignoring the amplitude Δ^{0} induced by the pairing of electrons with up–up and down–down spins. In this case, we are dealing with a two-band superconducting state similar to the A_2 state of superfluid ^{3}He [39]. This property is supported by recent low-temperature thermal conductivity measurements in a magnetic field [40].

Both the up–up spin ($V^{\uparrow\uparrow}$) and the down–down spin ($V^{\downarrow\downarrow}$) pairing amplitudes are determined by the susceptibility component parallel to the direction of the spontaneous magnetization χ^{u}_{zz}, which greatly exceeds the susceptibility

[2] The case of UCoGe at a pressure of about 1.1 GPa when the Curie temperature is almost equal to the temperature of the superconducting transition requires a special treatment.

along the other crystallographic directions. On the other hand, the spin-up and the spin-down Cooper pairs interact with each other due to the susceptibility anisotropy $\chi_{xx} \neq \chi_{yy}$, which gives rise to a phase transition to an A_2-type state common to the spin-up and the spin-down bands. The susceptibility anisotropy does not exist in the exchange approximation and is completely determined by the spin–orbit coupling. Even in isotropic liquid ^{3}He, the spin–orbit coupling leads to entanglement between the spin-up and spin-down order parameters [41]. However, in view of the smallness of spin–orbit interaction, the entanglement between the spin-up and spin-down components is practically absent, which results in two subsequent phase transitions in a magnetic field: first to the spin-up A_1 state and then to the mixed spin-up and spin-down A_2 superfluid state [39].

We next find the susceptibility.

3.2 Magnetic susceptibility of an orthorhombic ferromagnet

We seek the static magnetic susceptibility following the phenomenological approach in the Landau theory of phase transitions. The free energy of an orthorhombic ferromagnet in a magnetic field $\mathbf{H}(\mathbf{r})$ is

$$\mathcal{F} = \int \mathrm{d}V (F_M + F_\nabla)\,, \tag{43}$$

where we take the orthorhombic anisotropy into account in expressions for the condensation energy density

$$F_M = \alpha_z M_z^2 + \alpha_y M_y^2 + \alpha_x M_x^2 + \beta_z M_z^4 + \beta_{xy} M_x^2 M_y^2 + \beta_{yz} M_z^2 M_y^2 + \beta_{xz} M_z^2 M_x^2 - \mathbf{MH} \tag{44}$$

and the gradient energy density

$$F_\nabla = \gamma_{ij}^{\alpha\beta} \frac{\partial M_\alpha}{\partial x_i} \frac{\partial M_\beta}{\partial x_j} \tag{45}$$

The z direction is always chosen along the spontaneous magnetization; hence, the x, y, z coordinates are respectively directed along the a, b, c crystallographic axes in URhGe and UCoGe, and along the b, c, a axes in UGe_2,

$$\alpha_z = \alpha_{z0}(T - T_\mathrm{C})\,, \quad \alpha_x > 0\,, \quad \alpha_y > 0\,, \tag{46}$$

where T_C is the Curie temperature and

$$\gamma_{ij}^{\alpha=\beta} = \begin{pmatrix} \gamma_{xx}^{\alpha} & 0 & 0 \\ 0 & \gamma_{yy}^{\alpha} & 0 \\ 0 & 0 & \gamma_{zz}^{\alpha} \end{pmatrix}, \qquad \alpha = x, y, z\,, \tag{47}$$

$$\gamma_{ij}^{\alpha\neq\beta} = \gamma_{ij}^{ij} = \begin{pmatrix} 0 & \gamma_{xy} & \gamma_{xz} \\ \gamma_{xy} & 0 & \gamma_{yz} \\ \gamma_{xz} & \gamma_{yz} & 0 \end{pmatrix}. \tag{48}$$

The corresponding energy density in the exchange approximation is

$$F_M^{\text{exchange}} + F_\nabla^{\text{exchange}} = \alpha \mathbf{M}^2 + \beta \mathbf{M}^4 - \mathbf{MH} + \gamma_{ij} \frac{\partial \mathbf{M}}{\partial x_i} \frac{\partial \mathbf{M}}{\partial x_j}\,, \tag{49}$$

where

$$\gamma_{ij} = \begin{pmatrix} \gamma_{xx} & 0 & 0 \\ 0 & \gamma_{yy} & 0 \\ 0 & 0 & \gamma_{zz} \end{pmatrix}, \tag{50}$$

and hence the gradient energy is determined only by three constants instead of the 12 constants that occur when taking small relativistic interactions into account.

We take the magnetic field as the sum of a constant field in the direction of spontaneous magnetization and the coordinate-dependent small addition

$$\mathbf{H}(\mathbf{r}) = \delta H_x(\mathbf{r})\hat{\mathbf{x}} + \delta H_y(\mathbf{r})\hat{\mathbf{y}} + \big(H_z + \delta H_z(\mathbf{r})\big)\hat{\mathbf{z}}\,. \tag{51}$$

By varying functional (43) with respect to the magnetization components, we arrive at the equations

$$\begin{aligned}
&2\alpha_x M_x + 2\beta_{xy} M_y^2 M_x + 2\beta_{xz} M_z^2 M_x \\
&\qquad - 2\gamma_{ij}^x \frac{\partial^2 M_x}{\partial x_i\, \partial x_j} - \gamma_{xy} \frac{\partial^2 M_y}{\partial x\, \partial y} - \gamma_{xz} \frac{\partial^2 M_z}{\partial x\, \partial z} = \delta H_x\,, \\
&2\alpha_y M_y + 2\beta_{xy} M_x^2 M_y + 2\beta_{yz} M_z^2 M_y \\
&\qquad - 2\gamma_{ij}^y \frac{\partial^2 M_y}{\partial x_i\, \partial x_j} - \gamma_{xy} \frac{\partial^2 M_x}{\partial x\, \partial y} - \gamma_{yz} \frac{\partial^2 M_z}{\partial y\, \partial z} = \delta H_y\,, \\
&2\alpha_z M_z + 4\beta_z M_z^3 + 2\beta_{xz} M_x^2 M_z + 2\beta_{yz} M_y^2 M_z \\
&\qquad - 2\gamma_{ij}^z \frac{\partial^2 M_z}{\partial x_i\, \partial x_j} - \gamma_{xz} \frac{\partial^2 M_x}{\partial x\, \partial z} - \gamma_{yz} \frac{\partial^2 M_y}{\partial y\, \partial z} = H_z + \delta H_z\,.
\end{aligned} \tag{52}$$

The equilibrium magnetization projections are determined by the equations

$$M_x = 0\,, \qquad M_y = 0\,, \tag{53}$$

$$M_z^2 = -\frac{\alpha_z}{2\beta_z} + \frac{H_z}{4\beta_z M_z}\,. \tag{54}$$

The first and last terms in the right-hand side of (54) correspond to the spontaneous and the induced parts of magnetization along the z direction.

The total magnetization is the sum of the constant part and the small coordinate-dependent addition

$$\mathbf{M}(\mathbf{r}) = M_z\hat{\mathbf{z}} + \delta\mathbf{M}_x(\mathbf{r}) + \delta\mathbf{M}_y(\mathbf{r}) + \delta\mathbf{M}_z(\mathbf{r})\,, \tag{55}$$

whose Fourier components $\delta\mathbf{M}(\mathbf{k})$ satisfy linear equations derived from Eqns (52):

$$\begin{aligned}
&2(\alpha_x + \beta_{xz} M_z^2 + \gamma_{ij}^x k_i k_j)\delta M_x(\mathbf{k}) + \gamma_{xy} k_x k_y \delta M_y(\mathbf{k}) \\
&\qquad + \gamma_{xz} k_x k_z \delta M_z(\mathbf{k}) = \delta H_x(\mathbf{k})\,, \\
&\gamma_{xy} k_x k_y \delta M_x(\mathbf{k}) + 2(\alpha_y + \beta_{yz} M_z^2 + \gamma_{ij}^y k_i k_j)\delta M_y(\mathbf{k}) \\
&\qquad + \gamma_{yz} k_y k_z \delta M_z(\mathbf{k}) = \delta H_y(\mathbf{k})\,, \\
&\gamma_{xz} k_x k_z \delta M_x(\mathbf{k}) + \gamma_{yz} k_y k_z \delta M_y(\mathbf{k}) \\
&\qquad + 2(\alpha_z + 6\beta_z M_z^2 + \gamma_{ij}^z k_i k_j)\delta M_z(\mathbf{k}) = \delta H_x(\mathbf{k})\,.
\end{aligned} \tag{56}$$

The coupling between the magnetization components in Eqns (56) is due to the small terms in the gradient energy originating from the relativistic interactions. Disregarding all the products of terms such as $\gamma_{xy} k_x k_y \gamma_{yz} k_y k_z$, we obtain a solution of this system of equations in the form

$$\chi_{xx} = \frac{\delta M_x}{\delta H_x} \approx \frac{1}{2(\alpha_x + \beta_{xz} M_z^2 + \gamma_{ij}^x k_i k_j)}\,, \tag{57}$$

$$\chi_{yy} = \frac{\delta M_y}{\delta H_y} \approx \frac{1}{2(\alpha_y + \beta_{yz} M_z^2 + \gamma_{ij}^y k_i k_j)}\,, \tag{58}$$

$$\chi_{zz} = \frac{\delta M_z}{\delta H_z} \approx \frac{1}{2(\alpha_z + 6\beta_z M_z^2 + \gamma_{ij}^z k_i k_j)}\,, \tag{59}$$

$$\chi_{xy}=\frac{\delta M_x}{\delta H_y}=\frac{\delta M_y}{\delta H_x}$$
$$\approx -\frac{\gamma_{xy}k_xk_y}{4(\alpha_x+\beta_{xz}M_z^2+\gamma_{ij}^x k_i k_j)(\alpha_y+\beta_{yz}M_z^2+\gamma_{ij}^y k_i k_j)}\,, \quad (60)$$

$$\chi_{xz}=\frac{\delta M_x}{\delta H_z}=\frac{\delta M_z}{\delta H_x}$$
$$\approx -\frac{\gamma_{xz}k_xk_z}{4(\alpha_x+\beta_{xz}M_z^2+\gamma_{ij}^x k_i k_j)(\alpha_z+6\beta_zM_z^2+\gamma_{ij}^z k_i k_j)}\,, \quad (61)$$

$$\chi_{yz}=\frac{\delta M_y}{\delta H_z}=\frac{\delta M_z}{\delta H_y}$$
$$\approx -\frac{\gamma_{yz}k_yk_z}{4(\alpha_y+\beta_{yz}M_z^2+\gamma_{ij}^y k_i k_j)(\alpha_z+6\beta_zM_z^2+\gamma_{ij}^z k_i k_j)}\,. \quad (62)$$

The expressions for the susceptibility components depend on the wave vectors through combinations like γk^2. They are derived for wave vectors much smaller than the inverse interatomic distance a^{-1}. The corresponding wave-vector-dependent terms in the susceptibility components found from an appropriate microscopic model then contain combinations of trigonometric functions like $\gamma\sin^2 ka/a^2$. These combinations at small $\mathbf{k}$ reproduce our phenomenological expressions, and at $k\approx k_{\rm F}$ are of the order of γ/a^2, as are the phenomenological expressions. This means that our formulas for susceptibilities are still qualitatively valid at large wave vector transfers $k\approx k_{\rm F}$ determining Cooper pairing. The Fermi wave vectors $k_{\rm F}$ are different at different points of the Fermi surface; hence, $k_{\rm F}$ is a function of direction in the reciprocal space with orthorhombic symmetry.

The odd part of the z component of the susceptibility is found as

$$\chi_{zz}^{\rm u}(\mathbf{k},\mathbf{k}')=\frac{1}{2}\left[\chi_{zz}(\mathbf{k}-\mathbf{k}')-\chi_{zz}(\mathbf{k}+\mathbf{k}')\right]$$
$$=\frac{2\gamma_{ij}k_ik'_j}{\left(\alpha_z+6\beta_zM_z^2+\gamma_{ij}(k_ik_j+k'_ik'_j)\right)^2-(2\gamma_{ij}k_ik'_j)^2}\,. \quad (63)$$

According to Eqns (33) and (34), the pairing interaction is determined by this formula. The situation is similar to the case of the weak-coupling singlet pairing, where the zero-frequency limit of the phonon propagator plays the role of a potential for the phonon-mediated attraction among electrons. We are interested in the pairing interaction inside the ferromagnetic state where $\alpha_z+6\beta_zM_z^2>0$. At the Curie temperature, this combination is equal to zero and $\chi_{zz}^{\rm u}(\mathbf{k},\mathbf{k}')$ diverges at coincident arguments corresponding to Cooper pairing. This is an inevitable property of a model with static interaction.

To avoid this pairing interaction divergence, Fay and Appel [42], in their theory of *p*-wave superconductivity in an itinerant ferromagnet, introduced a cutoff depending on the distance from the ferromagnetic phase transition. As a result, the critical temperature of the phase transition to the superconducting state with a finite value in both the ferromagnetic and the paramagnetic state turned out to be equal to zero at the transition between them. This misleading property does not take place in a model taking the retardation effect in pairing interaction into account.

At a finite value of $\alpha_z+6\beta_zM_z^2$, we can keep only the angular dependence in the numerator of Eqn (63), ignoring the angular dependence of $k_{\rm F}$ and the orthorhombic-symmetry terms $\gamma_{ij}^z(k_ik_j+k'_ik'_j)\approx 2\gamma^z k_{\rm F}^2$ in the denominator, as well as all the higher angular harmonics determined by the last term in the denominator. Calculations without these simplifications are much more cumbersome but do not lead to qualitatively different results. Thus, we obtain

$$\chi_{zz}^{\rm u}(\mathbf{k},\mathbf{k}')\approx\frac{\gamma_{ij}^z k_{\rm F}^2}{a_z^2}\,\hat{k}_i\hat{k}'_j\,, \quad (64)$$

$$a_z=\alpha_z+6\beta_zM_z^2+2\gamma^z k_{\rm F}^2=2\beta_z(3M_z^2-M_{z0}^2)+2\gamma^z k_{\rm F}^2\,, \quad (65)$$

where M_z is the solution of Eqn (54) and $M_{z0}=M_z(H_z=0)=(-\alpha_z/2\beta_z)^{1/2}$. At arbitrary temperatures below the Curie temperature, we can use the known experimental values of the field-dependent magnetization $M_z(H_z)$ and its almost temperature-independent spontaneous part $M_{z0}=M_z(H_z=0)$.

In a similar manner, we find the odd part of the susceptibility x and y components:

$$\chi_{xx}^{\rm u}(\mathbf{k},\mathbf{k}')\approx\frac{\gamma_{ij}^x k_{\rm F}^2}{a_x^2}\,\hat{k}_i\hat{k}'_j\,,\quad \chi_{yy}^{\rm u}(\mathbf{k},\mathbf{k}')\approx\frac{\gamma_{ij}^y k_{\rm F}^2}{a_y^2}\,\hat{k}_i\hat{k}'_j\,, \quad (66)$$

where

$$a_x=\alpha_x+\beta_{xz}M_z^2+2\gamma^x k_{\rm F}^2\,,$$
$$a_y=\alpha_y+\beta_{yz}M_z^2+2\gamma^y k_{\rm F}^2\,. \quad (67)$$

All the off-diagonal susceptibility components are linear in the anisotropy terms determined by the spin–orbit coupling:

$$\chi_{xy}^{\rm u}(\mathbf{k},\mathbf{k}')\approx\frac{\gamma_{xy}k_{\rm F}^2}{4\tilde{a}_x\tilde{a}_y}(\hat{k}_x\hat{k}'_y+\hat{k}'_x\hat{k}_y)\,, \quad (68)$$

$$\chi_{xz}^{\rm u}(\mathbf{k},\mathbf{k}')\approx\frac{\gamma_{xz}k_{\rm F}^2}{4\tilde{a}_x\tilde{a}_z}(\hat{k}_x\hat{k}'_z+\hat{k}'_x\hat{k}_z)\,, \quad (69)$$

$$\chi_{yz}^{\rm u}(\mathbf{k},\mathbf{k}')\approx\frac{\gamma_{yz}k_{\rm F}^2}{4\tilde{a}_y\tilde{a}_z}(\hat{k}_y\hat{k}'_z+\hat{k}'_y\hat{k}_z)\,, \quad (70)$$

$$\tilde{a}_x=\alpha_x+\beta_{xz}M_z^2\,,\quad \tilde{a}_y=\alpha_y+\beta_{yz}M_z^2\,,$$
$$\tilde{a}_z=\alpha_z+6\beta_zM_z^2=4\beta_zM_z^2+\frac{H_z}{2M_z}\,. \quad (71)$$

Here, we completely disregard the fourth order terms in respect of the products of wave vector components. They have the same symmetry as Eqns (68)–(70), but seriously complicate the corresponding expressions.

3.3 Pairing amplitudes

Equations (33)–(39) express the pairing amplitudes through the susceptibility components in a ferromagnetic metal with arbitrary symmetry. Explicit formulas for the susceptibility components in an orthorhombic ferromagnet are found in Section 3.2. The structure of superconducting states in an orthorhombic crystal is determined by the angular dependence of pairing amplitudes:

$$V^{\uparrow\uparrow}(\mathbf{k},\mathbf{k}')=V^{\downarrow\downarrow}(\mathbf{k},\mathbf{k}')=-\mu_{\rm B}^2I^2\chi_{zz}^{\rm u}$$
$$=-\frac{\mu_{\rm B}^2I^2k_{\rm F}^2\gamma_{ij}^z\hat{k}_i\hat{k}'_j}{4\left[\beta_z(3M_z^2-M_{z0}^2)+\gamma^z k_{\rm F}^2\right]^2}=-V_{1ij}\hat{k}_i\hat{k}'_j\,, \quad (72)$$

$$V^{\uparrow\downarrow}(\mathbf{k},\mathbf{k}')=-V_{2ij}\hat{k}_i\hat{k}'_j+{\rm i}V_3(\hat{k}_x\hat{k}'_y+\hat{k}_y\hat{k}'_x)\,, \quad (73)$$

$$V^{\downarrow\uparrow}(\mathbf{k},\mathbf{k}')=\left(V^{\uparrow\downarrow}(\mathbf{k},\mathbf{k}')\right)^*\,, \quad (74)$$

$$V^{00}(\mathbf{k},\mathbf{k}') = -W_{1ij}\hat{k}_i\hat{k}'_j\,, \tag{75}$$

$$V^{\uparrow 0}(\mathbf{k},\mathbf{k}') = \bigl(V^{0\uparrow}(\mathbf{k},\mathbf{k}')\bigr)^* = -W_2(\hat{k}_x\hat{k}'_z + \hat{k}_z\hat{k}'_x) + \mathrm{i}W_3(\hat{k}_y\hat{k}'_z + \hat{k}_z\hat{k}'_y)\,, \tag{76}$$

$$V^{\downarrow 0}(\mathbf{k},\mathbf{k}') = \bigl(V^{0\downarrow}(\mathbf{k},\mathbf{k}')\bigr)^* = -\bigl(V^{\uparrow 0}(\mathbf{k},\mathbf{k}')\bigr)^*\,, \tag{77}$$

where the constants are

$$V_{1ij} = \mu_{\mathrm{B}}^2 I^2 k_{\mathrm{F}}^2 \frac{\gamma^z_{ij}}{a_z^2} = \frac{\mu_{\mathrm{B}}^2 I^2 k_{\mathrm{F}}^2 \gamma^z_{ij}}{4\bigl[\beta_z(3M_z^2 - M_{z0}^2) + \gamma^z k_{\mathrm{F}}^2\bigr]^2}\,, \tag{78}$$

$$V_{2ij} = \mu_{\mathrm{B}}^2 I^2 k_{\mathrm{F}}^2 \left(\frac{\gamma^x_{ij}}{a_x^2} - \frac{\gamma^y_{ij}}{a_y^2}\right), \qquad V_3 = \frac{\mu_{\mathrm{B}}^2 I^2 k_{\mathrm{F}}^2 \gamma_{xy}}{4\tilde{a}_x\tilde{a}_y}\,, \tag{79}$$

$$W_{1ij} = \frac{\mu_{\mathrm{B}}^2 I^2 k_{\mathrm{F}}^2}{2}\left(\frac{\gamma^x_{ij}}{a_x^2} + \frac{\gamma^y_{ij}}{a_y^2} - \frac{\gamma^z_{ij}}{a_z^2}\right), \qquad W_2 = \frac{\mu_{\mathrm{B}}^2 I^2 k_{\mathrm{F}}^2 \gamma_{xz}}{4\tilde{a}_x\tilde{a}_z}\,, \qquad W_3 = \frac{\mu_{\mathrm{B}}^2 I^2 k_{\mathrm{F}}^2 \gamma_{yz}}{4\tilde{a}_y\tilde{a}_z}\,. \tag{80}$$

The pairing interaction between the particles in the same spin-up or spin-down band plays the most important role. The corresponding amplitude originates from the odd part of the magnetic susceptibility component χ^{u}_{zz}, which depends on the temperature and the magnetic field. The amplitudes V_{1ij} and W_{1ij} are mainly determined by the exchange interaction. The amplitude V_{2ij} is equal to zero in the exchange approximation, but it can have a nonnegligible magnitude corresponding to a strong orthorhombic anisotropy of the susceptibility, $\chi_{xx} \neq \chi_{yy}$. The amplitudes V_3, W_2, and W_3 are determined by the spin–orbit terms in the gradient energy of an orthorhombic ferromagnet, and we treat them as the smallest among the amplitudes.

3.4 Critical temperature of the phase transition to a paramagnetic superconducting state in UCoGe

Equations (30)–(32) are also applicable to finding the critical temperature of the phase transition from the normal to the paramagnetic superconducting state observed in UCoGe at high pressures (Fig. 1c). In this case, the internal magnetic field is absent; hence, the normal-state Green's functions for the spin-up and spin-down electrons are equal, $G^{\uparrow} = G^{\downarrow} = G$, and the order parameter is spatially homogeneous. The equations then take the form

$$\Delta^{\uparrow}(\mathbf{k}) = -T\sum_n \sum_{\mathbf{k}'}\bigl[V^{\uparrow\uparrow}(\mathbf{k},\mathbf{k}')\Delta^{\uparrow}(\mathbf{k}') + V^{\uparrow\downarrow}(\mathbf{k},\mathbf{k}')\Delta^{\downarrow}(\mathbf{k}') + 2V^{\uparrow 0}(\mathbf{k},\mathbf{k}')\Delta^{0}(\mathbf{k}')\bigr]G(\mathbf{k}',\omega_n)G(-\mathbf{k}',-\omega_n)\,, \tag{81}$$

$$\Delta^{\downarrow}(\mathbf{k}) = -T\sum_n \sum_{\mathbf{k}'}\bigl[V^{\downarrow\uparrow}(\mathbf{k},\mathbf{k}')\Delta^{\uparrow}(\mathbf{k}') + V^{\downarrow\downarrow}(\mathbf{k},\mathbf{k}')\Delta^{\downarrow}(\mathbf{k}') + 2V^{\downarrow 0}(\mathbf{k},\mathbf{k}')\Delta^{0}(\mathbf{k}')\bigr]G(\mathbf{k}',\omega_n)G(-\mathbf{k}',-\omega_n)\,, \tag{82}$$

$$\Delta^{0}(\mathbf{k}) = -T\sum_n \sum_{\mathbf{k}'}\bigl[2V^{0\uparrow}(\mathbf{k},\mathbf{k}')\Delta^{\uparrow}(\mathbf{k}') + V^{0\downarrow}(\mathbf{k},\mathbf{k}')\Delta^{\downarrow}(\mathbf{k}') + V^{00}(\mathbf{k},\mathbf{k}')\Delta^{0}(\mathbf{k}')\bigr]G(\mathbf{k}',\omega_n)G(-\mathbf{k}',-\omega_n)\,. \tag{83}$$

Substituting the paramagnetic-state order parameter components (see Section 2.2)

$$\Delta^{\uparrow} = -\hat{k}_x\eta_x + \mathrm{i}\hat{k}_y\eta_y\,, \quad \Delta^{\downarrow} = \hat{k}_x\eta_x + \mathrm{i}\hat{k}_y\eta_y\,, \quad \Delta^{0} = \hat{k}_z\eta_z\hat{z} \tag{84}$$

in these equations gives five equations for the three amplitudes η_x, η_y, and η_z. Two of these equations coincide with two others, and we are left with the system of three independent equations

$$\begin{aligned}
&(\lambda^{-1} - g_{1x} + g_{2x})\eta_x + g_{3y}\eta_y + 2w_{2z}\eta_z = 0\,,\\
&g_{3x}\eta_x + (\lambda^{-1} - g_{1y} - g_{2y})\eta_y + 2w_{3z}\eta_z = 0\,,\\
&2w_{2x}\eta_x + 2w_{3y}\eta_y + (\lambda^{-1} - w_{1z})\eta_z = 0\,.
\end{aligned} \tag{85}$$

The pairing coupling constants are

$$\begin{aligned}
&g_{1x} = V_{1xx}\bigl\langle\hat{k}_x^2 N_0(\mathbf{k})\bigr\rangle\,, \qquad g_{2x} = V_{2xx}\bigl\langle\hat{k}_x^2 N_0(\mathbf{k})\bigr\rangle\,,\\
&g_{1y} = V_{1yy}\bigl\langle\hat{k}_y^2 N_0(\mathbf{k})\bigr\rangle\,, \qquad g_{2y} = V_{2yy}\bigl\langle\hat{k}_y^2 N_0(\mathbf{k})\bigr\rangle\,,\\
&w_{1z} = W_{1zz}\bigl\langle\hat{k}_z^2 N_0(\mathbf{k})\bigr\rangle\,, \qquad g_{3x} = V_3\bigl\langle\hat{k}_x^2 N_0(\mathbf{k})\bigr\rangle\,,\\
&g_{3y} = V_3\bigl\langle\hat{k}_y^2 N_0(\mathbf{k})\bigr\rangle\,, \qquad w_{2x} = W_2\bigl\langle\hat{k}_x^2 N_0(\mathbf{k})\bigr\rangle\,,\\
&w_{2z} = W_2\bigl\langle\hat{k}_z^2 N_0(\mathbf{k})\bigr\rangle\,, \qquad w_{3z} = W_3\bigl\langle\hat{k}_z^2 N_0(\mathbf{k})\bigr\rangle\,,\\
&w_{3y} = W_3\bigl\langle\hat{k}_y^2 N_0(\mathbf{k})\bigr\rangle\,.
\end{aligned}$$

The angular brackets denote averaging over the Fermi surface and $N_0(\mathbf{k})$ is the angular-dependent density of electronic states on the Fermi surface. We have

$$\lambda(T) = 2\pi T\sum_{n\geqslant 0}\frac{1}{\omega_n} = \ln\frac{\varepsilon}{T}\,,$$

where $\varepsilon = 2\gamma\varepsilon_0/\pi$, $\ln\gamma = 0.577$ is the Euler constant, and ε_0 is the cutoff energy for the pairing interaction. The critical temperature of the phase transition

$$T_{\mathrm{SC}} = \varepsilon\exp\left(-\frac{1}{g}\right) \tag{86}$$

is expressed in terms of the maximal eigenvalue of the matrix corresponding to system of linear equations (85).

3.5 Phase transition from the paramagnetic to ferromagnetic superconducting state in UCoGe

Equations (81)–(83) can also be used to determine the critical temperature of the phase transition that must separate the paramagnetic superconducting and ferromagnetic superconducting states in UCoGe (Fig. 1c), but which has not been discovered experimentally. The Green's function of the paramagnetic superconducting state must be used here:

$$G(\mathbf{k},\omega_n) = -\frac{\mathrm{i}\omega_n + \xi_{\mathbf{k}}}{\omega_n^2 + \xi_{\mathbf{k}}^2 + \eta_x^2\hat{k}_x^2 + \eta_y^2\hat{k}_y^2 + \eta_z^2\hat{k}_z^2}\,. \tag{87}$$

Substituting the ferromagnetic-state order parameter components (see Section 2.2)

$$\Delta^{\uparrow} = -\hat{k}_x\eta_x^{\uparrow} + \mathrm{i}\hat{k}_y\eta_y^{\uparrow}\,, \quad \Delta^{\downarrow} = \hat{k}_x\eta_x^{\downarrow} + \mathrm{i}\hat{k}_y\eta_y^{\downarrow}\,, \quad \Delta^{0} = \hat{k}_z\eta_z^{0}\hat{z} \tag{88}$$

in Eqns (81)–(83) gives five equations for the five amplitudes $\eta_x^{\uparrow}$, $\eta_y^{\uparrow}$, $\eta_x^{\downarrow}$, $\eta_y^{\downarrow}$, and η_z^0. The maximum eigenvalue of this system determines the critical temperature of the phase transition from the paramagnetic to the ferromagnetic superconducting state.

This phase transition occurs in the itinerant electron subsystem. Mathematically, it is described by a smooth development of an inequality in the spin-up and spin-down amplitudes of the order parameter, that is, by the development of a spontaneous magnetic moment of a purely super-

conducting nature. Simultaneously, magnetization related to the subsystem of localized moments appears. Its emergence, induced by the superconducting electron magnetic moment, is similar to the crossover between paramagnetic and ferromagnetic normal states in an external magnetic field. It can be expected that due to the smallness of the magnetization, the superconductor remains in the Meissner state below the transition line.

There is another possible scenario of the phase transition from the paramagnetic to ferromagnetic superconducting state. It is realized when the transition driving force is the ordering in the subsystem of localized moments. In this case, the subsystem of superconducting electrons is rearranged under the action of spontaneous magnetization.

The theory of the phase transition from the paramagnetic to the ferromagnetic superconducting state must include the effect of the emergence of supercurrents and the field dependence of the magnetization, which can be important in view of the divergence of the magnetic susceptibility near the Curie temperature. A satisfactory treatment of this phenomenon is currently absent.[3]

3.6 Superconducting states in orthorhombic ferromagnets

We now find what kind of superconducting state emerges at the phase transition from a normal ferromagnetic to the superconducting ferromagnetic state. Performing the Taylor expansion of Eqns (30)–(32) in powers of $\mathbf{q}$ up to the second order and then passing to the coordinate representation by the substitution

$$\mathbf{q} \to \mathbf{D} = -\mathrm{i}\nabla_{\mathbf{r}} + 2e\mathbf{A}(\mathbf{r})\,, \tag{89}$$

we obtain the equations

$$\begin{aligned}
\Delta^{\uparrow}(\mathbf{k},\mathbf{r}) &= T\sum_n \int \frac{\mathrm{d}^3\mathbf{k}'}{(2\pi)^3}\, V_{1ij}\hat{k}_i\hat{k}'_j \\
&\times \left(G^{\uparrow}G^{\uparrow} + \frac{1}{2}\,G^{\uparrow}\,\frac{\partial^2 G^{\uparrow}}{\partial k'_l\,\partial k'_m}\,D_l D_m\right)\Delta^{\uparrow}(\mathbf{k}',\mathbf{r}) \\
&+ T\sum_n \int \frac{\mathrm{d}^3\mathbf{k}'}{(2\pi)^3}\left[V_{2ij}\hat{k}_i\hat{k}'_j - \mathrm{i}V_3(\hat{k}_x\hat{k}'_y + \hat{k}'_x\hat{k}_y)\right] \\
&\times \left(G^{\downarrow}G^{\downarrow} + \frac{1}{2}\,G^{\downarrow}\,\frac{\partial^2 G^{\downarrow}}{\partial k'_l\,\partial k'_m}\,D_l D_m\right)\Delta^{\downarrow}(\mathbf{k}',\mathbf{r}) \\
&+ T\sum_n \int \frac{\mathrm{d}^3\mathbf{k}'}{(2\pi)^3}\left[W_2(\hat{k}_x\hat{k}'_z + \hat{k}_z\hat{k}'_x) - \mathrm{i}W_3(\hat{k}_y\hat{k}'_z + \hat{k}_z\hat{k}'_y)\right] \\
&\times \left(G^{\uparrow}G^{\downarrow} + \frac{1}{2}\,G^{\uparrow}\,\frac{\partial^2 G^{\downarrow}}{\partial k'_l\,\partial k'_m}\,D_l D_m + G^{\downarrow}G^{\uparrow}\right. \\
&\left. + \frac{1}{2}\,G^{\downarrow}\,\frac{\partial^2 G^{\uparrow}}{\partial k'_l\,\partial k'_m}\,D_l D_m\right)\Delta^{0}(\mathbf{k}',\mathbf{r})\,,
\end{aligned} \tag{90}$$

$$\begin{aligned}
\Delta^{\downarrow}(\mathbf{k},\mathbf{r}) &= T\sum_n \int \frac{\mathrm{d}^3\mathbf{k}'}{(2\pi)^3}\left[V_{2ij}\hat{k}_i\hat{k}'_j + \mathrm{i}V_3(\hat{k}_x\hat{k}'_y + \hat{k}'_x\hat{k}_y)\right] \\
&\times \left(G^{\uparrow}G^{\uparrow} + \frac{1}{2}\,G^{\uparrow}\,\frac{\partial^2 G^{\uparrow}}{\partial k'_l\,\partial k'_m}\,D_l D_m\right)\Delta^{\uparrow}(\mathbf{k}',\mathbf{r}) \\
&+ T\sum_n \int \frac{\mathrm{d}^3\mathbf{k}'}{(2\pi)^3}\, V_{1ij}\hat{k}_i\hat{k}'_j \\
&\times \left(G^{\downarrow}G^{\downarrow} + \frac{1}{2}\,G^{\downarrow}\,\frac{\partial^2 G^{\downarrow}}{\partial k'_l\,\partial k'_m}\,D_l D_m\right)\Delta^{\downarrow}(\mathbf{k}',\mathbf{r}) \\
&+ T\sum_n \int \frac{\mathrm{d}^3\mathbf{k}'}{(2\pi)^3}\left[-W_2(\hat{k}_x\hat{k}'_z + \hat{k}_z\hat{k}'_x) - \mathrm{i}W_3(\hat{k}_y\hat{k}'_z + \hat{k}_z\hat{k}'_y)\right] \\
&\times \left(G^{\uparrow}G^{\downarrow} + \frac{1}{2}\,G^{\uparrow}\,\frac{\partial^2 G^{\downarrow}}{\partial k'_l\,\partial k'_m}\,D_l D_m + G^{\downarrow}G^{\uparrow}\right. \\
&\left. + \frac{1}{2}\,G^{\downarrow}\,\frac{\partial^2 G^{\uparrow}}{\partial k'_l\,\partial k'_m}\,D_l D_m\right)\Delta^{0}(\mathbf{k}',\mathbf{r})\,,
\end{aligned} \tag{91}$$

$$\begin{aligned}
\Delta^{0}(\mathbf{k}',\mathbf{r}) &= T\sum_n \int \frac{\mathrm{d}^3\mathbf{k}'}{(2\pi)^3}\left[W_2(\hat{k}_x\hat{k}'_z + \hat{k}_z\hat{k}'_x) + \mathrm{i}W_3(\hat{k}_y\hat{k}'_z + \hat{k}_z\hat{k}'_y)\right] \\
&\times \left(G^{\uparrow}G^{\uparrow} + \frac{1}{2}\,G^{\uparrow}\,\frac{\partial^2 G^{\uparrow}}{\partial k'_l\,\partial k'_m}\,D_l D_m\right)\Delta^{\uparrow}(\mathbf{k}',\mathbf{r}) \\
&+ T\sum_n \int \frac{\mathrm{d}^3\mathbf{k}'}{(2\pi)^3}\left[-W_2(\hat{k}_x\hat{k}'_z + \hat{k}_z\hat{k}'_x) + \mathrm{i}W_3(\hat{k}_y\hat{k}'_z + \hat{k}_z\hat{k}'_y)\right] \\
&\times \left(G^{\downarrow}G^{\downarrow} + \frac{1}{2}\,G^{\downarrow}\,\frac{\partial^2 G^{\downarrow}}{\partial k'_l\,\partial k'_m}\,D_l D_m\right)\Delta^{\downarrow}(\mathbf{k}',\mathbf{r}) \\
&+ T\sum_n \int \frac{\mathrm{d}^3\mathbf{k}'}{(2\pi)^3}\, W_{1ij}\hat{k}_i\hat{k}'_j\left(G^{\uparrow}G^{\downarrow} + \frac{1}{2}\,G^{\uparrow}\,\frac{\partial^2 G^{\downarrow}}{\partial k'_l\,\partial k'_m}\,D_l D_m\right. \\
&\left. + G^{\downarrow}G^{\uparrow} + \frac{1}{2}\,G^{\downarrow}\,\frac{\partial^2 G^{\uparrow}}{\partial k'_l\,\partial k'_m}\,D_l D_m\right)\Delta^{0}(\mathbf{k}',\mathbf{r})\,.
\end{aligned} \tag{92}$$

Here, as before, the arguments in the products of the Green's functions are

$$G^{\uparrow}G^{\uparrow} = G^{\uparrow}(\mathbf{k}',\omega_n)G^{\uparrow}(-\mathbf{k}',-\omega_n)\,,$$

$$G^{\uparrow}\,\frac{\partial^2 G^{\uparrow}}{\partial k'_l\,\partial k'_m} = G^{\uparrow}(\mathbf{k}',\omega_n)\,\frac{\partial^2 G^{\uparrow}(-\mathbf{k}',-\omega_n)}{\partial k'_l\,\partial k'_m}\,,\quad \ldots\,.$$

In a single-domain ferromagnet in the absence of an external field, $H = 0$, or in an external field directed along the spontaneous magnetization axis $\hat{\mathbf{z}}$, the order parameter components are independent of z, and the operators of so-called long derivatives are

$$D_x = -\mathrm{i}\,\frac{\partial}{\partial x}\,,\qquad D_y = -\mathrm{i}\,\frac{\partial}{\partial y} + \frac{2e}{c}(H + H_{\mathrm{int}})x\,. \tag{93}$$

Here, we introduce an internal electromagnetic field corresponding to the spontaneous magnetization $H_{\mathrm{int}} = 4\pi M$ and ignore the difference between the external field and the magnetic field induced inside the medium by the external field.

With the dependence of the pairing interaction in Eqns (90)–(92) on the wave vector taken into account, we can choose the superconducting order parameter as the linear combinations

$$\begin{aligned}
\Delta^{\uparrow}(\mathbf{k},\mathbf{r}) &= \hat{k}_x\eta^{\uparrow}_x(\mathbf{r}) + \mathrm{i}\hat{k}_y\eta^{\uparrow}_y(\mathbf{r}) + \hat{k}_z\zeta^{\uparrow}_z(\mathbf{r})\,, \\
\Delta^{\downarrow}(\mathbf{k},\mathbf{r}) &= \hat{k}_x\eta^{\downarrow}_x(\mathbf{r}) + \mathrm{i}\hat{k}_y\eta^{\downarrow}_y(\mathbf{r}) + \hat{k}_z\zeta^{\downarrow}_z(\mathbf{r})\,, \\
\Delta^{0}(\mathbf{k},\mathbf{r}) &= \hat{k}_x\zeta^{0}_x(\mathbf{r}) + \mathrm{i}\hat{k}_y\zeta^{0}_y(\mathbf{r}) + \hat{k}_z\eta^{0}_z(\mathbf{r})\,.
\end{aligned}$$

Substituting these expressions in Eqns (90)–(92) leads to two independent systems of differential equations

$$\eta_{\alpha}(\mathbf{r}) = A_{\alpha\beta}\eta_{\beta}(\mathbf{r})\,,\qquad \zeta_{\alpha}(\mathbf{r}) = B_{\alpha\beta}\zeta_{\beta}(\mathbf{r})\,, \tag{94}$$

for the components of the vectors

$$\eta_{\alpha}(\mathbf{r}) = \left(\eta^{\uparrow}_x(\mathbf{r}), \eta^{\downarrow}_x(\mathbf{r}), \eta^{\uparrow}_y(\mathbf{r}), \eta^{\downarrow}_y(\mathbf{r}), \eta^{0}_z(\mathbf{r})\right), \tag{95}$$

$$\zeta_{\alpha}(\mathbf{r}) = \left(\zeta^{\uparrow}_z(\mathbf{r}), \zeta^{\downarrow}_z(\mathbf{r}), \zeta^{0}_x(\mathbf{r}), \zeta^{0}_y(\mathbf{r})\right), \tag{96}$$

[3] However, see Ref. [109], which appeared after this review was written.

which correspond to *two different superconducting states with different critical temperatures pertaining to corepresentations* A *and* B. Thereby, the *derived microscopic equations confirm the conclusions that were made in Section 2 based on pure symmetry considerations*.

3.7 Equal-spin-pairing states

We next simplify the problem and work with Eqns (40) and (41) that correspond to superconducting states of pairs of different-spin electrons. Then state A is described by the four-component order parameter

$$\Delta^{\uparrow}(\mathbf{k},\mathbf{r}) = \hat{k}_x\eta_x^{\uparrow}(\mathbf{r}) + \mathrm{i}\hat{k}_y\eta_y^{\uparrow}(\mathbf{r})\,, \tag{97}$$

$$\Delta^{\downarrow}(\mathbf{k},\mathbf{r}) = \hat{k}_x\eta_x^{\downarrow}(\mathbf{r}) + \mathrm{i}\hat{k}_y\eta_y^{\downarrow}(\mathbf{r})\,, \tag{98}$$

and state B by the two-component order parameter

$$\Delta^{\uparrow}(\mathbf{k},\mathbf{r}) = \hat{k}_z\zeta_z^{\uparrow}(\mathbf{r})\,, \tag{99}$$

$$\Delta^{\downarrow}(\mathbf{k},\mathbf{r}) = \hat{k}_z\zeta_z^{\downarrow}(\mathbf{r})\,. \tag{100}$$

Equations (94) for the critical temperatures of phase transitions to these states are determined by the 4×4 and 2×2 matrices

$$A_{\alpha\beta} = \begin{pmatrix} g_{1x}^{\uparrow}\lambda + L_{1x}^{\uparrow} & g_{2x}^{\downarrow}\lambda + L_{2x}^{\downarrow} + \mathrm{i}L_{3yx}^{\downarrow} & \mathrm{i}L_{1xy}^{\uparrow} & -g_{3y}^{\downarrow}\lambda + \mathrm{i}L_{2xy}^{\downarrow} - L_{3y}^{\downarrow} \\ g_{2x}^{\uparrow}\lambda + L_{2x}^{\uparrow} - \mathrm{i}L_{3yx}^{\uparrow} & g_{1x}^{\downarrow}\lambda + L_{1x}^{\downarrow} & g_{3y}^{\uparrow}\lambda + \mathrm{i}L_{2xy}^{\uparrow} + L_{3y}^{\uparrow} & \mathrm{i}L_{1xy}^{\downarrow} \\ -\mathrm{i}L_{1yx}^{\uparrow} & g_{3x}^{\downarrow}\lambda - \mathrm{i}L_{2yx}^{\downarrow} + L_{3x}^{\downarrow} & g_{1y}^{\uparrow}\lambda + L_{1y}^{\uparrow} & g_{2y}^{\downarrow}\lambda + L_{2y}^{\downarrow} + \mathrm{i}L_{3xy}^{\downarrow} \\ -g_{3x}^{\uparrow}\lambda - \mathrm{i}L_{2yx}^{\uparrow} - L_{3x}^{\uparrow} & -\mathrm{i}L_{1yx}^{\downarrow} & g_{2y}^{\uparrow}\lambda + L_{2y}^{\uparrow} - \mathrm{i}L_{3xy}^{\uparrow} & g_{1y}^{\downarrow}\lambda + L_{1y}^{\downarrow} \end{pmatrix}, \tag{101}$$

$$B_{\alpha\beta} = \begin{pmatrix} g_{1z}^{\uparrow}\lambda + L_{1z}^{\uparrow} & g_{2z}^{\downarrow}\lambda + L_{2z}^{\downarrow} \\ g_{2z}^{\uparrow}\lambda + L_{2z}^{\uparrow} & g_{1z}^{\downarrow}\lambda + L_{1z}^{\downarrow} \end{pmatrix}. \tag{102}$$

Here,

$$g_{1x}^{\uparrow} = V_{1xx}\langle\hat{k}_x^2 N_0^{\uparrow}(\mathbf{k})\rangle = \frac{\mu_{\mathrm{B}}^2 I^2 k_{\mathrm{F}}^2 \gamma_{xx}^z \langle\hat{k}_x^2 N_0^{\uparrow}(\mathbf{k})\rangle}{4\left[\beta_z(3M_z^2 - M_{z0}^2) + \gamma^z k_{\mathrm{F}}^2\right]^2} \tag{103}$$

is one of the pairing interaction constants, the angular brackets mean averaging over the Fermi surface, and $N_0^{\uparrow}(\mathbf{k})$ is the angular-dependent density of electronic states on the Fermi surface of the band $\uparrow$. Accordingly,

$$g_{2x}^{\downarrow} = V_{2xx}\langle\hat{k}_x^2 N_0^{\downarrow}(\mathbf{k})\rangle\,, \qquad g_{3x}^{\downarrow} = V_3\langle\hat{k}_x^2 N_0^{\downarrow}(\mathbf{k})\rangle\,. \tag{104}$$

All the other pairing interaction constants are obtained by the obvious substitutions $x\leftrightarrow y$ and $\uparrow\leftrightarrow\downarrow$ or $x\to z$. We have

$$\lambda(T) = 2\pi T\sum_{n\geqslant 0}\frac{1}{\omega_n} = \ln\frac{\varepsilon}{T}\,, \tag{105}$$

where $\varepsilon = 2\gamma\varepsilon_0/\pi$, $\ln\gamma = 0.577$ is the Euler constant, and ε_0 is the cutoff energy for the pairing interaction. We assume here that it has the same value for both bands.

The differential operator

$$L_{1x}^{\uparrow} = \frac{1}{2}\,V_{1xx}T\sum_n\int\frac{\mathrm{d}^3\mathbf{k}}{(2\pi)^3}\,\hat{k}_x^2 G^{\uparrow}(\mathbf{k},\omega_n)\mathcal{D}^{\uparrow} \tag{106}$$

and the operator $L_{2y}^{\downarrow}$ and other operators with the same structure are obtained by the obvious substitutions $x\to y, z$, $1\to 2$, and $\uparrow\to\downarrow$, but a similar operator with the index 3 is

$$L_{3x}^{\uparrow} = \frac{1}{2}\,V_3T\sum_n\int\frac{\mathrm{d}^3\mathbf{k}}{(2\pi)^3}\,\hat{k}_y^2 G^{\uparrow}(\mathbf{k},\omega_n)\mathcal{D}^{\uparrow}\,, \tag{107}$$

where

$$\mathcal{D}^{\uparrow} = \frac{\partial^2 G^{\uparrow}(-\mathbf{k},-\omega_n)}{\partial k_x^2}\,D_x^2 + \frac{\partial^2 G^{\uparrow}(-\mathbf{k},-\omega_n)}{\partial k_y^2}\,D_y^2\,. \tag{108}$$

Operators of the second type are

$$L_{1xy}^{\uparrow} = \frac{1}{2}\,V_{1xx}T\sum_n\int\frac{\mathrm{d}^3\mathbf{k}}{(2\pi)^3}\,\hat{k}_x\hat{k}_y G^{\uparrow}(\mathbf{k},\omega_n) \times\frac{\partial^2 G^{\uparrow}(-\mathbf{k},-\omega_n)}{\partial k_x\,\partial k_y}(D_xD_y + D_yD_x)\,, \tag{109}$$

and $L_{2yx}^{\uparrow}$ and other operators of this type are obtained by the obvious substitutions $x\to y$, $1\to 2$, and $\uparrow\to\downarrow$. A similar operator with the index 3 has the form

$$L_{3xy}^{\uparrow} = \frac{1}{2}\,V_3T\sum_n\int\frac{\mathrm{d}^3\mathbf{k}}{(2\pi)^3}\,\hat{k}_x\hat{k}_y G^{\uparrow}(\mathbf{k},\omega_n) \times\frac{\partial^2 G^{\uparrow}(-\mathbf{k},-\omega_n)}{\partial k_x\,\partial k_y}(D_xD_y + D_yD_x)\,. \tag{110}$$

3.8 Equal-spin-pairing states near the critical temperature

As noted in Section 2, the internal field acting on the electron charges in uranium ferromagnets is much weaker than the upper critical field at zero temperature. In this case, the gradient terms produce only small corrections of the order $O(H_{\mathrm{int}}/(H_{c2}(T=0)))$ to the eigenvalues of linear differential equations (94). Neglecting these, we arrive at the system of algebraic equations

$$\begin{aligned} \eta_x^{\uparrow} &= (g_{1x}^{\uparrow}\eta_x^{\uparrow} + g_{2x}^{\downarrow}\eta_x^{\downarrow} + g_{3y}^{\downarrow}\eta_y^{\downarrow})\lambda\,, \\ \eta_x^{\downarrow} &= (g_{2x}^{\uparrow}\eta_x^{\uparrow} + g_{1x}^{\downarrow}\eta_x^{\downarrow} - g_{3y}^{\uparrow}\eta_y^{\uparrow})\lambda\,, \\ \eta_y^{\uparrow} &= (g_{1y}^{\uparrow}\eta_y^{\uparrow} + g_{2y}^{\downarrow}\eta_y^{\downarrow} - g_{3x}^{\downarrow}\eta_x^{\downarrow})\lambda\,, \\ \eta_y^{\downarrow} &= (g_{2y}^{\uparrow}\eta_y^{\uparrow} + g_{1y}^{\downarrow}\eta_y^{\downarrow} + g_{3x}^{\uparrow}\eta_x^{\uparrow})\lambda\,, \end{aligned} \tag{111}$$

for the A state and

$$\begin{aligned} \zeta_z^{\uparrow} &= (g_{1z}^{\uparrow}\zeta_z^{\uparrow} + g_{2z}^{\downarrow}\zeta_z^{\downarrow})\lambda\,, \\ \zeta_z^{\downarrow} &= (g_{2z}^{\uparrow}\zeta_z^{\uparrow} + g_{1z}^{\downarrow}\zeta_z^{\downarrow})\lambda \end{aligned} \tag{112}$$

for the B state. Taking into account that the coupling constants with indices 1 and 2 significantly exceed the constants with index 3 originating from the spin–orbit terms in the gradient energy of a ferromagnet,

$$g_1, g_2 \gg g_3\,,$$

we obtain three independent systems of equations for the x, y, and z components of the order parameter:

$$\begin{aligned} \eta_x^{\uparrow} &= (g_{1x}^{\uparrow}\eta_x^{\uparrow} + g_{2x}^{\downarrow}\eta_x^{\downarrow})\lambda\,, \\ \eta_x^{\downarrow} &= (g_{2x}^{\uparrow}\eta_x^{\uparrow} + g_{1x}^{\downarrow}\eta_x^{\downarrow})\lambda\,, \end{aligned} \tag{113}$$

$$\begin{aligned} \eta_y^{\uparrow} &= (g_{1y}^{\uparrow}\eta_y^{\uparrow} + g_{2y}^{\downarrow}\eta_y^{\downarrow})\lambda\,, \\ \eta_y^{\downarrow} &= (g_{2y}^{\uparrow}\eta_y^{\uparrow} + g_{1y}^{\downarrow}\eta_y^{\downarrow})\lambda\,, \end{aligned} \tag{114}$$

$$\begin{aligned} \zeta_z^{\uparrow} &= (g_{1z}^{\uparrow}\zeta_z^{\uparrow} + g_{2z}^{\downarrow}\zeta_z^{\downarrow})\lambda\,, \\ \zeta_z^{\downarrow} &= (g_{2z}^{\uparrow}\zeta_z^{\uparrow} + g_{1z}^{\downarrow}\zeta_z^{\downarrow})\lambda\,. \end{aligned} \tag{115}$$

Thus, in the exchange approximation for the energy of magnetic inhomogeneity, we have three different superconducting states $(\hat{k}_x\eta_x^{\uparrow},\hat{k}_x\eta_x^{\downarrow})$, $(\hat{k}_y\eta_y^{\uparrow},\hat{k}_y\eta_y^{\downarrow})$, and $(\hat{k}_z\zeta_z^{\uparrow},\hat{k}_z\zeta_z^{\downarrow})$ with different critical temperatures determined by the vanishing of the determinants of Eqns (113)–(115).

4. Physical properties

4.1 Critical temperature

Assuming that the highest critical temperature corresponds to the $(\hat{k}_x\eta_x^{\uparrow},\hat{k}_x\eta_x^{\downarrow})$ superconducting state and equating the determinant of system (113) to zero, we obtain the BCS-type formula

$$T=\varepsilon\exp\left(-\frac{1}{g}\right), \tag{116}$$

where the coupling constant

$$g(T)=\frac{g_{1x}^{\uparrow}+g_{1x}^{\downarrow}}{2}+\sqrt{\frac{(g_{1x}^{\uparrow}-g_{1x}^{\downarrow})^2}{4}+g_{2x}^{\uparrow}g_{2x}^{\downarrow}} \tag{117}$$

is a function of temperature. Thereby, formula (116) is in fact an equation for the critical temperature of the transition to the superconducting state. We now discuss the simplest case of a single-band (say, spin-up) superconducting state with $g=g_{1x}^{\uparrow}$.

In URhGe, the transition to the superconducting state occurs at a temperature much lower than the Curie temperature. Hence, the temperature dependence of the coupling constant can be ignored. Then the critical temperature is determined by the relation

$$\ln\frac{\varepsilon}{T_{SC}}\approx\frac{1}{g_{1x}^{\uparrow}}\propto\frac{(\alpha_{0z}T_C+\gamma_z k_F^2)^2}{\mu_B^2 I^2\gamma_{xx}^z k_F^2\langle\hat{k}_x^2 N_0^{\uparrow}(\mathbf{k})\rangle}, \tag{118}$$

where we have used Eqns (54) and (103) for $g_{1x}^{\uparrow}$ in the absence of a magnetic field. The Curie temperature T_C in URhGe is an increasing function of pressure (Fig. 1b). The pressure dependence of all other quantities in the right-hand side of this equation is unknown. Assuming that the right-hand side as a whole also increases with pressure, we see that this should be accompanied by a slow decrease in the temperature of transition to the superconducting state. And, vice versa, when the right-hand side decreases with pressure, the temperature $T_{SC}(P)$ increases. The first case obviously corresponds to the observed pressure dependences $T_C(P)$ and $T_{SC}(P)$ in URhGe; the second corresponds to the situation in UCoGe (Fig. 1c). In the latter case, of course, this argument is only applicable in the region where T_{SC} is significantly smaller than T_C.

Here, we do not consider UGe_2, where the superconducting state arises in the phase diagram region below the line of the first-order phase transition from the paramagnetic to the ferromagnetic state.

4.2 Upper critical field parallel to the *c* axis in UCoGe

The upper critical field $H_{c2}(T)$ parallel to the spontaneous magnetization axis in UCoGe [43] exhibits a peculiar bent upward (Fig. 4). A natural explanation of this phenomenon is that the critical temperature itself is a function of the magnetic field. Indeed, near T_{SC}, the temperature dependence of the upper critical field is

$$H_{c2}=AT_{SC}(T_{SC}-T), \tag{119}$$

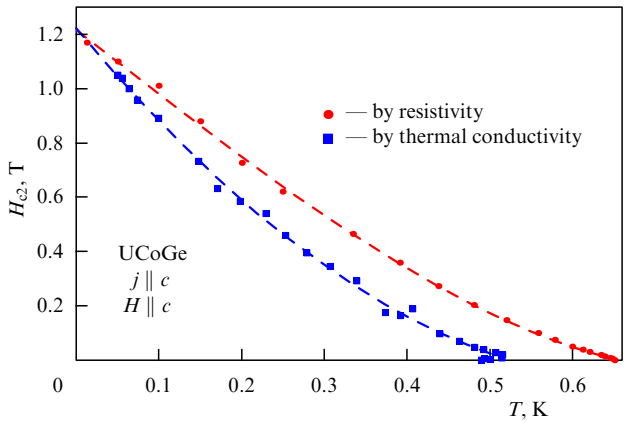

Figure 4. (Color online.) The upper critical field H_{c2} in UCoGe extracted from resistivity and thermal conductivity measurements. (M Taupin, unpublished (2016).)

where $A\approx\phi_0/v_F^2$ is a constant and the critical temperature of the $(\hat{k}_x\eta_x^{\uparrow},\hat{k}_x\eta_x^{\downarrow})$ state in the single-band approximation with $H\neq 0$ is given by

$$\ln\frac{\varepsilon}{T_{SC}}=\frac{1}{g_{1x}^{\uparrow}}\propto\left[\beta_z(3M_z^2-M_{z0}^2)+\gamma^z k_F^2\right]^2. \tag{120}$$

At temperatures well below the Curie temperature, the magnetization is almost temperature independent. On the other hand, the UCoGe magnetic moment in a field directed parallel to the c axis rapidly increases [44]. In fields of about 1 T, $M_z=M_z(H)$ is about twice as big as $M_{z0}=M_z(H=0)$. Hence, in accordance with (120), increasing the magnetic field leads to a decrease in the coupling constant $g_{1x}^{\uparrow}$ and the critical temperature $T_{SC}(g_{1x}^{\uparrow})$.

The temperature dependence of the upper critical field can be rewritten as a dependence of the transition temperature T_{SC}^{orb} on the magnetic field, determined by the orbital effect and by the field dependence of the pairing interaction $g_{1x}^{\uparrow}=g_{1x}^{\uparrow}(H)$:

$$T_{SC}^{orb}=T_{SC}(g_{1x}^{\uparrow})-\frac{H}{AT_{SC}(g_{1x}^{\uparrow})}. \tag{121}$$

Obviously, the field dependence $T_{SC}(g_{1x}^{\uparrow}(H))$ not only shifts the linear field dependence $T_{SC}^{orb}(H)$ down but also creates an upward curvature, in accordance with the experimental temperature dependence of the upper critical field shown in Fig. 4.

In URhGe, the dependence $H_{c2}^z(T)$ does not reveal an upward curvature [45] (Fig. 5). Unlike the magnetization change in UCoGe, the change in the magnetic moment in the field H_z smaller than 1 T is negligibly small in URhGe [46]. Hence, the field dependence of the pairing constant plays no role.

4.3 Upper critical field in URhGe

The superconducting critical temperature in all uranium ferromagnets increases with improving the sample quality, as it should in unconventional superconducting states where the $T_{SC}(l)$ dependence on the electron mean free path at $l>\xi_0$ is described by [36]

$$T_{SC}\approx T_{SC0}-\frac{\pi v_F}{8l}, \tag{122}$$

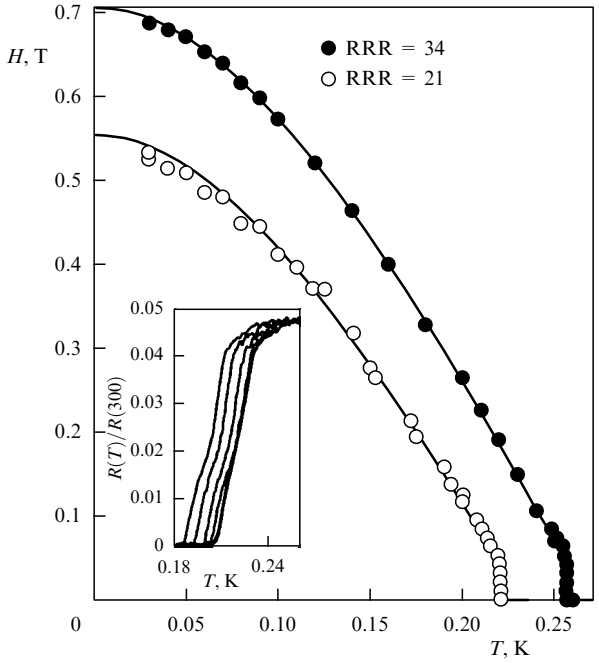

Figure 5. Temperature dependence of the applied field at which superconductivity is destroyed for two URhGe crystals with RRR = 34 and RRR = 21 for fields applied parallel to the c axis [45].

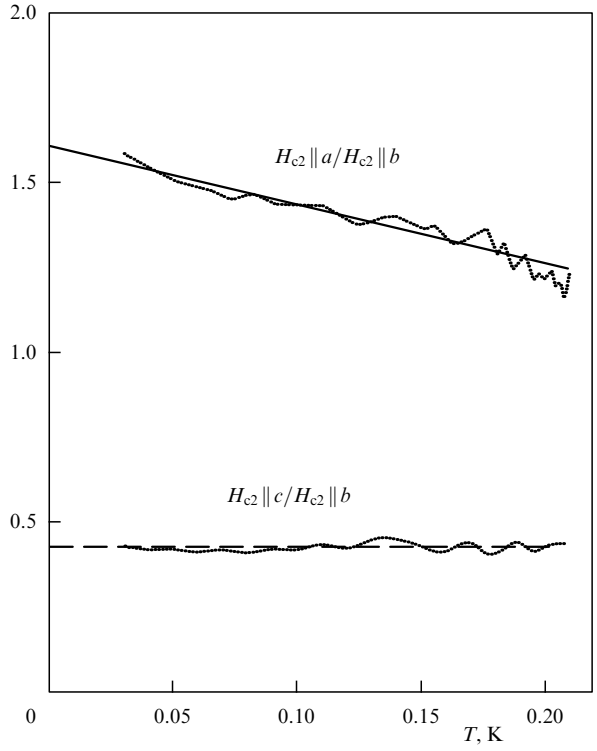

Figure 6. Temperature dependence of the ratio of the upper critical fields parallel to different axes in URhGe [45].

and the zero-temperature upper critical field increases with the sample purity as the square of the critical temperature:

$$H_{c2} \approx \frac{\phi_0}{\pi \xi_0^2} \propto T_{SC}^2 . \tag{123}$$

The last relation has been demonstrated by measurements of the upper critical field in URhGe in samples of differing quality [45] (see Fig. 5).

Another peculiar property revealed by Hardy and Huxley [45] is the temperature dependence of the upper critical field anisotropy. The ratio of $H_{c2}(T)$ along the c axis to that along the b axis is independent of the temperature. But the ratio of $H_{c2}(T)$ parallel to the a and b axes (or a and c axes) increases linearly by approximately 20% as the temperature decreases from T_c to zero (Fig. 6). This is consistent with the temperature behavior of the upper critical field in the single-band phase with the order parameter at $H = 0$:

$$\Delta^{\uparrow}(\mathbf{k}, \mathbf{r}) = \eta_x^{\uparrow} k_x .$$

It can be shown in this case [47] that the solutions of the linear Gor'kov equations corresponding to the maximal upper critical field for the different crystallographic directions are

$$\Delta^{\uparrow}(\mathbf{k}, \mathbf{r}) \sim A(H,T)(k_x + \mathrm{i}k_z)\psi_0(x,z) + B(H,T)(k_x - \mathrm{i}k_z)\psi_2(x,z) , \quad H \| b , \tag{124}$$

$$\Delta^{\uparrow}(\mathbf{k}, \mathbf{r}) \sim A(H,T)(k_x + \mathrm{i}k_y)\psi_0(x,y) + B(H,T)(k_x - \mathrm{i}k_y)\psi_2(x,y) , \quad H \| c , \tag{125}$$

$$\Delta^{\uparrow}(\mathbf{k}, \mathbf{r}) \sim k_x \psi_0(y,z) , \quad H \| a , \tag{126}$$

where $\psi_n(x,y)$ are the Landau functions of a particle with the charge $2e$ in a magnetic field, n is the Landau level number, and $A(H,T)$ and $B(H,T)$ are functions of the magnetic field and temperature. We see that the solutions for the field along the c and b axes have the same structure and differ from the solution for the field along the a axis, which naturally explains the observed temperature dependence of the upper critical field anisotropy.

This property is still valid in a multi-band superconductor with equal-spin-pairing if we assume (as we did in the single-band case) that our superconducting state is an A state whose order parameter components in a zero field are

$$\Delta^{\uparrow}(\mathbf{k}, \mathbf{r}) = \eta_x^{\uparrow} k_x , \quad \Delta^{\downarrow}(\mathbf{k}, \mathbf{r}) = \eta_x^{\downarrow} k_x . \tag{127}$$

Thus, the observed temperature dependence of the upper critical field anisotropy strongly points to the preferable order parameter structure for the superconducting state in URhGe.

4.4 Zeros in the spectrum and specific heat at low temperatures

As we have already noted, even in the absence of an external field in a ferromagnetic superconductor, there is an internal field H_{int} acting on the electron charges. The internal magnetic field in all uranium ferromagnets is larger than the lower critical field H_{c1}. Hence, the Meissner state is absent and the superconductor is in an Abrikosov vortex state with spatially inhomogeneous distributions of the order parameter and the internal magnetic field. At low temperatures, when due to $H_{int} \ll H_{c2}$ the distance between vortices is much larger than the core radius, contributions to the specific heat on the Fermi surface from the vortex cores and the inter-vortex space can be separated.

It is customary to operate not with the specific heat but with the ratio $C/T = \gamma$, which, in a normal metal, is directly proportional to the electron density of states on the Fermi surface. The core contribution to the specific heat is due to the almost gapless excitations localized in the vortex cores.

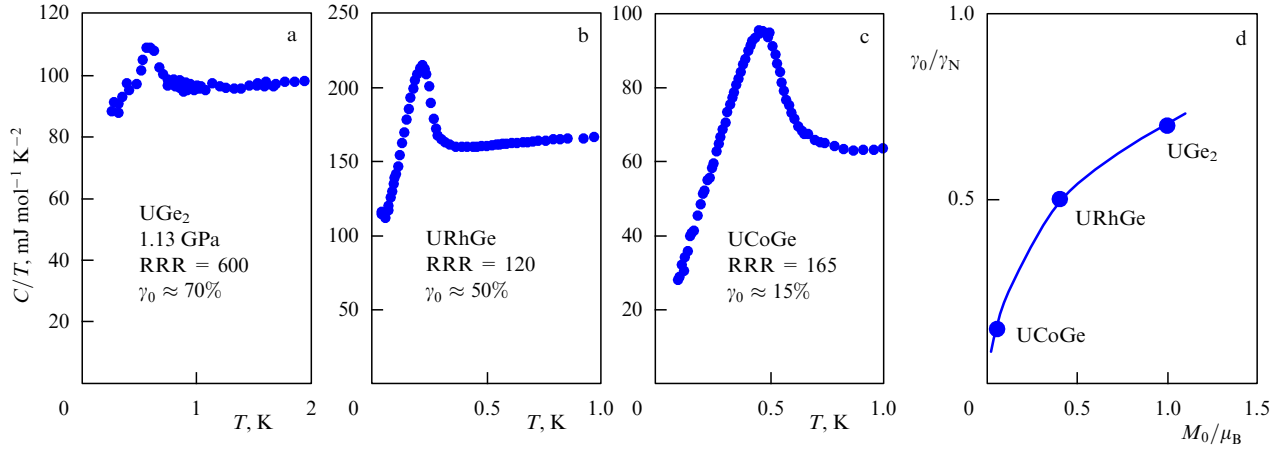

Figure 7. (Color online.) Specific heat divided by temperature $C/T = \gamma$ in (a) UGe_2, (b) URhGe, and (c) UCoGe. (d) Scaled residual γ_0/γ_N-value as a function of the ordered moment [9].

Hence, due to the vortex cores, γ preserves a finite value in the limit $T = 0$:

$$\gamma_v \approx \frac{H_{int}}{H_{c2}}\,\gamma_N\,, \tag{128}$$

where γ_N is the normal-state value of γ.

Another contribution to the density of states originates from the so-called Volovik effect [48] taking place in the inter-vortex space. In this case, the energy of excitations is given by Eqns (19) and (20). In the absence of additional phase transitions, there are either A or B superconducting states with the respective order parameters (97), (98) and (99), (100). The A-state order parameter vanishes at isolated points $k_x = k_y = 0$; hence, the inter-vortex space contribution to the density of states is given by [48]

$$\gamma_{iv}^{A} \approx \frac{H_{int}}{H_{c2}}\,\ln\left(\frac{H_{c2}}{H_{int}}\right)\gamma_N\,. \tag{129}$$

The B-state order parameter vanishes on the line $k_z = 0$; hence, the inter-vortex space contribution to the density of states is given by [48]

$$\gamma_{iv}^{B} \approx \sqrt{\frac{H_{int}}{H_{c2}}}\,\gamma_N\,. \tag{130}$$

As shown in Section 3, the mixing of the x and y components of the order parameter in the A state is in fact quite small, owing to the smallness of the V_3 amplitude of pairing. Therefore, the gap in the A-state spectrum is almost equal to zero either on the line $k_x = 0$ or on the line $k_y = 0$. Hence, the inter-vortex contribution to the density of states in the A state can be given by the same square-root formula as for the B state.

Equations (129) and (130) are applicable to defect-free superconducting crystals. In the presence of inhomogeneities created by impurities, dislocations, and domain walls, the gap in the quasiparticle spectrum is suppressed in a finite vicinity of the order parameter zeros [36] as well as in a finite vicinity of the inter-domain walls. As a result, the zero-energy density of states acquires a field-independent contribution. At a high enough impurity concentration, the square-root field dependence can also be modified [49].

Qualitatively, the low-temperature dependence of γ on the magnetic field at moderate amounts of impurity is described by

$$\gamma_0 = \gamma_{dw} + \gamma_{iv} + \gamma_v \approx \left(a + \sqrt{\frac{H_{int}}{H_{c2}}} + \frac{H_{int}}{H_{c2}}\right)\gamma_N \tag{131}$$

with a constant $a \ll 1$.

We can estimate the magnitude of the internal field as

$$H_{int} = \text{const}\,\frac{\mu_U}{a_{UU}^3}\,, \tag{132}$$

where μ_U is the magnetic moment per uranium atom at zero temperature and a_{UU} is the distance between nearest-neighbor uranium atoms. The inter-uranium distances in UCoGe, URhGe, and UGe_2 are close to each other. But the corresponding magnetic moments $0.05\mu_B$, $0.4\mu_B$, and μ_B are quite different, which determines the difference in H_{int} in these materials. An indeterminacy is also introduced by the unknown prefactors in Eqn (132). Another way to determine the internal field is to set it equal to the external field along the direction of spontaneous magnetization that suppresses the ferromagnet multi-domain structure.

The internal fields estimated in review [9] are about 100 G for UCoGe, 800 G for URhGe, and 2800 G for UGe_2, in accordance with the higher value of the magnetic moments μ_U in these materials. The zero-temperature upper critical field directed along the spontaneous magnetization is 1.2 T in UCoGe [43] and approximately 2.2 T in UGe_2 [19]. The known value 0.6 T of H_{c2} for URhGe has been measured [45], albeit in a single crystal with a low relative residual resistance, equal to 21. We can therefore expect that the real value of the low-temperature upper critical field in URhGe is roughly the same as in UCoGe. Then the part of the ratio γ_0/γ_N that depends on the field and is found from Eqn (131) is approximately 0.1 for UCoGe, 0.3 for URhGe, and 0.5 for UGe_2. The corresponding experimentally established values are presented in Fig. 7.

5. Reentrant superconductivity in URhGe

URhGe has a peculiar property. At a sufficiently low temperature, a magnetic field of about 1.3 T directed along the b axis suppresses the superconducting state [45], but in a

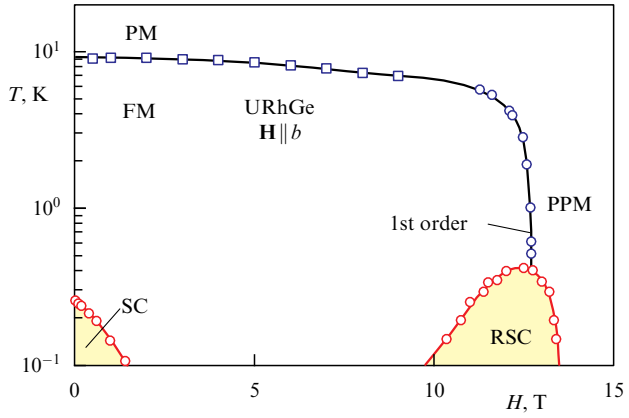

Figure 8. (Color online.) Temperature–field phase diagram for the magnetic field parallel to the b axis in URhGe. PM, FM, and PPM denote paramagnetic, ferromagnetic, and strongly polarized paramagnetic states. SC and RSC denote superconducting and reentrant superconducting states [50].

much stronger field of about 10 T, superconductivity is restored and exists in the fields up to 13 T [30]. The maximum critical temperature in this field interval is ≈ 0.4 K. In the same field interval, the material transfers from the ferromagnetic to the paramagnetic state via a first-order phase transition. The superconducting state exists not only inside the ferromagnetic state but also in the paramagnetic state separated from the ferromagnetic state by a first-order phase transition (Fig. 8).

The observation of an abrupt collapse of spontaneous magnetization in a sufficiently strong external field along the b axis was already reported in the first publication on magnetic-field-induced superconductivity in the ferromagnet URhGe [30]. Recently, the first-order character of the transition has been confirmed by the direct observation of hysteresis [50] in the Hall resistivity in the vicinity of the transition field $H_R \sim 12.5$ T.

In Sections 5.1–5.4, we develop a phenomenological description of the ferromagnetic–paramagnetic phase transition in an external magnetic field perpendicular to the spontaneous magnetization direction. We find the magnetic susceptibility and show that the magnetic susceptibility corresponding to longitudinal magnetic fluctuations increases greatly in the vicinity of the first-order phase transition, stimulating the reentrance of the superconducting state.

5.1 Phase transition in an orthorhombic ferromagnet in a magnetic field perpendicular to spontaneous magnetization

The Landau free energy of an orthorhombic ferromagnet in a magnetic field $\mathbf{H}(\mathbf{r})$ is

$$\mathcal{F} = \int \mathrm{d}V (F_M + F_\nabla) , \tag{133}$$

where, in writing

$$F_M = \alpha_z M_z^2 + \beta_z M_z^4 + \delta_z M_z^6 + \alpha_y M_y^2 + \alpha_x M_x^2 + \beta_{xy} M_x^2 M_y^2 + \beta_{yz} M_z^2 M_y^2 + \beta_{xz} M_z^2 M_x^2 - \mathbf{MH} , \tag{134}$$

we took the orthorhombic anisotropy and the sixth-order term in powers of M_z into account. The density of the gradient energy is taken in the exchange approximation,

$$F_\nabla = \gamma_{ij} \frac{\partial \mathbf{M}}{\partial x_i} \frac{\partial \mathbf{M}}{\partial x_j} , \tag{135}$$

where x, y, z are the coordinates along the respective a, b, c crystallographic directions, and

$$\alpha_z = \alpha_{z0}(T - T_{C0}) , \quad \alpha_x > 0, \quad \alpha_y > 0 , \tag{136}$$

$$\gamma_{ij} = \begin{pmatrix} \gamma_{xx} & 0 & 0 \\ 0 & \gamma_{yy} & 0 \\ 0 & 0 & \gamma_{zz} \end{pmatrix} . \tag{137}$$

In the constant magnetic field $\mathbf{H} = H_y \hat{\mathbf{y}}$, the equilibrium magnetization projections along the x and y directions are obtained by minimizing free energy (134) with respect to M_x and M_y:

$$M_x = 0 , \qquad M_y = \frac{H_y}{2(\alpha_y + \beta_{yz} M_z^2)} . \tag{138}$$

Substituting these expressions in (106), we obtain

$$F_M = \alpha_z M_z^2 + \beta_z M_z^4 + \delta_z M_z^6 - \frac{1}{4} \frac{H_y^2}{\alpha_y + \beta_{yz} M_z^2} , \tag{139}$$

which, after the expansion of the denominator in the last term, gives

$$F_M = -\frac{H_y^2}{4\alpha_y} + \tilde{\alpha}_z M_z^2 + \tilde{\beta}_z M_z^4 + \tilde{\delta}_z M_z^6 + \ldots , \tag{140}$$

where

$$\tilde{\alpha}_z = \alpha_{z0}(T - T_{C0}) + \frac{\beta_{yz} H_y^2}{4\alpha_y^2} , \tag{141}$$

$$\tilde{\beta}_z = \beta_z - \frac{\beta_{yz}}{\alpha_y} \frac{\beta_{yz} H_y^2}{4\alpha_y^2} , \tag{142}$$

$$\tilde{\delta}_z = \delta_z + \frac{\beta_{yz}^2}{\alpha_y^2} \frac{\beta_{yz} H_y^2}{4\alpha_y^2} . \tag{143}$$

We see that in the magnetic field perpendicular to the spontaneous magnetization direction, the Curie temperature decreases as

$$T_C = T_C(H_y) = T_{C0} - \frac{\beta_{yz} H_y^2}{4\alpha_y^2 \alpha_{z0}} . \tag{144}$$

The coefficient $\tilde{\beta}_z$ also decreases with H_y and reaches zero at

$$H_y^{cr} = \frac{2\alpha_y^{3/2} \beta_z^{1/2}}{\beta_{yz}} . \tag{145}$$

In this field, under the condition

$$\frac{\alpha_{z0} \beta_{yz} T_{C0}}{\alpha_y \beta_z} > 1 , \tag{146}$$

Curie temperature (144) is still positive and at $H_y > H_y^{cr}$ the phase transition from the paramagnetic to the ferromagnetic state becomes a first-order transition (Fig. 9). The point $(H_y^{cr}, T_C(H_y^{cr}))$ on the paramagnetic–ferromagnetic phase transition line is a tricritical point.

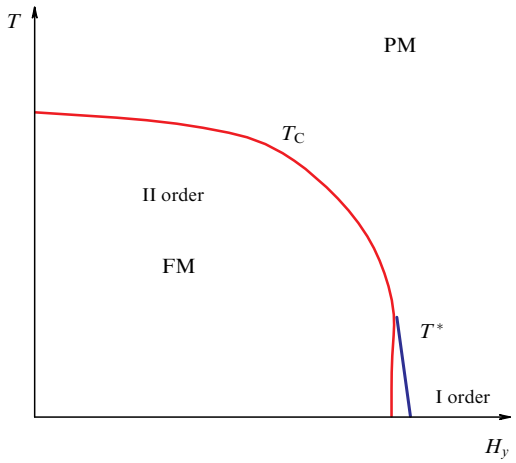

Figure 9. (Color online.) Phase diagram of a uniaxial ferromagnet in a magnetic field perpendicular to the spontaneous magnetization axis. PM and FM denote paramagnetic and ferromagnetic states. The red line is the Curie temperature. The blue line is the first-order transition.

Minimizing the free energy in Eqn (140) gives the value of the order parameter in the ferromagnetic state,

$$M_z^2 = \frac{1}{3\tilde{\delta}_z}\left(-\tilde{\beta}_z + \sqrt{\tilde{\beta}_z^2 - 3\tilde{\alpha}_z\tilde{\delta}_z}\right). \tag{147}$$

Minimizing the free energy in the paramagnetic state

$$F_{\rm para} = \alpha_y M_y^2 - H_y M_y \tag{148}$$

with respect to M_y gives the equilibrium value of the magnetization projection on the y axis in the paramagnetic state:

$$M_y = \frac{H_y}{2\alpha_y}. \tag{149}$$

Substituting this in Eqn (148) yields the equilibrium value of the free energy in the paramagnetic state

$$F_{\rm para} = -\frac{H_y^2}{4\alpha_y}. \tag{150}$$

On the line of the first-order phase transition from the paramagnetic to ferromagnetic state determined by the equations [51]

$$F_M = F_{\rm para}\,, \qquad \frac{\partial F_M}{\partial M_z} = 0\,, \tag{151}$$

the order parameter M_z experiences a jump (Fig. 10) from

$$M_z^{*2} = -\frac{\tilde{\beta}_z}{2\tilde{\delta}_z} \tag{152}$$

in the ferromagnetic state to zero in the paramagnetic state. Substituting (152) in the equation $F_M = F_{\rm para}$ gives the equation of the first-order transition line

$$4\tilde{\alpha}_z\tilde{\delta}_z = \tilde{\beta}_z^2\,, \tag{153}$$

that is,

$$T^* = T^*(H_y) = T_{C0} - \frac{\beta_{yz}H_y^2}{4\alpha_y^2\alpha_{z0}} + \frac{\tilde{\beta}_z^2}{4\alpha_{z0}\tilde{\delta}_z}. \tag{154}$$

The corresponding jump of M_y (see Fig. 10) is given by

$$M_y^* = M_y^{\rm ferro} - M_y^{\rm para} = \frac{H_y}{2(\alpha_y + \beta_{yz}M_z^{*2})} - \frac{H_y}{2\alpha_y}. \tag{155}$$

5.2 Susceptibilities

In a field perpendicular to the magnetization direction, magnetic susceptibility components can be found in the same manner as in Section 3.2 in the case of a parallel field. In the ferromagnetic state at $T < T^*$, they are

$$\begin{aligned}
\chi_{xx}^{\rm f}(\mathbf{k}) &\approx \left[2(\alpha_x + \beta_{xz}M_z^2 + \beta_{xy}M_y^2 + \gamma_{ij}k_ik_j)\right]^{-1},\\
\chi_{yy}^{\rm f}(\mathbf{k}) &\approx \left[2(\alpha_y + \beta_{yz}M_z^2 + \gamma_{ij}k_ik_j)\right]^{-1},\\
\chi_{zz}^{\rm f}(\mathbf{k}) &\approx \left[2(\alpha_z + 6\beta_zM_z^2 + 15\delta_zM_z^4 + \beta_{yz}M_y^2 + \gamma_{ij}k_ik_j)\right]^{-1}\\
&= \left[2(4\beta_zM_z^2 + 12\delta_zM_z^4 + \gamma_{ij}k_ik_j)\right]^{-1},
\end{aligned} \tag{156}$$

and in the paramagnetic state at $T > T^*$,

$$\begin{aligned}
\chi_{xx}^{\rm p}(\mathbf{k}) &\approx \left[2(\alpha_x + \beta_{xy}M_y^2 + \gamma_{ij}k_ik_j)\right]^{-1},\\
\chi_{yy}^{\rm p}(\mathbf{k}) &\approx \left[2(\alpha_y + \gamma_{ij}k_ik_j)\right]^{-1},\\
\chi_{zz}^{\rm p}(\mathbf{k}) &\approx \left[2(\tilde{\alpha}_z + \gamma_{ij}k_ik_j)\right]^{-1}\\
&= \left[2(\alpha_{z0}(T - T_C(H_y)) + \gamma_{ij}k_ik_j)\right]^{-1}.
\end{aligned} \tag{157}$$

The spin-triplet pairing interaction is expressed through the odd part of the susceptibility components:

$$\chi_{ii}^{\rm u}(\mathbf{k},\mathbf{k}') = \frac{1}{2}\left[\chi_{ii}(\mathbf{k}-\mathbf{k}') - \chi_{ii}(\mathbf{k}+\mathbf{k}')\right], \quad i = x,y,z\,. \tag{158}$$

Hence, for the ferromagnetic state at $T < T^*$, we have

$$\begin{aligned}
&\chi_{xx}^{\rm fu}(\mathbf{k},\mathbf{k}') \approx \frac{\gamma_{ij}k_{\rm F}^2}{(a_x^{\rm f})^2}\hat{k}_i\hat{k}_j'\,, \qquad \chi_{yy}^{\rm fu}(\mathbf{k},\mathbf{k}') \approx \frac{\gamma_{ij}k_{\rm F}^2}{(a_y^{\rm f})^2}\hat{k}_i\hat{k}_j'\,,\\
&\chi_{zz}^{\rm fu}(\mathbf{k},\mathbf{k}') \approx \frac{\gamma_{ij}k_{\rm F}^2}{(a_z^{\rm f})^2}\hat{k}_i\hat{k}_j'
\end{aligned} \tag{159}$$

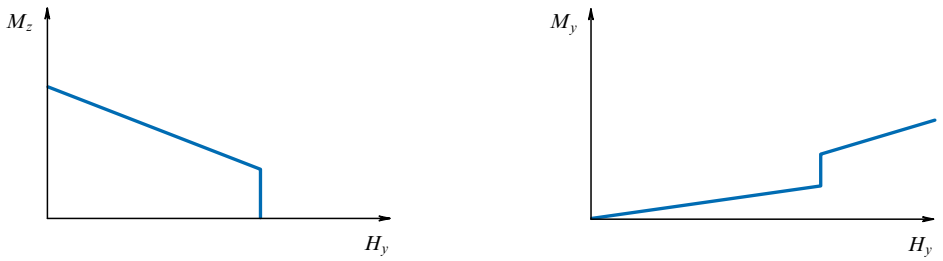

Figure 10. Magnetic field dependences of $M_z(H_y)$ and $M_y(H_y)$ with jumps at the first-order transition.

with

$$a_x^{\rm f} = \alpha_x + \beta_{xz} M_z^2 + \beta_{xy} M_y^2 + 2\gamma k_{\rm F}^2 ,$$
$$a_y^{\rm f} = \alpha_y + \beta_{yz} M_z^2 + 2\gamma k_{\rm F}^2 , \qquad (160)$$
$$a_z^{\rm f} = 4\beta_z M_z^2 + 12\delta_z M_z^4 + 2\gamma k_{\rm F}^2 ,$$

where $M_z(H_y)$ and $M_y(H_y)$ are equilibrium values of the magnetization components. It is instructive to compare the expressions obtained for the odd parts of the susceptibility components with Eqns (64)–(67) found at $\delta_z = 0, H_y = 0$, but $H_z \neq 0$.

For the paramagnetic state at $T > T^*$,

$$\chi_{xx}^{\rm pu}(\mathbf{k},\mathbf{k}') \approx \frac{\gamma_{ij} k_{\rm F}^2}{(a_x^{\rm p})^2}\, \hat{k}_i \hat{k}'_j , \qquad \chi_{yy}^{\rm pu}(\mathbf{k},\mathbf{k}') \approx \frac{\gamma_{ij} k_{\rm F}^2}{(a_y^{\rm p})^2}\, \hat{k}_i \hat{k}'_j ,$$
$$\chi_{zz}^{\rm pu}(\mathbf{k},\mathbf{k}') \approx \frac{\gamma_{ij} k_{\rm F}^2}{(a_z^{\rm p})^2}\, \hat{k}_i \hat{k}'_j , \qquad (161)$$

$$a_x^{\rm p} = \alpha_x + \beta_{xy} M_y^2 + 2\gamma k_{\rm F}^2 ,$$
$$a_y^{\rm p} = \alpha_y + 2\gamma k_{\rm F}^2 , \qquad (162)$$
$$a_z^{\rm p} = 2\alpha_{z0}\big(T - T_{\rm C}(H_y)\big) + 2\gamma k_{\rm F}^2 .$$

Thus, under the first-order transition from the paramagnetic to the ferromagnetic state, the susceptibility components change their values jump-wise.

As we saw in Section 3.1, the pairing interaction in the ferromagnetic state is mostly determined by the odd part of the z component of the susceptibility:

$$\chi_{zz}^{\rm fu}(\mathbf{k},\mathbf{k}') \approx \frac{\gamma_{ij} k_{\rm F}^2}{4(2\beta_z M_z^2 + 6\delta_z M_z^4 + \gamma k_{\rm F}^2)^2}\, \hat{k}_i \hat{k}'_j . \qquad (163)$$

The equilibrium magnetization $M_z(H_y)$ decreases with the magnetic field H_y (see Fig. 10). It can be expected that the jump of M_z at the first-order transition is much smaller than the low-temperature magnetization at the zero field $H_y = 0$:

$$M_z\Big|_{H_y=0,\, T=0} \gg M_z^* . \qquad (164)$$

In this case, according to Eqn (163), the susceptibility $\chi_{zz}^{\rm fu}$ on the first-order transition line substantially exceeds its initial value at $H_y = 0$, which stimulates the reentrance of superconductivity.

5.3 Superconducting state in the vicinity of the first-order transition

The suppression of the Curie temperature by the magnetic field perpendicular to spontaneous magnetization leads to an effective increase in pairing interaction. This effect can in principle compensate the suppression of superconductivity by orbital depairing. In URhGe, the Curie temperature is much higher than $T_{\rm SC}$. Hence, the orbital effect succeeds in suppressing the superconducting state ($H_{\rm c2}^b(T=0) \approx 1.3$ T (see [45])) well before the effect of decreasing the Curie temperature and the stimulation of pairing intensity manifests itself. But at fields higher than 10 T, the last effect starts to overcome the orbital depairing and the superconducting state is restored. The critical temperature of the superconducting transition begins to increase and approaches the line of the first-order transition from the ferromagnetic to paramagnetic state and intersects it [30, 50]. Here, we discuss

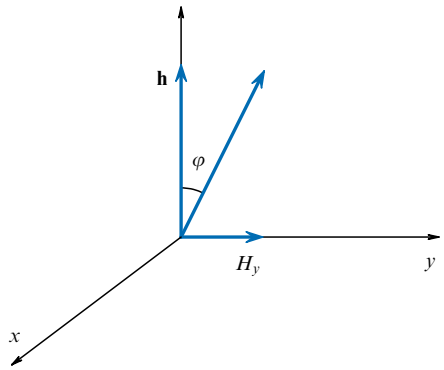

Figure 11. Magnetic field H_y directed perpendicular to the exchange field **h**.

what happens to the superconducting phase transition line at the intersection with the line of the first-order ferromagnet–paramagnet phase transition $T^*(H_y)$.

In the external field oriented along the b axis, which is perpendicular to the exchange field h (Fig. 11), it is natural to choose the spin quantization axis along the direction of the total magnetic field $h\hat{\mathbf{z}} + H_y\hat{\mathbf{y}}$. The normal-state matrix Green's function then retains its diagonal form

$$\hat{G}_n = \begin{pmatrix} G^{\uparrow} & 0 \\ 0 & G^{\downarrow} \end{pmatrix} , \qquad (165)$$

where

$$G^{\uparrow,\downarrow} = \left({\rm i}\omega_n - \xi_{\mathbf{k}}^{\uparrow,\downarrow} \pm \mu_{\rm B}\sqrt{h^2 + H_y^2} \right)^{-1} . \qquad (166)$$

We can use the formulas obtained in Section 3.1, but with the susceptibility tensor written in the new coordinate system,

$$\chi_{ij} \to \tilde{\chi}_{ij} = R_{il}\, \chi_{lm} R_{jm} , \qquad (167)$$

where

$$R = \begin{pmatrix} 1 & 0 & 0 \\ 0 & \cos\varphi & -\sin\varphi \\ 0 & \sin\varphi & \cos\varphi \end{pmatrix} \qquad (168)$$

is the matrix of rotation around the $\hat{x}$ direction through the angle given by $\tan\varphi = H_y/h$.

For simplicity, we can work with the equal-spin-pairing superconductivity, ignoring the amplitude Δ^0. Also, the gradient energy of the orthorhombic ferromagnet in Eqn (135) was taken in the exchange approximation such that the pairing amplitude $V_3 = 0$. In contrast to the case of a parallel field, *we here disregard the orbital effects*, ignoring the order parameter coordinate dependence. In this case, the critical temperature $T_{\rm SC}(H_y)$ of transition to the superconducting state is determined from the self-consistency equations

$$\Delta^{\uparrow}(\mathbf{k}) = \mu_{\rm B} I^2 T \sum_n \sum_{\mathbf{k}'} \Big\{ \big[\chi_{zz}^{\rm fu}(\mathbf{k},\mathbf{k}')\cos^2\varphi$$
$$+ \chi_{yy}^{\rm fu}(\mathbf{k},\mathbf{k}')\sin^2\varphi\big] G_1^{\uparrow} G_2^{\uparrow} \Delta^{\uparrow}(\mathbf{k}')$$
$$+ \big[\big(\chi_{xx}^{\rm fu}(\mathbf{k},\mathbf{k}') - \chi_{yy}^{\rm fu}(\mathbf{k},\mathbf{k}')\big)\cos^2\varphi$$
$$+ \big(\chi_{xx}^{\rm fu}(\mathbf{k},\mathbf{k}') - \chi_{zz}^{\rm fu}(\mathbf{k},\mathbf{k}')\big)\sin^2\varphi\big] G_1^{\downarrow} G_2^{\downarrow} \Delta^{\downarrow}(\mathbf{k}') \Big\} , \qquad (169)$$

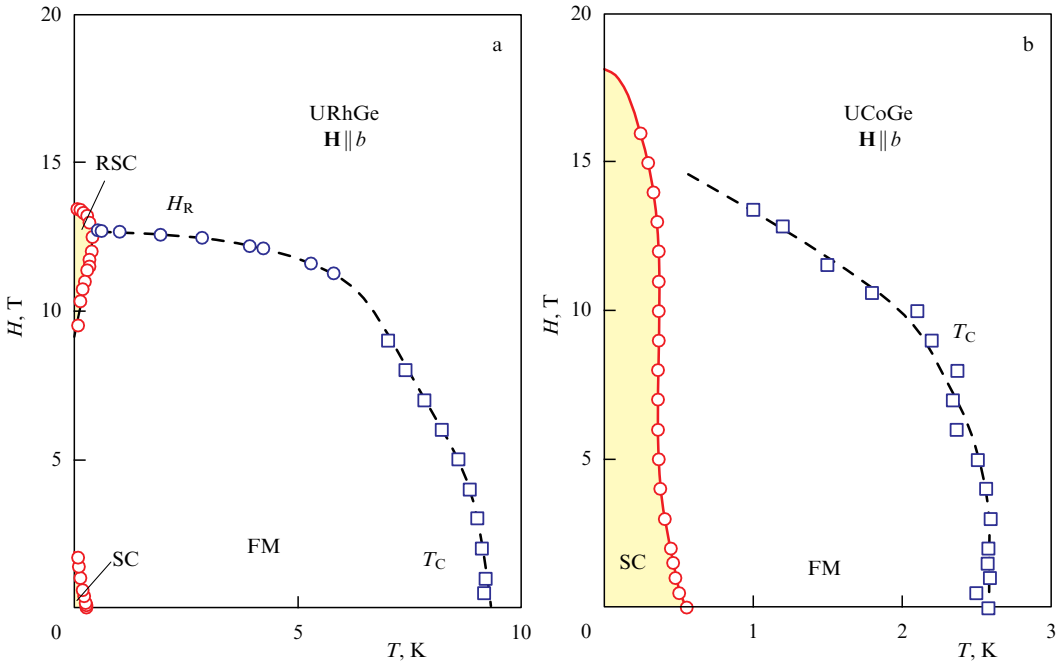

Figure 12. (Color online.) Field–temperature phase diagram of (a) URhGe and (b) UCoGe for the field directed along the *b* axis. SC, FM, and RSC denote the superconducting, ferromagnetic, and reentrant superconducting states [9].

$$\Delta^{\downarrow}(\mathbf{k}) = \mu_B I^2 T \sum_n \sum_{\mathbf{k}'} \Big\{ \big[\big(\chi^{\rm fu}_{xx}(\mathbf{k},\mathbf{k}') - \chi^{\rm fu}_{yy}(\mathbf{k},\mathbf{k}')\big)\cos^2\varphi + \big(\chi^{\rm fu}_{xx}(\mathbf{k},\mathbf{k}') - \chi^{\rm fu}_{zz}(\mathbf{k},\mathbf{k}')\big)\sin^2\varphi \big] G_1^{\uparrow} G_2^{\uparrow} \Delta^{\uparrow}(\mathbf{k}',\mathbf{q}) + \big[\chi^{\rm fu}_{zz}(\mathbf{k},\mathbf{k}')\cos^2\varphi + \chi^{\rm fu}_{yy}(\mathbf{k},\mathbf{k}')\sin^2\varphi\big] G_1^{\downarrow} G_2^{\downarrow} \Delta^{\downarrow}(\mathbf{k}') \Big\}, \tag{170}$$

where $G_1^{\uparrow} = G^{\uparrow}(\mathbf{k}',\omega_n)$ and $G_2^{\uparrow} = G^{\uparrow}(-\mathbf{k}',-\omega_n)$, and similarly for the Green's functions $G_1^{\downarrow}$ and $G_2^{\downarrow}$ given by Eqn (166). In the ferromagnetic state near the first-order transition, the angle is $\varphi \approx \pi/4$, and the susceptibilities are determined by Eqns (159) and (160).

In the paramagnetic state, the susceptibilities are determined by Eqns (161) and (162). The angle is $\varphi = \pi/2$,

$$G^{\uparrow,\downarrow}_{\rm para} = \frac{1}{\mathrm{i}\omega_n - \xi_{\mathbf{k}} \pm \mu_B H_y}, \tag{171}$$

and the equations for $\Delta^{\uparrow}$ and $\Delta^{\downarrow}$ are independent of Δ^0 [27]:

$$\Delta^{\uparrow}(\mathbf{k},\mathbf{q}) = \mu_B I^2 T \sum_n \sum_{\mathbf{k}'} \Big\{ \chi^{\rm pu}_{yy}(\mathbf{k},\mathbf{k}') G_1^{\uparrow} G_2^{\uparrow} \Delta^{\uparrow}(\mathbf{k}') + \big(\chi^{\rm pu}_{xx}(\mathbf{k},\mathbf{k}') - \chi^{\rm pu}_{zz}(\mathbf{k},\mathbf{k}')\big) G_1^{\downarrow} G_2^{\downarrow} \Delta^{\downarrow}(\mathbf{k}',\mathbf{q}) \Big\}, \tag{172}$$

$$\Delta^{\downarrow}(\mathbf{k},\mathbf{q}) = \mu_B I^2 T \sum_n \sum_{\mathbf{k}'} \Big\{ \big(\chi^{\rm pu}_{xx}(\mathbf{k},\mathbf{k}') - \chi^{\rm pu}_{zz}(\mathbf{k},\mathbf{k}')\big) \times G_1^{\uparrow} G_2^{\uparrow} \Delta^{\uparrow}(\mathbf{k}',\mathbf{q}) + \chi^{\rm pu}_{yy}(\mathbf{k},\mathbf{k}') G_1^{\downarrow} G_2^{\downarrow} \Delta^{\downarrow}(\mathbf{k}',\mathbf{q}) \Big\}. \tag{173}$$

As we have mentioned, the susceptibility components undergo a finite jump at the first-order phase transition from the ferromagnetic to paramagnetic state. The Fermi surfaces of split spin-up and spin-down electron bands and the corresponding densities of states also undergo jumpwise changes. The equations for the superconductivity onset temperature $T_{\rm SC}(H_y)$ are quite different on the different sides of the ferromagnet–paramagnet phase transition. Hence, $T_{\rm SC}(H_y)$ should undergo a jump at crossing the first-order phase transition line $T^*(H_y)$, which is indeed observed in experiment [30].

5.4 Concluding remarks

Using the phenomenological description of the phase diagram in URhGe in a magnetic field directed along the crystallographic *b* axis perpendicular to the spontaneous magnetization direction, we have found that the phase transition between the ferromagnetic and paramagnetic states becomes a first-order transition in a sufficiently strong field. The reentrance of superconductivity is explained by a significant increase in the magnetic susceptibility in the vicinity of the first-order transition in comparison with its zero-field value. The reentrant superconductivity near the first-order transition line $T^*(H_y)$ exists in both the ferromagnetic and paramagnetic states. The critical temperature of the transition to the superconducting state undergoes an abrupt fall at the intersection with the ferromagnet–paramagnet phase transition line.

The decrease in the Curie temperature in a magnetic field perpendicular to the spontaneous magnetization direction enhances the pairing interaction. This effect compensates the suppression of superconductivity by the magnetic field. In UCoGe, where the Curie temperature does not greatly exceed the temperature of the transition to the superconducting state, this mechanism stimulates the increase in the upper critical field along the *b* axis, which is observed in the fields above 5 T and is shown in Fig. 12. The superconductivity enhancement in UCoGe is accompanied by an enhancement of the nuclear relaxation rate caused by the increase in the magnetic susceptibility in approaching the Curie temperature in the magnetic field parallel to the *b* axis [52].

The crystallographic *a* direction is magnetically much harder than the *b* direction. Hence, the decrease in the Curie temperature due to the magnetic field directed along the *a* axis is much less pronounced and practically unobservable in available magnetic fields [52]. However, we can expect a

similar development of superconductivity stimulation at much higher fields along the a direction.

If, in the vicinity of the first-order phase transition, we activate the field H_x directed along the a axis in addition to the field $H_y \approx 12$ T, thus increasing the total magnetic field to $H = (H_y^{*2} + H_x^2)^{1/2}$, this would introduce negligible changes to the pairing interaction that was in the absence of a field along the hard a axis. At the same time, the orbital upper critical field in the a direction is larger than that in the b direction by a factor of 1.5 [45]. This roughly explains the stability of reentrant superconductivity in URhGe up to the fields $H = (H_y^{*2} + H_x^2)^{1/2} \approx 30$ T [53].

It is known that in the presence of an external field along the spontaneous magnetization direction $\hat{\mathbf{z}}$, the first-order transition line $T^*(H_y)$ spreads to two first-order transition surfaces $T^*(H_y, \pm H_z)$. On these surfaces, the jump in the spontaneous magnetization decreases with an increase in $|H_z|$ and disappears completely on lines beginning at the tricritical point $T_C(H_y^{cr}, H_z = 0)$. It was suggested in [53] that these lines terminate at the zero temperature at some quantum critical points on the (H_y, H_z) plane and that quantum critical magnetic fluctuations stimulate superconductivity in the vicinity of the ferromagnet–paramagnet first-order phase transition line. This idea looks promising. It can be noted, however, that in general the tricritical line $T^{cr}(H_y, H_z)$ can never reach the zero temperature or simply be located far from the superconducting region on the phase diagram. Motivated by the desire to find critical fluctuations, the recent measurements in [54] demonstrated a huge increase in the NMR relaxation rate in $URh_{0.9}Co_{0.1}Ge$ at $H_y \approx 13$ T. These experiments have been performed at a temperature of 1.6 K, that is, in the region near the second-order phase transition between the ferromagnetic and the paramagnetic states. The reentrant superconductivity occurs at much lower temperatures near the first-order transition line, where the role of critical fluctuations is certainly less important.

Here, we have demonstrated that the reentrant superconductivity in URhGe can arise even in the absence of critical fluctuations due to a drastic increase in the longitudinal susceptibility in the vicinity of the first-order transition line from the paramagnetic to the ferromagnetic state.

6. Critical magnetic relaxation in ferromagnetic uranium compounds

6.1 Critical magnetic relaxation in ferromagnets

Excitations in magnetic systems are measured by neutron scattering. The inelastic magnetic neutron scattering intensity

$$I(\mathbf{Q}, \omega) = A(k_i, k_f)(\delta_{\alpha\beta} - \hat{Q}_\alpha \hat{Q}_\beta)\left|F(\mathbf{Q})\right|^2 S_{\alpha\beta}(\mathbf{q}, \omega) \quad (174)$$

is related to the dynamical structure factor

$$S_{\alpha\beta}(\mathbf{q}, \omega) = \int_{-\infty}^{\infty} \mathrm{d}t \, \exp(\mathrm{i}\omega t)\left\langle M_{\alpha\mathbf{q}}(t) M_{\beta-\mathbf{q}}(0)\right\rangle ,$$

which is a correlation function of magnetic moments [55], related by the fluctuation–dissipation theorem to the imaginary part of susceptibility:

$$S_{\alpha\beta}(\mathbf{q}, \omega) = \frac{2}{1 - \exp(-\omega/T)} \, \chi''_{\alpha\beta}(\mathbf{q}, \omega) . \quad (175)$$

The total transferred wave vector is $\mathbf{Q} = \mathbf{q} + \boldsymbol{\tau}$, where $\boldsymbol{\tau}$ is a reciprocal lattice vector and $\mathbf{q}$ lies in the first Brillouin zone; $\hat{Q}_\alpha$ is the direction cosine of $\mathbf{Q}$ along the α direction; and $F(\mathbf{Q})$ is the magnetic form factor measured by elastic neutron scattering. We put the Planck constant equal to unity, $\hbar = 1$.

For each crystallographic direction, we can take the imaginary part of the susceptibility as the function

$$\frac{\chi''(\mathbf{q}, \omega)}{\omega} = \frac{A}{\omega^2 + \Gamma_\mathbf{q}^2} , \quad (176)$$

that depends on the experimentally measured amplitude A and width $\Gamma_\mathbf{q}$ of the scattering intensity. Then the Kramers–Kronig relation allows finding the real part of the susceptibility:

$$\chi_{(\mathbf{q})} = \chi'(\mathbf{q}, 0) = \frac{1}{\pi} \int \frac{\chi''(\mathbf{q}, \omega)}{\omega} \, \mathrm{d}\omega = \frac{A}{\Gamma_\mathbf{q}} . \quad (177)$$

In the absence of walls and spin–orbit coupling, the magnetization is a conserved quantity; hence, in a Heisenberg ferromagnet above the Curie temperature, the only mechanism leading to magnetization relaxation is the spin diffusion, which results in [55, 56]

$$S(\mathbf{q}, \omega) = \frac{2\omega\chi(\mathbf{q})}{1 - \exp(-\omega/T)} \frac{\Gamma_\mathbf{q}}{\omega^2 + \Gamma_\mathbf{q}^2} , \quad (178)$$

where the linewidth of quasi-elastic scattering

$$\Gamma_\mathbf{q} = Dq^2 \quad (179)$$

is determined by the diffusion coefficient D. The q^2 dependence of $\Gamma_\mathbf{q}$ has been observed in a wide temperature range above the Curie temperature in Ni and Fe (see Ref. [57] and the references therein); near T_C, it is superseded by a $\Gamma \propto q^{2.5}$ dependence, according to predictions of the mode–mode coupling theory [58].

In weak itinerant ferromagnets at $T > T_C$, another mechanism of dissipationless relaxation dominates, with the structure factor given by the same Eqn (178) but with the linewidth determined by the equality [59, 60]

$$\chi(\mathbf{q})\Gamma_\mathbf{q} = \chi_P \omega(\mathbf{q}) , \quad (180)$$

where χ_P is the Pauli susceptibility in the free-electron gas and $\omega(\mathbf{q})$ is the Landau damping, equal to $(2/\pi)qv_F$ for a spherical Fermi surface. A line width linear in the wave vector was observed in MnSi [61]; however, in other weak itinerant ferromagnets MnP [62] and Ni_3Al [63], the dependence of the linewidth on the wave vector is closer to the dynamical scaling theory predictions [58].

6.2 Magnetic relaxation in ferromagnet uranium compounds

The magnetic susceptibility along the easy axis in uranium ferromagnets is much larger than in the directions perpendicular to it. In UGe_2, the easy axis is along the a crystallographic direction. Neutron scattering measurements reported in [33] with the scattering wave vector $\mathbf{q}$ parallel to the a axis revealed no extra scattering relative to the background, while for $\mathbf{q}$ parallel to the c axis, a strongly temperature-dependent contribution was found, as it should be according to Eqn (174). Magnetic relaxation measure-

ments in UGe_2 in [33, 64] show that $\Gamma_{\mathbf{q}}$ does not vanish as $q \to 0$ at temperatures different from T_C. The same result was found for UCoGe [65] for scattering with $\mathbf{q}$ parallel to the a axis, because the easy axis in this material is along the c direction.[4] Hence, there is a mechanism of the uniform magnetization relaxation to equilibrium in uranium ferromagnets.

The magnetization in an electron gas relaxes due to spin-flip processes caused by spin–orbit coupling, either between the electrons [66] or between the itinerant Bloch electron spins and the potential of ions in a vibrating crystal lattice [67, 68]. Both mechanisms produce such a tiny homogeneous relaxation rate that it is unobservable in ferromagnetic materials, while the relaxation rate $\Gamma_{\mathbf{q}=0}$ found in UGe_2 [33] is of the order of several Kelvins. In what follows, to be specific, we discuss UGe_2.

The magnetic susceptibility of single UGe_2 crystals has been measured in [69–72]. The easy-axis magnetization at zero temperature was found to be $1.43\,\mu_B$/f.u., which, in the case of itinerant ferromagnetism, corresponds to a single completely polarized electron band. On the other hand, neutron scattering measurements of the magnetic form factor $M(q)$ [16] show that (i) the shape of $M(q)$ is not distinguishable from that of free U^{3+} or U^{4+} ions, (ii) at low temperature, $M(q \to 0)$ coincides with the magnetization measured by a magnetometer with an accuracy of the order of 1%. Thus, practically the whole magnetic moment in both the paramagnetic and ferromagnetic state is concentrated in uranium atoms.[5]

The static magnetic properties of UGe_2 are described well [71] in terms of the crystal-field splitting of the U^{4+} state, which is the $^3H_4$ term of the $5f^2$ configuration of localized electrons. Itinerant electron states filling the bands are formed by two 7s, one 6d, and one 5f uranium orbitals, as well as by germanium orbitals. Thus, local and itinerant states of f-electrons coexist in UGe_2. The $^3H_4$ term of each atom of UGe_2 in the paramagnetic state mostly consists of a superposition of three quasi-doublets and three singlets arising from the state with the total momentum $J = 4$ split by the crystal field [71]. The temperature decrease causes a change in the populations of these states, leading to a temperature dependence of the magnetic moment. The degeneracy removal for the ground state formed by the lower quasi-doublet allows the system to order magnetically with the spontaneous magnetic moment $\sim 1.5\mu_B$ per uranium atom, which is twice smaller than the Curie–Weiss moment deduced from susceptibility in the paramagnetic state. The itinerant electron subsystem formed by 7s, 6d, and partly 5f electrons is also present, making a contribution of $0.02\mu_B$ to the ferromagnetic ordering, as was demonstrated by muon spin-relaxation measurements [72, 73]. All the mentioned experimental observations as well the theoretical treatment in [71] unequivocally point to the local nature of the UGe_2 ferromagnetism. This means that quasielastic neutron scattering occurs mostly on magnetization fluctuations in the localized moment subsystem.

[4] A small residual linewidth $\Gamma_0 \sim 0.02$ meV has also been registered in ferromagnet MnP [62].

[5] The same property of the strong localization of magnetization in U atoms has been revealed in URhGe [17] and in UCoGe [18]. In the latter case, there are also more recent data [20, 21] partly contesting the results in [18].

The interaction between localized and itinerant electron subsystems leads to the magnetization relaxation measured by neutron scattering in paramagnetic and ferromagnetic states of UGe_2. This type of relaxation can be considered an analog of *spin–lattice relaxation* well known in the physics of nuclear magnetic resonance [74]. In our case, *the magnetization created by the local moments of uranium atoms making the dominant contribution to neutron scattering plays the role of the 'spin' subsystem, whereas the itinerant electrons represent the 'lattice' degrees of freedom* absorbing and dissolving fluctuations of magnetization. Unlike the NMR relaxation determined by the nucleus and electron magnetic moment interaction, *the spin–lattice relaxation between localized and conducting electrons is determined by spin–spin exchange processes* and has no relativistic smallness typical of NMR relaxation. Deviations of magnetization from the equilibrium value relax to equilibrium by the transfer to itinerant electrons. According to this, we treat the magnetization that is almost completely determined by the local moments of uranium atoms as a nonconserved quantity [34].

The process of the easy-axis magnetization relaxation to equilibrium is described by the Landau–Khalatnikov kinetic equation [75]

$$\frac{\partial M}{\partial t} = -A\,\frac{\delta \mathcal{F}}{\delta M}\,, \tag{181}$$

where

$$\mathcal{F} = \int \mathrm{d}V \left(\alpha_0 (T - T_C) M^2 + \gamma_{ij}\,\frac{\partial M}{\partial x_i}\frac{\partial M}{\partial x_j} - MH \right) \tag{182}$$

is the energy of the order parameter fluctuations in the paramagnetic region in a quasistationary magnetic field along the easy axis. The gradient energy in an orthorhombic crystal written in the exchange approximation is determined by three nonzero constants $\gamma_{xx}, \gamma_{yy}, \gamma_{zz}$. The coordinate axes x, y, and z are directed along the b, c, and a axes. The kinetic equation can be rewritten as

$$\frac{\partial M}{\partial t} + \nabla_i j_i = -\frac{M_\alpha}{\tau} + AH\,, \tag{183}$$

where $\tau^{-1} = 2A\alpha_0 (T - T_C)$ and

$$j_i = -2A\gamma_{ij}\,\frac{\partial M}{\partial x_j} \tag{184}$$

are the components of the spin diffusion currents. Substituting

$$M = m_{\mathbf{q}\omega} \exp\left[\mathrm{i}(\mathbf{qr} - \omega t)\right],$$
$$H = h_{\mathbf{q}\omega} \exp\left[\mathrm{i}(\mathbf{qr} - \omega t)\right]$$

in Eqn (183), we obtain the susceptibility

$$\chi(\mathbf{q}, \omega) = \frac{m_{\mathbf{q}\omega}}{h_{\mathbf{q}\omega}} = \frac{A}{-\mathrm{i}\omega + \Gamma_{\mathbf{q}}}\,. \tag{185}$$

The width of quasielastic scattering for $\mathbf{q} \parallel c$ is

$$\Gamma_{\mathbf{q}} = 2A\left[\alpha_0 (T - T_C) + \gamma_{yy} q_c^2\right]. \tag{186}$$

Below the Curie temperature T_C in the ferromagnetic state, the equilibrium magnetization $M = M_0(T)$ and the

energy of fluctuations are given by

$$\mathcal{F} = \int \mathrm{d}V \left[2\alpha_0 (T_\mathrm{C} - T)(M - M_0)^2 + \gamma_{ij} \frac{\partial M}{\partial x_i} \frac{\partial M}{\partial x_j} - (M - M_0)H \right]. \quad (187)$$

The expression for the susceptibility has the same form as in (185) and the quasielastic scattering linewidth is

$$\Gamma_\mathbf{q} = 2A\left[2\alpha_0 (T_\mathrm{C} - T) + \gamma_{yy} q_c^2\right]. \quad (188)$$

6.3 Concluding remarks

Experimentally, two independent values were determined: the width $\Gamma_\mathbf{q}$ and the amplitude $A = \chi(\mathbf{q})\Gamma_\mathbf{q}$ of distribution (178) (Fig. 13). Calculations show that (1) the linewidth of quasielastic neutron scattering near the Curie temperature is a linear function of $T - T_\mathrm{C}$; (2) the absolute value of the derivative $|\mathrm{d}\Gamma_{q_c}/\mathrm{d}T|$ in the ferromagnetic region is roughly twice as large as in the paramagnetic region; (3) the dependence on the wave vector q_c is parabolic. All of these findings are in qualitative correspondence with the experimental observations reported in [33] (see Fig. 14a, b).

At the same time, it has been found experimentally [33] (see the inset in Fig. 14c) that the product $\chi(\mathbf{q})\Gamma_\mathbf{q}$ is independent of temperature for $T > T_\mathrm{C}$ but rapidly decreases for $T < T_\mathrm{C}$. Such behavior means that the decrease in the UGe_2 susceptibility $\chi(\mathbf{q})$ with temperature below T_C is much faster than the mean-field theory predicts.

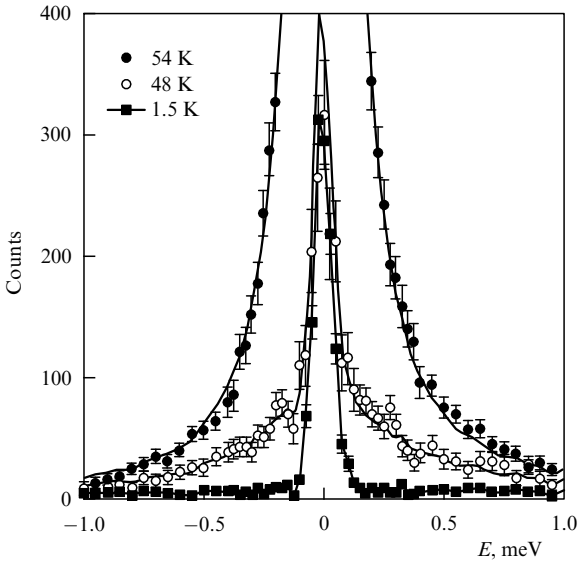

Figure 13. Detected neutron scattering (normalized to a fixed incident beam monitor count) shown as a function of energy transfer at $\mathbf{Q} = (0, 0, 1.04)$ (expressed in the reciprocal lattice units), just above the Curie temperature, at 48 K, and at 1.5 K [33].

Many experimental observations point to the local nature of magnetism in ferromagnetic uranium compounds. The interaction between localized and itinerant electron subsystems gives rise to a specific mechanism of magnetization relaxation similar to the 'spin–lattice' relaxation known in

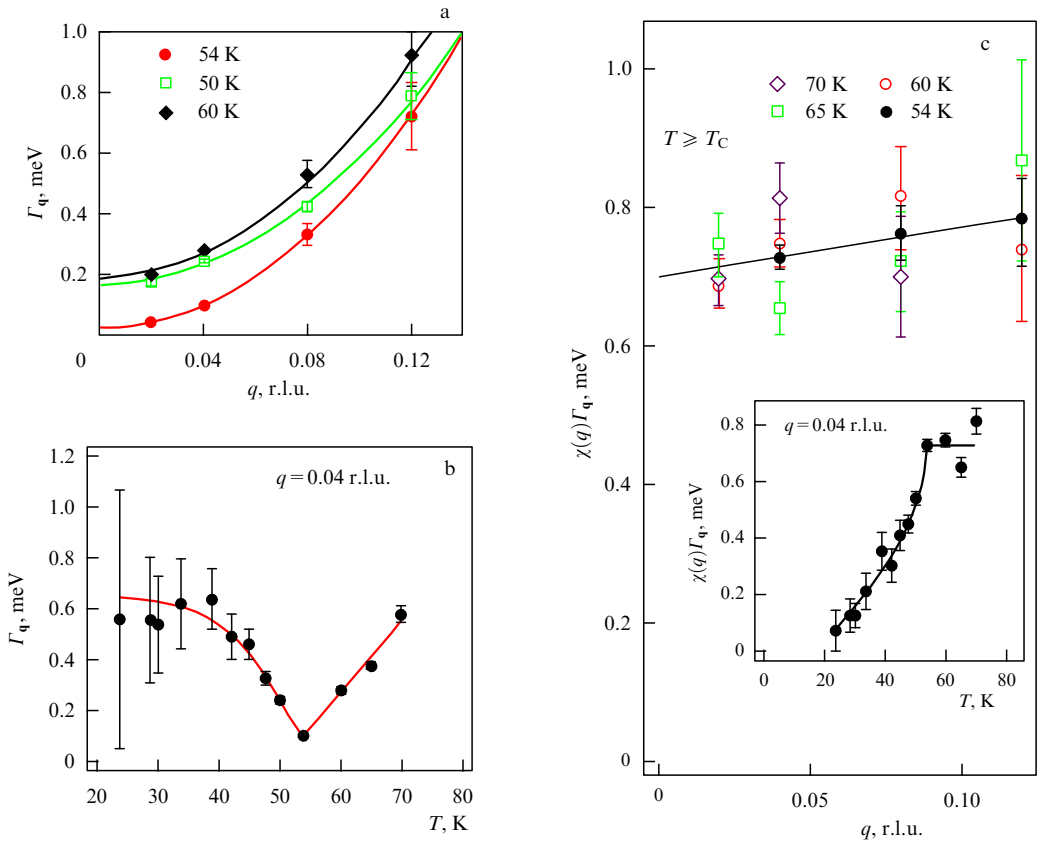

Figure 14. (Color online.) (a) The q dependence ($\mathbf{q} \| c$) of $\Gamma_\mathbf{q}$ at three different temperatures. (b) The temperature dependence of $\Gamma_\mathbf{q}$ at $\mathbf{q} = (0, 0, 0.04)$. (c) The q dependence of the product $\chi(\mathbf{q})\Gamma_\mathbf{q}$ at different temperatures above T_C. The inset in (c) shows the temperatures dependence of $\chi(\mathbf{q})\Gamma_\mathbf{q}$ at $\mathbf{q} = (0, 0, 0.04)$ above and below T_C [33].

the physics of NMR. This relaxation, determined by the exchange spin–spin coupling, is much faster than the NMR relaxation supported by the much weaker interaction between electron and nucleus magnetic moments. The phenomenological description of quasielastic magnetic relaxation is based on the specific property of uranium compounds that the magnetization supported by the moments located at uranium atoms is not a conserved quantity. As a result, the linewidth of quasielastic neutron scattering at $q \to 0$ acquires a nonvanishing value at all temperatures except the Curie temperature.

This conclusion has been confirmed by the microscopic calculations [76] of magnetic relaxation near the transition to the ferromagnetic state in a system consisting of localized and itinerant electrons.

7. Anisotropy of nuclear magnetic relaxation and the upper critical field in UCoGe

Nuclear magnetic resonance measurements with the ^{59}Co nuclei in UCoGe show that the magnetic field along the crystallographic c axis strongly suppresses magnetic fluctuations along this direction [31, 77]. It was also revealed that the upper critical field value in this superconducting material drops abruptly at small field deviations from both the a and b axes toward the spontaneous magnetization direction c [9, 32]. Therefore, the magnetic field component along the c axis very efficiently suppresses the superconducting state. As we have seen, triplet pairing in uranium ferromagnet superconductors is mostly determined by longitudinal fluctuations of magnetization with the amplitude proportional to the odd part of the susceptibility χ^{u}_{zz}. Here, we demonstrate that both mentioned phenomena have the same origin and are explained by a strong increase in magnetization [44, 78] and the corresponding decrease in differential susceptibility (59) of UCoGe in the magnetic field directed along the c axis.

7.1 Nuclear magnetic relaxation

The nuclear spin–lattice relaxation rate measured in a field along the α direction is expressed in terms of the imaginary part of the dynamical susceptibility along the β and γ directions perpendicular to α as

$$\frac{1}{T_1^{\alpha}} \propto T\sum_{\mathbf{k}}\left(|A^{\beta}_{\mathrm{hf}}|^2\,\frac{\chi''_{\beta}(\mathbf{k},\omega)}{\omega}+|A^{\gamma}_{\mathrm{hf}}|^2\,\frac{\chi''_{\gamma}(\mathbf{k},\omega)}{\omega}\right). \quad (189)$$

At low temperatures with $H \| c$, $1/T_1$ is more than an order of magnitude smaller than the relaxation rate measured in the other two field directions [77]. Therefore, if we are interested in the relaxation rate in a field tilted at an angle θ to the b axis in the bc plane, such that θ is noticeably smaller than $\pi/2$, we can use the expression

$$\frac{1}{T_1(\theta)} \propto T\sum_{\mathbf{k}}|A^{z}_{\mathrm{hf}}|^2\,\frac{\chi''_{zz}(\mathbf{k},\omega)}{\omega}\cos^2\theta\,. \quad (190)$$

Assuming that fluctuations of the hyperfine electromagnetic field at the Co sites are determined by fluctuations of the magnetization of the subsystem of localized moments, as we did in discussing the neutron scattering relaxation rate, we can use the formula

$$\frac{\chi''_{zz}(\mathbf{q},\omega)}{\omega}=\frac{A}{\omega^2+\Gamma^2_{\mathbf{k}}}\,, \qquad \Gamma_{\mathbf{k}}=2A(a+\gamma_{ij}k_ik_j)\,, \quad (191)$$

where

$$a=\alpha_z+\beta_{yz}M_y^2+6\beta_zM_z^2=2\beta_z(3M_z^2-M_{z0}^2)\,. \quad (192)$$

To obtain the last equality, as in Eqn (65), we used the equilibrium condition

$$2\alpha_z+2\beta_{yz}M_y^2+4\beta_zM_z^2=\frac{H_z}{M_z}\,,$$

where

$$M_z=M_z(H_y,H_z)=M_z(H\cos\theta,H\sin\theta)\,, \quad M_{z0}=M_z(H,0) \quad (193)$$

are the equilibrium magnetization components in the field

$$\mathbf{H}=H_y\hat{\mathbf{y}}+H_z\hat{\mathbf{z}}=H\cos\theta\,\hat{\mathbf{y}}+H\sin\theta\,\hat{\mathbf{z}}\,. \quad (194)$$

At all temperatures below the Curie temperature, experimental values can be used for the magnetization $M_z(H_y,H_z)$.

The NMR measurements are performed at frequencies $\omega \ll \Gamma_{\mathbf{q}}$; hence, the relaxation rate is determined as

$$\frac{1}{T_1}(\theta) \propto T|A_{\mathrm{hf}}|^2A\cos^2\theta\int\frac{\mathrm{d}^3k}{(2\pi)^3\Gamma^2_{\mathbf{k}}}\,. \quad (195)$$

For simplicity, we can calculate the converging integral in the spherical approximation,

$$\int\frac{\mathrm{d}^3k}{(2\pi)^3\Gamma^2_{\mathbf{k}}}\approx\int_0^{\infty}\frac{4\pi k^2\,\mathrm{d}k}{(2\pi)^3(2A)^2(a+\gamma k^2)^2}=\frac{1}{32\pi A^2\sqrt{a\gamma^3}}\,.$$

Then, keeping only the field-dependent part in Eqn (195), we obtain

$$\frac{1}{T_1}(\theta)\propto\frac{\cos^2\theta}{\sqrt{a}}=\frac{1-H_z^2/H^2}{\sqrt{2\beta_z(3M_z^2-M_{z0}^2)}}\,. \quad (196)$$

Measurements of the NMR relaxation rate dependence on the magnetic field orientation were performed in relatively small fields $H < 3.5$ T [31]. In this case, $M_{z0}=M_z(H,0)$ is almost independent of the field $H=H_y$, and it can be set approximately equal to the spontaneous magnetization $M_{z0}(0,0)$. On the other hand, $M_z=M_z(H_y,H_z)\approx M_z(0,H_z)$ rapidly increases with an increase in H_z. For instance, in the field $H_z=1$ T, the magnetization $M_z(0,H_z)$ is twice as large as at $H_z=0$ [44]. Hence, according to Eqn (196), taking $H=3.5$ T and $H_z=1$ T, we obtain

$$\frac{1}{T_1}(H_z=1\text{ T})\approx 0.4\,\frac{1}{T_1}(H_z=0)\,. \quad (197)$$

The measured relaxation rate $1/T_1$ [31] as a function of the magnetic field H_z (H_c in Fig. 15) decreases faster than this estimate. This is not surprising in view of the roughness of our approximations made in deriving Eqn (196).

Thus, the NMR relaxation rate dependence on the magnetic field along the easy magnetization axis originates from the corresponding field dependence of the longitudinal magnetic susceptibility component.

7.2 Upper critical field anisotropy

The anomalous upper critical field anisotropy in UCoGe [9, 32] also finds a natural explanation in terms of the strong field

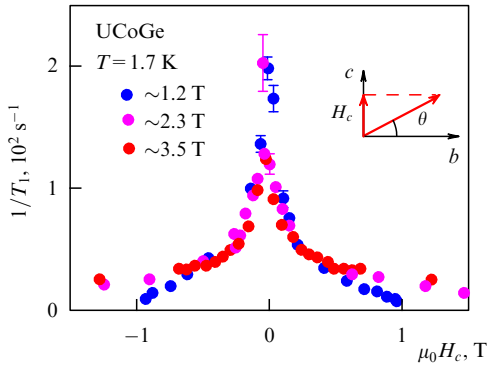

Figure 15. (Color online.) Plot of $1/T_1$ vs. H_c [31].

dependence of the longitudinal susceptibility determining the pairing coupling constant. In Section 4.2, we already derived this dependence in the case of a magnetic field parallel to the spontaneous magnetization direction (the c axis). If the magnetic field is directed along the crystallographic b axis, the critical temperature, ignoring orbital effects, is determined by Eqns (169) and (170). In a field directed in the bc plane, $\mathbf{H} = H_y\hat{\mathbf{y}} + H_z\hat{\mathbf{z}}$, Eqns (169) and (170) retain their form, but the Green's functions become

$$G^{\uparrow,\downarrow} = \left[\mathrm{i}\omega_n - \xi_{\mathbf{k}}^{\uparrow,\downarrow} \pm \mu_{\mathrm{B}}\sqrt{(h+H_z)^2 + H_y^2}\,\right]^{-1}, \qquad (198)$$

and the angle φ is found from $\tan\varphi = H_y/(h+H_z)$. The susceptibilities are

$$\chi^{\mathrm{u}}_{zz}(\mathbf{k},\mathbf{k}') \approx \frac{\gamma_{ij}k_{\mathrm{F}}^2}{4\left[\beta_z(3M_z^2 - M_{z0}^2) + \gamma k_{\mathrm{F}}^2\right]^2}\,\hat{k}_i\hat{k}'_j\,, \qquad (199)$$

$$\chi^{\mathrm{u}}_{yy}(\mathbf{k},\mathbf{k}') \approx \frac{\gamma_{ij}k_{\mathrm{F}}^2}{(\alpha_y + \beta_{yz}M_z^2 + 2\gamma k_{\mathrm{F}}^2)^2}\,\hat{k}_i\hat{k}'_j\,, \qquad (200)$$

where

$$M_z = M_z(H_y, H_z) = M_z(H\cos\theta, H\sin\theta), \quad M_{z0} = M_z(H,0)$$

are the equilibrium magnetization components in the field $\mathbf{H} = H_y\hat{\mathbf{y}} + H_z\hat{\mathbf{z}}$.

As usual, we can neglect χ^{u}_{yy} in view of its smallness compared to χ^{u}_{zz}. Then, as in Section 4.2, assuming that the highest critical temperature corresponds to the $(\hat{k}_x\eta_x^{\uparrow}, \hat{k}_x\eta_x^{\downarrow})$ superconducting state, in the single-band approximation we have

$$\ln\frac{\varepsilon}{T_{\mathrm{SC}}} = \frac{1}{g_{1x}^{\uparrow}} \propto \frac{\left[\beta_z(3M_z^2 - M_{z0}^2) + \gamma^z k_{\mathrm{F}}^2\right]^2}{\cos^2\varphi}\,. \qquad (201)$$

There are no experimental data on the low-temperature behavior of $M_z = M_z(H_y, H_z)$ as a function of both of its arguments. All measurements have been performed in the field directed along the crystallographic axes a, b, c [44, 78]. However, judging by the data in [78], where the phenomenon of strong upper critical field anisotropy has been revealed, we can expect that the increase in H_z at a fixed H_y would significantly increase M_z. A decrease in H_y, causing an increase in the Curie temperature $T_{\mathrm{C}}(H_y)$, increases M_z as well. Thus, a magnetic field deflection from the b or a direction toward the c axis leads to an increase in $M_z = M_z(H_y, H_z)$ and hence to a sharp drop in the pairing coupling constant described by Eqn (201). This explains the strong anisotropy of the upper critical field observed in UCoGe at low temperatures in strong magnetic fields [9, 32] (Fig. 16).

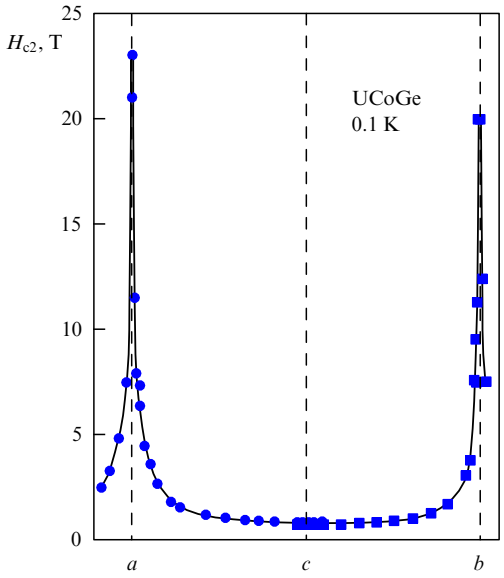

Figure 16. (Color online.) Angular dependence of H_{c2} at 0.1 K in UCoGe. $T_{\mathrm{SC}}(H=0) \approx 0.6$ K [9].

8. First-order phase transition to the ferromagnetic state in UGe_2

The pressure–temperature phase diagrams of several weak ferromagnets exhibit similarity. The transition from the paramagnetic to ferromagnetic states at ambient pressure occurs via a second-order phase transition. The phase transition temperature decreases as the pressure increases such that it reaches the zero value at some pressure P_0. In a pressure interval below P_0, magnetic ordering vanishes discontinuously. Hence, at high pressures and low temperatures, the ferromagnetic and paramagnetic states are separated by a first-order phase transition, whereas at higher temperatures and lower pressures this is a second-order transition. Such type of behavior is typical of MnSi [79–82], UGe_2 [83, 84] (Fig. 17), and $ZrZn_2$ [85]. The same behavior has been established in the ferromagnetic compounds $Co(Si_{1-x}Se_x)_2$ [86] and $(Sr_{1-x}Ca_x)RuO_3$ [82], where the role of pressure is played by the concentration of Se or Ca.

8.1 Phase transition to the ferromagnetic state in the Fermi liquid theory

The phase transition from the paramagnetic state to the itinerant ferromagnetic state is usually considered in the framework of the Stoner theory, where it is a second-order transition [59]. Some time ago, Belitz, Kirkpatrick, and Vojta (BKV) argued that in clean itinerant ferromagnets at low temperatures, this must be a first-order transition, due to the correlation effects that lead to a logarithmic term in the free energy density expansion in powers of the dimensionless magnetization M [87]:

$$E = E_0 + \alpha M^2 + \beta M^4 + vM^4\ln|M| + \ldots\,. \qquad (202)$$

Indeed, at a positive coefficient v, the effective fourth-order term in this formula is negative at small M, and the transition to the ferromagnetic state is a first-order one.

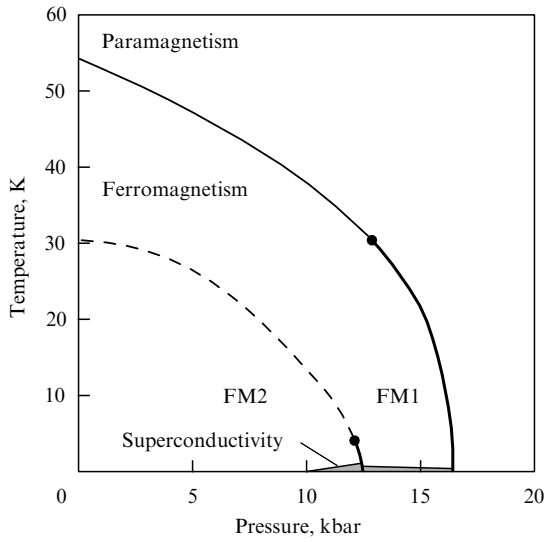

Figure 17. Phase diagram of UGe_2. Thick lines denote first order transitions and fine lines second order transitions. The dashed line is a crossover. Dots mark the positions of critical (tricritical) points. The region where superconductivity occurs is shaded [33].

The logarithmic correction to the fourth-order term has a long history. It was first calculated in 1970 by Kanno [88] in the dilute Fermi gas model in the second order with respect to the dimensionless gas parameter $k_F a$, where k_F is the Fermi momentum related to the total particle density

$$n = n^{\uparrow} + n^{\downarrow} = \frac{k_F^3}{3\pi^2} ,$$

and $a > 0$ is the s-wave scattering length. In general, to solve the phase transition problem at $T = 0$, we must calculate the Fermi-gas energy density

$$E(x) = \frac{3}{5} n\varepsilon_F f(M)$$

as a function of the dimensionless spin polarization (magnetization)

$$M = \frac{n^{\uparrow} - n^{\downarrow}}{n^{\uparrow} + n^{\downarrow}}$$

at a fixed $k_F a$. Here, $\varepsilon_F = k_F^2/(2m)$.

In the first order in $k_F a$, the phase transition to the ferromagnetic state is of the second order and occurs at $k_F a = \pi/2$ [89]. The second-order perturbation theory predicts a first-order phase transition [90–92] at $k_F a = 1.054$, consistent with the BKV argument. But because the critical gas parameter is expected to be of the order of unity, perturbative predictions may be unreliable. Nonperturbative effects have been studied in [93] by summing particle–particle ladder diagrams to all orders in the gas parameter. The theory predicts a second-order phase transition at $k_F a = 0.858$, which is in good agreement with the recent quantum Monte Carlo result $k_F a = 0.86$ [94]. This indicates that the ferromagnetic transition to the Fermi liquid does not occur by the BKV scenario.

Thus, the first-order phase transition in UGe_2 cannot be explained in the framework of the isotropic Fermi liquid theory even if we forget that this compound is a strongly anisotropic ferromagnetic metal with magnetization mostly supported by the magnetic moments localized at uranium atoms.

We also note that an isotropic ferromagnetic Fermi liquid is unstable with respect to transverse inhomogeneous deflections of magnetization [95, 96]. Therefore, the question of the isotropic Fermi liquid phase transition to the ferromagnetic state is only of academic interest.

8.2 Magneto-elastic mechanism of the development of first-order instability

The magneto-elastic mechanism of the development of a first-order instability has been proposed in [97], where it was demonstrated that the change in the transition order from second to first occurs at high compressibility and at a quite acute steepness of the exchange interaction dependence on the interatomic distance. This can easily be demonstrated in the framework of the Landau theory of phase transitions. Indeed, neglecting the shear deformation, the free energy density near the phase transition in an Ising-type ferromagnet has the form

$$F = \alpha_0(T - T_C)M^2 + \beta M^4 + \frac{K}{2}\varepsilon^2 - q\varepsilon M^2 , \qquad (203)$$

where M is the magnetization density, ε is the relative volume change, and K is the bulk modulus. The coefficient q is related to the Curie temperature pressure dependence as

$$q = \alpha_0 \frac{dT_C}{d\varepsilon} = -\alpha_0 K \frac{dT_C}{dP} . \qquad (204)$$

At a fixed pressure, that is, when changes in the specimen volume are not accompanied by pressure changes in the ambient medium, $\partial F/\partial\varepsilon = 0$, the deformation is determined by the magnetization squared, $\varepsilon = (q/K)M^2$, whence

$$F = \alpha M^2 + \left(\beta - \frac{q^2}{2K}\right) M^4 . \qquad (205)$$

Therefore, the phase transition changes its order from second to first at $q^2/(2K) > \beta$. The last inequality can be rewritten in terms of measurable parameters as

$$\frac{K\Delta C}{T_C}\left(\frac{dT_C}{dP}\right)^2 > 1 , \qquad (206)$$

where we use the formal expression $\Delta C = \alpha_0^2/(2\beta)T_C$ for the specific heat jump at a second-order phase transition.

The magneto-elastic interaction also produces another general mechanism for the instability of a second-order phase transition to the discontinuous formation of a ferromagnetic state from a paramagnetic one. This was first noted by Rice [98], who demonstrated that at a very small distance from a volume-dependent critical temperature $T_C(V)$, where the specific heat $C_{fl}(\tau) \sim \tau^{-\alpha}$, with $\tau = T/T_C(V) - 1$, tends to infinity due to critical fluctuations, the system bulk modulus

$$K = -V\frac{\partial P}{\partial V} = V\frac{\partial^2 FV}{\partial V^2} ,$$

expressed in terms of the free energy density $F = F_0 + F_{fl}$, $F_{fl} \sim -T_C\tau^{2-\alpha}$, becomes negative,

$$K = K_0 - A\frac{C_{fl}(\tau)V^2}{T_C}\left(\frac{\partial T_C}{\partial V}\right)^2 = K_0 - AK_0^2\frac{C_{fl}(\tau)}{T_C}\left(\frac{\partial T_C}{\partial P}\right)^2\Bigg|_{\tau\to 0} < 0 , \qquad (207)$$

which contradicts the thermodynamic stability of the system. In reality, as the temperature decreases but before the temperature corresponding to $K = 0$ is reached, the system undergoes a first-order transition, jumping over the instability region directly to the ferromagnetic state with a finite magnetization and the corresponding striction deformation. This transition is similar to the jump over the region with $\partial P/\partial V > 0$ on the van der Waals isotherm at the liquid–gas transition.

The condition of first-order instability (207) can be written similarly to Eqn (206):

$$\frac{K_0 C_{\rm fl}(\tau)}{T_{\rm C}} \left(\frac{\partial T_{\rm C}}{\partial P}\right)^2 > 1\,. \tag{208}$$

Unlike Eqn (206), this formula demonstrates that the first-order instability is inevitable due to the infinite increase in the fluctuation specific heat.

The striction interaction can change the form of the free energy compared with its form at a fixed volume. A more elaborate treatment [99] taking this effect into account leads to the following condition for the first-order instability:

$$\frac{1}{T_{\rm C}} \frac{4\mu K}{3K + 4\mu} f''(x) \left(\frac{\partial T_{\rm C}}{\partial P}\right)^2 > 1\,. \tag{209}$$

Here, the function $f(x)$ determines the fluctuation part of free energy $F = -T_{\rm C} f[(T - T_{\rm C})/T_{\rm C}]$, and μ is the shear modulus.

Usually, the left-hand side of Eqn (208) is quite small and a first-order transition occurs at a temperature T^* close to the critical temperature, where the fluctuation specific heat is large enough. This means that the temperature difference $T^* - T_{\rm C}$ is much smaller than the critical temperature $T_{\rm C}$. The latent heat

$$q \approx C_{\rm fl}(T^* - T_{\rm C}) \tag{210}$$

is extremely small in this transition, and hence the first-order phase transition is practically indistinguishable from a second-order one; it is called a *weak first-order phase transition or a phase transition of the first order close to the second order*.

According to Eqns (206) and (208), the magneto-elastic mechanism effectively leads to a first-order transition when the critical temperature is highly pressure dependent. This is the case with all the materials mentioned above. To check criteria (206) and (208), we must calculate the mean-field jump and the fluctuation part of the specific heat near the Curie temperature for each particular material. In Sections 8.3 and 8.4, we do these calculations for UGe_2 [35] characterized by strong magnetic anisotropy and by a precipitous drop in the critical temperature with a pressure increase near 14–15 kbar [3].

8.3 Specific heat near the Curie temperature

UGe_2 is an orthorhombic material that exhibits a transition to the ferromagnetic state at ambient pressure at $T_{\rm C} = 53$ K. Magnetic measurements reveal a very strong magnetocrystalline anisotropy [100] with **a** being the easy axis (which we take to be the z direction). As in Section 7, we take only the easy-axis order parameter fluctuations into account. Above the Curie temperature, they are determined by deviations of the system free energy

$$\mathcal{F} = \int \mathrm{d}^3\mathbf{r} \left[\alpha M^2 + \beta M^4 + \gamma_{ij} \nabla_i M \nabla_j M - \frac{1}{2} \frac{\partial^2 M(\mathbf{r})}{\partial z^2} \int \frac{M(\mathbf{r}')}{|\mathbf{r} - \mathbf{r}'|}\, \mathrm{d}^3\mathbf{r}'\right] \tag{211}$$

from the equilibrium value $\alpha = \alpha_0(T - T_{\rm C})$. The gradient energy is determined by three constants γ_{xx}, γ_{yy}, and γ_{zz}. The coordinates x, y, z correspond to the crystallographic axes b, c, a. The last nonlocal term in Eqn (211) corresponds to the magnetostatic energy [101] $-\mathbf{MH} - H^2/8\pi$ of the internal magnetic field **H** created by magnetization and is related to it by the Maxwell equations

$$\mathrm{rot}\,\mathbf{H} = 0\,, \qquad \mathrm{div}\,(\mathbf{H} + 4\pi\mathbf{M}) = 0\,.$$

We use the following estimates for the coefficients in the Landau functional:

$$\alpha_0 = \frac{1}{m^2 n}\,, \tag{212}$$

$$\beta = \frac{T_{\rm C}}{2(m^2 n)^2 n}\,, \tag{213}$$

$$\gamma_x \approx \gamma_y \approx \gamma_z \approx \frac{T_{\rm C} a^2}{m^2 n}\,. \tag{214}$$

Here, m is the magnetic moment per uranium atom at zero temperature, $m = 1.4\mu_{\rm B}$ at ambient pressure [16], and $n = a^{-3}$ is the density of uranium atoms, which can be approximately taken to be the cube of the inverse nearest-neighbor uranium atom separation $a = 3.85$ Å [19].

The mean-field magnetization and the jump in the specific heat are

$$M^2 = -\frac{\alpha}{2\beta} = (mn)^2\, \frac{T_{\rm C} - T}{T_{\rm C}}\,, \tag{215}$$

$$\Delta C = \frac{T_{\rm C}\alpha_0^2}{2\beta} = n\,. \tag{216}$$

The experimentally found specific heat jump $\Delta C_{\rm exp} \approx 10$ J mol^{-1} K^{-1} ≈ 1 per uranium atom [19] is in remarkable correspondence with Eqn (216).

To calculate the fluctuation specific heat, we use the Fourier representation of the part of Eqn (211) that is quadratic in the order parameter:

$$\mathcal{F} = \sum_{\mathbf{k}} \left(\alpha + \gamma_{ij} k_i k_j + \frac{2\pi k_z^2}{k^2}\right) M_{\mathbf{k}} M_{-\mathbf{k}}\,, \tag{217}$$

where $M_{\mathbf{k}} = \int M(\mathbf{r}) \exp(-\mathrm{i}\mathbf{k}\mathbf{r})\, \mathrm{d}^3\mathbf{r}$. The last term in this expression corresponds to the magnetostatic energy [35, 101]. The corresponding thermodynamic potential and the specific heat found in a similar uniaxial segnetoelectric model are [102]

$$\mathcal{F}_{\rm fl} = -\frac{T}{2} \sum_{\mathbf{k}} \ln \frac{\pi T}{\alpha + \gamma_{ij} k_i k_j + 2\pi k_z^2/k^2}\,, \tag{218}$$

$$C_{\rm fl0} = \frac{T^2 \alpha_0^2}{2(2\pi)^3} \int \frac{\mathrm{d}k_x\, \mathrm{d}k_y\, \mathrm{d}k_z}{(\alpha + \gamma_{ij} k_i k_j + 2\pi \hat{k}_z^2)^2}\,. \tag{219}$$

Passing to spherical coordinates and integrating over the modulus k, we arrive at

$$C_{\rm fl0} = \frac{T^2\alpha_0^2}{32\pi^2}\int_0^1 {\rm d}\zeta \int_0^{2\pi} \frac{{\rm d}\varphi}{(\alpha + 2\pi\zeta^2)^{1/2}\left[\gamma_\perp + \zeta^2(\gamma_z - \gamma_\perp)\right]^{3/2}}\,, \tag{220}$$

where $\gamma_\perp(\varphi) = \gamma_x \cos^2\varphi + \gamma_y \sin^2\varphi$. At the critical temperature, $\alpha = 0$ and the integral diverges. Integrating over ζ with logarithmic accuracy, we obtain

$$C_{\rm fl0} = \frac{T_{\rm C}^2\alpha_0^2}{32\pi\sqrt{2\pi}\gamma^{3/2}} \ln\frac{2\pi}{\alpha} \approx \frac{n}{32\pi}\sqrt{\frac{T_{\rm C}}{2\pi m^2 n}} \ln\frac{2\pi m^2 n}{T - T_{\rm C}}\,, \tag{221}$$

where

$$\frac{1}{\gamma^{3/2}} = \frac{1}{2\pi}\int_0^{2\pi} \frac{{\rm d}\varphi}{\gamma_\perp^{3/2}(\varphi)}\,.$$

The condition $\alpha \ll 2\pi$ at $T_{\rm C} = 10$ K used here is realized at

$$\frac{T - T_{\rm C}}{T_{\rm C}} < \frac{2\pi m^2 n}{T_{\rm C}} \approx 0.015\,. \tag{222}$$

In view of the roughness of the parameters, the region of the logarithmic increase of specific heat can in fact be broader.

Calculations taking the interaction of fluctuations into account in the formally similar uniaxial segnetoelectric model were performed by Larkin and Khmelnitskii [103]. In our notation, the expression for the fluctuation specific heat at constant pressure obtained in that paper is

$$C_{\rm fl} = \frac{3^{1/3}T_{\rm C}^2\alpha_0^2}{16\pi\gamma_{\rm LK}^{2/3}\gamma^{3/2}} \left(\ln\frac{2\pi}{\alpha}\right)^{1/3}, \tag{223}$$

where $\gamma_{\rm LK} = 3T_{\rm C}\beta/(\sqrt{32\pi}\,\gamma^{3/2})$ is the effective coupling constant. Using Eqns (212)–(214), we can rewrite Eqn (223) as

$$C_{\rm fl} \approx \frac{n}{10}\left(\frac{T_{\rm C}}{2\pi m^2 n}\right)^{1/6} \left(\ln\frac{2\pi m^2 n}{T - T_{\rm C}}\right)^{1/3}. \tag{224}$$

The power of the logarithm $\{\ln[\alpha/(2\pi)]\}^{1/3}$ is a very slowly varying function slightly exceeding unity; hence, in the temperature range defined by inequality (222) we can estimate the fluctuation specific heat as

$$C_{\rm fl} \approx \frac{n}{5}\,. \tag{225}$$

We see that the fluctuation specific heat is smaller than the mean field jump given by Eqn (216). Hence, criterion (206) can be used to check a tendency to the first-order phase transition in UGe_2.

8.4 Second-order transition instability

The Curie temperature in UGe_2 decreases monotonically with increasing pressure: from 53 K at ambient pressure to a precipitous decrease above 15 kbar [3]. The average value of the critical temperature derivative with respect to pressure can be estimated as

$$\frac{\partial T_{\rm C}}{\partial P} \approx \frac{40\ {\rm K}}{14\ {\rm kbar}} = 4\times 10^{-25}\ {\rm cm}^3\,. \tag{226}$$

For the bulk modulus, we obtain

$$K = \rho c^2 \approx 10^{11}\ {\rm erg\ cm}^{-3}\,, \tag{227}$$

where we use the speed of sound $c \approx 10^5$ cm s^{-1} typical for metals and the known [104] density $\rho = 10.26$ g cm^{-3}. Hence, for the combination in Eqn (206), we have

$$\frac{Kn}{T_{\rm C}}\left(\frac{\partial T_{\rm C}}{\partial P}\right)^2 = 0.2\,. \tag{228}$$

At $T_{\rm C} \approx 10$ K, the pressure derivative of the critical temperature is much higher (and its square is even higher) than its average value given by Eqn (226). We therefore conclude that at a critical temperature of the order of 10 K, criterion (206) is fulfilled, and the phase transition to the ferromagnetic state becomes a first-order transition.

8.5 Concluding remarks

The magneto-elastic interaction contributes to the development of the first-order instability at the phase transition to the ordered state in any ferromagnet. But the actual temperature range where this instability develops is typically very small, and the first-order transition is almost indistinguishable from a second-order one. In the anisotropic ferromagnet UGe_2, the precipitous drop in the Curie temperature as a function of pressure near 14–15 kbar is sufficient for the second-order phase transition to the ferromagnetic state to be replaced by a first-order transition.

At low temperatures, according to the Nernst law and the Clausius–Clapeyron relation

$$\frac{{\rm d}T_{\rm C}}{{\rm d}P} = \left.\frac{v_1 - v_2}{s_1 - s_2}\right|_{T\to 0} \to \infty\,, \tag{229}$$

the decrease in the first-order transition temperature with pressure becomes infinitely fast, meaning that even a weak first-order transition tends to be stronger as the temperature approaches the absolute zero. Hence, the effect of the magneto-elastic interaction in ferromagnets or, more generally, of the order parameter interaction with elastic degrees of freedom at an arbitrary type of ordering raises doubts about the existence of quantum critical phenomena.

9. Superconducting order in ferromagnetic UIr

UIr has a monoclinic PbBi-type structure without inversion symmetry, as shown in Fig. 18. At ambient pressure, it is an Ising-like ferromagnet with the Curie temperature $T_{\rm C} = 46$ K.

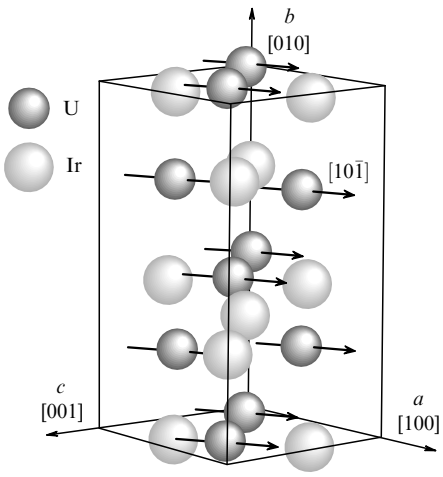

Figure 18. Monoclinic structure of UIr. The arrows indicate the spontaneous magnetization direction [105].

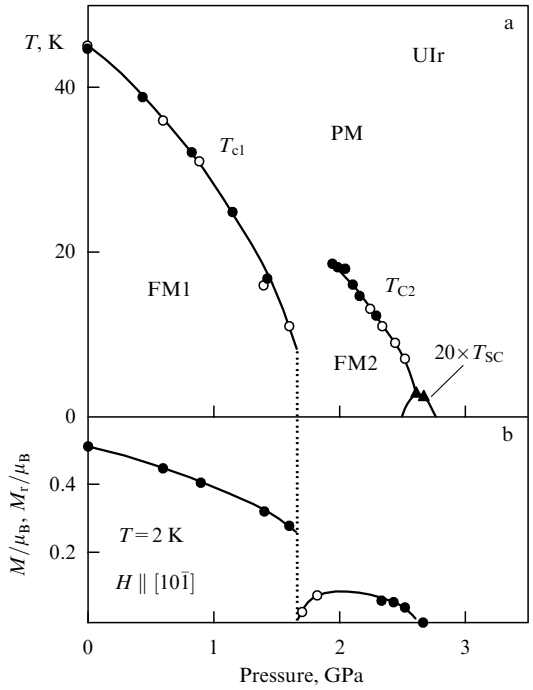

Figure 19. (a) $P-T$ phase diagram of UIr. Filled and unfilled dots respectively show the resistivity and magnetization measurements. Superconductivity is observed near the critical pressure where the FM2 phase disappears. (b) Pressure dependence of the ordered moment along $[1, 0, \bar{1}]$ at 2 K. Filled dots are the ordered moments determined from the Arrott plot. Unfilled dots are the residual magnetization M_r [106].

The magnetic susceptibility follows the Curie–Weiss law with the effective moment $\mu_{\text{eff}} = 2.4\mu_B$ per uranium atom, while the ordered moment at low temperatures is $0.5\mu_B$ per uranium atom. The pressure–temperature phase diagram of UIr consists of a low-pressure phase FM1, a high-pressure magnetic phase FM2, and a superconducting phase as shown in Fig. 19a. The discrete change in the ordered moment indicates that the FM1–FM2 transition is of the first order. The FM2–nonmagnetic transition is of the second order [106].

For UIr, it is still not clear whether superconductivity coexists with magnetic ordering [106]. However, if this is the case, we are dealing with a unique situation where the superconducting state arises in a material with broken space and time parity. We here describe the symmetry and order parameter of this type of superconductivity.

The symmetry group of the normal nonmagnetic state of UIr

$$\mathrm{G_N} = (\mathrm{E}, \mathrm{C}_{2b}) \times \mathrm{R} \times \mathrm{U}(1) \tag{230}$$

includes the point symmetry group $\mathrm{C}_2 = (\mathrm{E}, \mathrm{C}_{2b})$, where C_{2b} is the rotation around the b axis through the angle π (see Fig. 19), the time reversal R, and the gauge group U(1). In the FM2 state, the time reversal is broken and the symmetry group

$$\mathrm{G_F} = (\mathrm{E}, \mathrm{RC}_{2b}) \times \mathrm{U}(1) \tag{231}$$

includes a combination of the rotation C_{2b} and the operation R reversing the direction of spontaneous magnetization lying in the (a, c) plane. Finally, in a superconducting state coexisting with the FM2 state, the gauge symmetry is broken and the symmetry group is

$$\mathrm{G_{FSC}} = \left(\mathrm{E}, \exp(2\mathrm{i}\varphi)\mathrm{RC}_{2b}\right). \tag{232}$$

The space parity is broken; hence, the magnetic pairing interaction inevitably includes the Dzyaloshinskii–Moriya coupling [38]. As a result, the superconducting order parameter is the sum of triplet and singlet parts:

$$\hat{\Delta} = \mathrm{i}(\mathbf{d}\boldsymbol{\sigma})\sigma_y + \mathrm{i}d_0\sigma_y\,. \tag{233}$$

The triplet part has the usual form

$$\mathbf{d}(\mathbf{k}, \mathbf{r}) = \frac{1}{2}\left[-(\hat{\mathbf{x}} + \mathrm{i}\hat{\mathbf{y}})\Delta^{\uparrow}(\mathbf{k}, \mathbf{r}) + (\hat{\mathbf{x}} - \mathrm{i}\hat{\mathbf{y}})\Delta^{\downarrow}(\mathbf{k}, \mathbf{r})\right] + \Delta^0(\mathbf{k}, \mathbf{r})\hat{\mathbf{z}}\,, \tag{234}$$

but in contrast to the coordinate axes in orthorhombic crystals discussed in Section 2, the coordinate axes of nonunitary superconducting ordering do not coincide with monoclinic crystallographic directions. Namely, here, the unit vector $\hat{\mathbf{z}}$ is aligned parallel to the spontaneous magnetization in the (a, c) plane (direction $[1, 0, \bar{1}]$), $\hat{\mathbf{x}}$ is the unit vector directed along the b axis, and $\hat{\mathbf{y}} = \hat{\mathbf{z}} \times \hat{\mathbf{x}}$:

$$\begin{aligned}
\Delta^{\uparrow}(\mathbf{k}, \mathbf{r}) &= k_x\eta_x^{\uparrow}(\mathbf{r}) + \mathrm{i}k_y\eta_y^{\uparrow}(\mathbf{r})\,,\\
\Delta^{\downarrow}(\mathbf{k}, \mathbf{r}) &= k_x\eta_x^{\downarrow}(\mathbf{r}) + \mathrm{i}k_y\eta_y^{\downarrow}(\mathbf{r})\,,\\
\Delta^{0}(\mathbf{k}, \mathbf{r}) &= k_z\eta_z^{0}(\mathbf{r})\,,
\end{aligned} \tag{235}$$

where k_x, k_y, k_z are momentum projections on the axes $\hat{x}, \hat{y}, \hat{z}$ defined above. The singlet part of the order parameter is

$$d_0(\mathbf{k}, \mathbf{r}) = F\eta_0(\mathbf{r})\,, \tag{236}$$

where F is a function of k_x^2, k_y^2, k_z^2.

10. Conclusion

The treatment of the properties of uranium compounds developed in this paper is based on the symmetry of superconducting states with triplet pairing in orthorhombic ferromagnets. The phenomenological considerations are supported by microscopic calculations performed in the framework of the weak-coupling superconductivity theory with pairing interaction expressed through the frequency-independent magnetic susceptibility of an anisotropic ferromagnetic medium. This approach reproduces the structure of superconducting states found on purely symmetry grounds and allows us to qualitatively explain many experimental observations.

A topic outside the scope of this paper is ARPES experiments and band structure calculations, which are still not in complete agreement. We can recommend two recent papers reporting the ARPES studies in URhGe [107] and in UGe_2 and UCoGe [108], a comparison with band structure calculations, and a long list of references to previous studies.

Acknowledgements
I am grateful to A Huxley, J-P Brison, S Raymond, K Ishida, D Aoki, M Zhitomirsky, and J Flouquet for the discussions of the physics of uranium ferromagnets. I am also indebted to M Sadovskii, who invited me to give lectures at the Winter Theoretical School *Kourovka-2016*, which obviously helped this paper to emerge.

References

1. Maple M B *J. Magn. Magn. Mater.* **31–34** 479 (1983)
2. Maple M B *Physica B* **215** 110 (1995)
3. Saxena S S et al. *Nature* **406** 587 (2000)
4. Aoki D et al. *Nature* **413** 613 (2001)
5. Huy N T et al. *Phys. Rev. Lett.* **99** 067006 (2007)
6. Akazawa T et al. *J. Phys. Soc. Jpn.* **73** 3129 (2004)
7. Aoki D et al. *C.R. Phys.* **12** 573 (2011)
8. Aoki D, Flouquet J *J. Phys. Soc. Jpn.* **81** 011003 (2012)
9. Aoki D, Flouquet J *J. Phys. Soc. Jpn.* **83** 061011 (2014)
10. Aso N et al. *Physica B* **359 – 361** 1051 (2005)
11. Kotegawa H et al. *J. Phys. Soc. Jpn.* **74** 705 (2005)
12. de Visser A et al. *Phys. Rev. Lett.* **102** 167003 (2009)
13. Sakarya S, van Dijk N H, Brück E *Phys. Rev. B* **71** 174417 (2005)
14. Hykel D J et al. *Phys. Rev. B* **90** 184501 (2014)
15. Kobayashi T C et al. *J. Phys. Soc. Jpn.* **76** 051007 (2007)
16. Kernavanois N et al. *Phys. Rev. B* **64** 174509 (2001)
17. Prokeš K et al. *Acta Phys. Polon. B* **34** 1473 (2003)
18. Prokeš K et al. *Phys. Rev. B* **81** 180407(R) (2010)
19. Huxley A et al. *Phys. Rev. B* **63** 144519 (2001)
20. Taupin M et al. *Phys. Rev. B* **92** 035124 (2015)
21. Butchers M W et al. *Phys. Rev. B* **92** 121107(R) (2015)
22. McHale P, Fulde P, Thalmeier P *Phys. Rev. B* **70** 014513 (2004)
23. Hattori K, Tsunetsugu H *Phys. Rev. B* **87** 064501 (2013)
24. Mineev V P *Phys. Rev. B* **66** 134504 (2002)
25. Mineev V P, Champel T *Phys. Rev. B* **69** 144521 (2004)
26. Mineev V P *Int. J. Mod. Phys. B* **18** 2963 (2004)
27. Mineev V P *Phys. Rev. B* **83** 064515 (2011)
28. Mineev V P *Phys. Rev. B* **90** 064506 (2014)
29. Mineev V P *Phys. Rev. B* **91** 014506 (2015)
30. Lévy F et al. *Science* **309** 1343 (2005)
31. Hattori T et al. *Phys. Rev. Lett.* **108** 066403 (2012)
32. Aoki D et al. *J. Phys. Soc. Jpn.* **78** 113709 (2009)
33. Huxley A D, Raymond S, Ressouche E *Phys. Rev. Lett.* **91** 207201 (2003)
34. Mineev V P *Phys. Rev. B* **88** 224408 (2013)
35. Mineev V P *J. Phys. Conf. Ser.* **400** 032053 (2012)
36. Mineev V P, Samokhin K V *Introduction to Unconventional Superconductivity* (Amsterdam: Gordon and Breach Sci. Publ., 1999); Translated from Russian: *Vvedenie v Teoriyu Neobychnoi Sverkhprovodimosti* (Moscow: Izd. MFTI, 1998)
37. Mineev V P *AIP Conf. Proc.* **1134** 68 (2009)
38. Samokhin K V, Mineev V P *Phys. Rev. B* **77** 104520 (2008)
39. Ambegaokar V, Mermin N D *Phys. Rev. Lett.* **30** 81 (1973)
40. Taupin M et al. *Phys. Rev. B* **90** 180501(R) (2014)
41. Yamaguchi A et al. *Nature* **444** 909 (2006)
42. Fay D, Appel J *Phys. Rev. B* **22** 3173 (1980)
43. Taupin M, unpublished
44. Huy N T et al. *Phys. Rev. Lett.* **100** 077002 (2008)
45. Hardy F, Huxley A D *Phys. Rev. Lett.* **94** 247006 (2005)
46. Hardy F et al. *Phys. Rev. B* **83** 195107 (2011)
47. Scharnberg K, Klemm R A *Phys. Rev. Lett.* **54** 2445 (1985)
48. Volovik G E *JETP Lett.* **58** 469 (1993); *Pis'ma Zh. Eksp. Teor. Fiz.* **58** 457 (1993)
49. Barash Yu S, Mineev V P, Svidzinskii A A *JETP Lett.* **65** 638 (1997); *Pis'ma Zh. Eksp. Teor. Fiz.* **65** 606 (1997)
50. Aoki D, Knebel G, Flouquet J *J. Phys. Soc. Jpn.* **83** 094719 (2014)
51. Landau L D, Lifshitz E M *Statistical Physics* Pt. 1 (Oxford: Butterworth-Heinemann, 1995); Translated from Russian: *Statisticheskaya Fizika* Pt. 1 (Moscow: Nauka, 1976)
52. Hattori T et al. *J. Phys. Soc. Jpn.* **83** 073708 (2014)
53. Lévy F, Sheikin I, Huxley A *Nature Phys.* **3** 460 (2007)
54. Tokunaga Y et al. *Phys. Rev. Lett.* **114** 216401 (2015)
55. Van Hove L *Phys. Rev.* **95** 1374 (1954)
56. Forster D *Hydrodynamic Fluctuations, Broken Symmetry, and Correlation Functions* (Reading, Mass.: W.A. Benjamin, 1975)
57. Shirane G et al. *J. Appl. Phys.* **55** 1887 (1984)
58. Halperin B I, Hohenberg P C *Phys. Rev.* **177** 952 (1969)
59. Hertz J A *Phys. Rev. B* **14** 1165 (1976)
60. Moriya T *J. Magn. Magn. Mater.* **14** 1 (1979)
61. Ishikawa Y et al. *Phys. Rev. B* **31** 5884 (1985)
62. Yamada K et al. *J. Appl. Phys.* **61** 3400 (1987)
63. Semadeni F et al. *Phys. Rev. B* **62** 1083 (2000)
64. Raymond S, Huxley A *Physica B* **350** 33 (2004)
65. Stock C et al. *Phys. Rev. Lett.* **107** 187202 (2011)
66. Overhauser A W *Phys. Rev.* **89** 689 (1953)
67. Elliott R J *Phys. Rev.* **96** 266 (1954)
68. Feher G, Kip A F *Phys. Rev.* **98** 337 (1955)
69. Menovsky A et al., in *High Field Magnetism. Proc. of the Intern. Symp. on High Field Magnetism, Osaka, Japan, September 13 – 14, 1982* (Ed. M Date) (Amsterdam: North-Holland, 1983) p. 189
70. Sakon T et al. *Phys. Scripta* **75** 546 (2007)
71. Troć R, Gajek Z, Pikul A *Phys. Rev. B* **86** 224403 (2012)
72. Yaouanc A et al. *Phys. Rev. Lett.* **89** 147001 (2002)
73. Sakarya S et al. *Phys. Rev. B* **81** 024429 (2010)
74. Slichter C P *Principles of Magnetic Resonance* (Berlin: Springer-Verlag, 1990)
75. Landau L D, Khalatnikov I M *Collected Papers of L.D. Landau* (Ed. D ter Haar) (London: Pergamon Press, 1965); Translated from Russian: *Dokl. Akad. Nauk SSSR* **96** 469 (1954)
76. Chubukov A V, Betouras J J, Efremov D V *Phys. Rev. Lett.* **112** 037202 (2014)
77. Ihara Y et al. *Phys. Rev. Lett.* **105** 206403 (2010)
78. Knafo W et al. *Phys. Rev. B* **86** 184416 (2012)
79. Pfleiderer C et al. *Phys. Rev. B* **55** 8330 (1997)
80. Stishov S M et al. *Phys. Rev. B* **76** 052405 (2007)
81. Otero-Leal M et al. *Phys. Rev. B* **79** 060401(R) (2009)
82. Uemura Y J et al. *Nature Phys.* **3** 29 (2007)
83. Pfleiderer C, Huxley A D *Phys. Rev. Lett.* **89** 147005 (2002)
84. Taufour V et al. *Phys. Rev. Lett.* **105** 217201 (2010)
85. Uhlarz M, Pfleiderer C, Hayden S M *Phys. Rev. Lett.* **93** 256041 (2004)
86. Goto T et al. *Phys. Rev. B* **56** 14019 (1997)
87. Belitz D, Kirkpatrick T R, Vojta T *Phys. Rev. Lett.* **82** 4707 (1999)
88. Kanno S *Prog. Theor. Phys.* **44** 813 (1970)
89. Huang K *Statistical Mechanics* (New York: Wiley, 1987)
90. Duine R A, MacDonald A H *Phys. Rev. Lett.* **95** 230403 (2005)
91. Conduit G J, Simons B D *Phys. Rev. A* **79** 053606 (2009)
92. Conduit G J, Green A G, Simons B D *Phys. Rev. Lett.* **103** 207201 (2009)
93. He L, Huang X-G *Phys. Rev. A* **85** 043624 (2012)
94. Pilati S et al. *Phys. Rev. Lett.* **105** 030405 (2010)
95. Mineev V P *Phys. Rev. B* **72** 144418 (2005)
96. Mineev V P, arXiv:1111.3208
97. Bean C P, Rodbell D S *Phys. Rev.* **126** 104 (1962)
98. Rice O K *J. Chem. Phys.* **22** 1535 (1954)
99. Larkin A I, Pikin S A *Sov. Phys. JETP* **29** 891 (1969); *Zh. Eksp. Teor. Fiz.* **56** 1664 (1969)
100. Ōnuki Y et al. *J. Phys. Soc. Jpn.* **61** 293 (1992)
101. Lifshitz E M, Pitaevskii L P *Statistical Physics* Pt. 2 (Oxford: Butterworth-Heinemann, 1995); *Statisticheskaya Fizika* Pt. 2 (Moscow: Nauka, 1978)
102. Levanyuk A P *Izv. Akad. Nauk SSSR Ser. Fiz.* **29** 879 (1965)
103. Larkin A I, Khmel'nitskii D E *Sov. Phys. JETP* **29** 1123 (1969); *Zh. Eksp. Teor. Fiz.* **56** 2087 (1969)
104. Boulet P et al. *J. Alloys Comp.* **247** 104 (1997)
105. Galatanu A et al. *J. Phys. Soc. Jpn.* **73** 766 (2004)
106. Kobayashi T C et al. *J. Phys. Condens. Matter* **19** 125205 (2007)
107. Fujimori S et al. *Phys. Rev. B* **89** 104518 (2014)
108. Fujimori S et al. *Phys. Rev. B* **91** 174503 (2015)
109. Mineev V P *Phys. Rev. B* **95** 104501 (2017)